REPUBLIQUE ALGERIENNE DEMOCRATIQUE ET POPULAIRE

Ministère de l'Enseignement Supérieur et de la Recherche Scientifique

École Nationale Polytechnique

Department: *Electronic*

Laboratory: *Communication and signal*

THESIS

For obtaining

Doctorate in electronic

Performance of novel architectures based on index modulation, considering multiuser interference and inter-symbols

Fadila BERRAHMA

Under the leadership of *Mrs. GHANEM Khalida research director*
And Mr. BOUSBIA-SALAH Hicham Professor / ENP Alger.

Presented on *21 /03 /2023*

Composition of jury :

President	Mr. M. ADNANE	**Professor/** ENP Alger.
Thesis authors	Mme. K. GHANEM	**Research director**/ CDTA Alger.
	Mr. H. BOUSBIA-SALAH	**Professor/** ENP Alger.
Examiners	Mr. C. LARBES	**Professor/** ENP Alger.
	Mr. A. HAMZA	**Professor/** USTHB Alger.
	Mr. A. MAALI	**Lecturer A/** EMP Alger.
	Mr. A. AMROUCHE	**Professor/** USTHB Alger.

ENP 2023

REPUBLIQUE ALGERIENNE DEMOCRATIQUE ET POPULAIRE

Ministère de l'Enseignement Supérieur et de la Recherche Scientifique

École Nationale Polytechnique

Department: *Electronic*

Laboratory: *Communication and signal*

THESIS

For obtaining

Doctorate in electronic

Performance of novel architectures based on index modulation, considering multiuser interference and inter-symbols

Fadila BERRAHMA

Under the leadership of *Mrs. GHANEM Khalida research director*
And Mr. BOUSBIA-SALAH Hicham Professor / ENP Alger.

Presented on *21 /03 /2023*

Composition of jury :

President	Mr. M. ADNANE	**Professor/** ENP Alger.
Thesis authors	Mme. K. GHANEM	**Research director**/ CDTA Alger.
	Mr. H. BOUSBIA-SALAH	**Professor/** ENP Alger.
Examiners	Mr. C. LARBES	**Professor/** ENP Alger.
	Mr. A. HAMZA	**Professor/** USTHB Alger.
	Mr. A. MAALI	**Lecturer A/** EMP Alger.
	Mr. A. AMROUCHE	**Professor/** USTHB Alger.

ENP 2023

REPUBLIQUE ALGERIENNE DEMOCRATIQUE ET POPULAIRE

Ministère de l'Enseignement Supérieur et de la Recherche Scientifique

École Nationale Polytechnique

Département : *Electronique*

Laboratoire : *Communication et signal*

THÈSE

En vue de l'obtention du

Doctorat en électronique

Performance de nouvelles architectures de communication à base de modulation d'indice, considérant l'agilité de la communication et l'interférence multi-usagers et inter-symboles

Fadila BERRAHMA

Sous la direction de *Mme. GHANEM Khalida Directrice de recherche*
Et Mr. BOUSBIA-SALAH Hicham Professeur / ENP Alger.

Présentée et soutenue le *21 /03 /2023*

Composition du jury :

Président	Mr. M. ADNANE	**Professeur/** ENP Alger.
Promoteurs	Mme. K. GHANEM	**Directrice de recherche**/ CDTA Alger.
	Mr. H. BOUSBIA-SALAH	**Professeur/** ENP Alger.
Examinateurs	Mr. C. LARBES	**Professeur/** ENP Alger.
	Mr. A. HAMZA	**Professeur/** USTHB Alger.
	Mr. A. MAALI	**Maître de conférences A/** EMP Alger.
	Mr. A. AMROUCHE	**Professeur/** USTHB Alger.

ENP 2023

ملخص :

في هذه المذكـرة، كنا مهتمين بتحليل و دراسة مدى كفاءة مختلف أنظمة الكشف المستخدمة في المخططات القائمة عموما على نظام "IM". تم التطرق إلى دراسة نظام متعدد المستخدمين والذي يعتمد على تقنية CDMA. بهدف مكافحة انتقائية تردد القناة في الاتصالات ذات السرعة العالية ، نقترح دمج IM مع تقنيات حديثة مثل GFDM. تم اقتراح أيضا مخطط جديد تم من خلاله تحسين الكفاءة و الذي يعتمد على استخدام انتقائية تردد القناة في نطاق تيراهرتز لبيئة طبيةIn-VIVO . يتيح هذا المخطط الحصول على معدلات بيانات عالية مع ضمان التواصل الجيد في الشبكة الطبية الحديثة.

تعتبر النتائج العامة المحصل عليها جد مرضية و تفتح أبواب جديدة للبحث.

كلمات مفتاحية: الأنظمة ذات المداخل و المخارج المتعددة ، التعديل الفهرسي، التقسيم العمودي للتردد، الحد الأدنى للخطأ.

Résumé :

Dans ce travail, nous nous sommes intéressés à l'analyse et à l'étude des performances des différentes architectures basées sur la modulation d'indice IM. Des structures permettant d'adresser le contexte multi-usagers sont d'intérêt, en adoptant des techniques à base de CDMA. Afin de combattre la sélectivité fréquentielle du canal dans les communications à très haut débit, nous proposons de combiner les architectures conventionnelles de l'IM avec les techniques récentes d'orthogonalisation des sous-canaux telles que la GFDM. Egalement, comme contribution, nous avons proposé une architecture novatrice d'accès multiple IM évoluant dans un canal sélectif en fréquence dans la bande Terahertz d'un environnement médical In-VIVO. Ce schéma permet d'obtenir des débits élevés tout en assurant une bonne communication dans le réseau de médecine moderne.

Mots clés: MIMO, Modulation d'indice IM, OFDM, GFDM, ZF.

Abstract:

In this thesis, we are interested in analyzing and studying the performance of the different architectures based on index modulation (IM). Extension architectures for a multi-user context are of interest, adopting CDMA-based techniques.
In order to combat channel frequency selectivity in communications that have a very high data rate, we propose to combine conventional IM with GFDM.
As a contribution, we propose an innovative scheme, based on multiple access IM, using a frequency selective channel in the Terahertz band in an In-VIVO environment. Very high data throughput can be offered while ensuring good communication in the modern medical network. The overall obtained results are considered satisfactory and open other interesting perspectives of research.

Keywords: MIMO, Index Modulation, OFDM, GFDM, ZF.

Acknowledgments

All the praises and deepest gratitude to ALLAH Almighty, the Omnipotent and the Benevolent, Who has bestowed upon me the quest for knowledge and granted unflinching determination to complete this work successfully.

I am extremely thankful to my thesis supervisor Mrs. GHANEM Khalida for providing me the opportunity to work with her, for her noble guidance, support with full encouragement and enthusiasm. I find it hard to imagine that anyone could be a better research adviser than what she has been. She is the true definition of a leader and the ultimate role model. I will never forget her sincerity and marvelous supervision helping me to grow professionally. Warmest thanks for my co-supervisor, Mr. BOUSBIA-SALAH Hicham, for facilitating my evolution during the project and within my institution, and for the valuable advices and directions. He has never failed to be present whenever needed.

For their participation in the scientific evaluation of this work, I would like to express my gratitude to the members of the jury committee.

I am grateful to Mr. ADNANE Mourad, the head of the Electronic Teaching and Research Unit, for everything he did to facilitate the administrative aspects and the coordination issues within the institution.

I also want to thank all ENP staff for all the assistance they kindly offered. I especially appreciate the interaction and suggestions from my friends and all colleagues at ENP, for whom I want to express my gratitude for their unfailing support during the six years of my studies.

I finally want to express my deep gratitude to my parents for their constant love and encouragement and for all they have sacrificed for the success of their children. It is to them that I dedicate this thesis.

Dedication

To my beloved father, mother, brothers and sisters

To all my family.

To all my friends.

To any one who ever wished me any thing good.

I dedicate this work.

Table of Contents

Acronyms

ABER	Average Bit Error Rate
ADSL	Asymetric digital subscriber line
AMPS	Advanced Mobile Phone System
AoA	Angle of Arrival
BPSK	Binary Phase Shift Keying
CDMA/FDD	Code Division Multiple Access/Frequency Division Duplex
DAB	Digital Audio Broadcasting
EGC	Equal Gain Combining
FBMC	Filter-Bank Multi-Carrier
FDMA/FDD	Frequency Division Multiple Access/Frequency Division Duplex
GSM	Global System for Mobile communications
HIPERLAN	High Performance Radio LAN
IAS	Inter-Antenna Synchronization
ICI	Inter Carrier Interference
IGCH	Information-Guided Channel-Hopping
IS-95	Interim Standard 95
IS-136	Interim Standard 136
ISI	Inter Symbol Interference
LED	Light-Emitting Diode
MAC	Media Access Control
MIMO	Multiple Input Multiple Output
MRC	Maximum Ratio Combining

OSDM	Orthogonal Space Division Multiplexing
PAM	Pulse Amplitude Modulation
PHY	Physical Layer
QAM	Quadrature Amplitude Modulation
QoS	Quality of Service
QPSK	Quadrature Phase Shift Keying
RF	Radio Frequency
TDMA/FDD	Time Division Multiplexing Access/Frequency Division
V-BLAST	Vertical Bell Labs Layered Space-Time

Symbols and Notations

Vectors and matrices

In this thesis, we will denote scalars in lower case, vectors and matrices in bold font. We will use C to represent the complex numbers. The following are the adopted notations:

$(.)^T$	The transpose operator
$(.)^*$	The conjugate operator
$(.)^H$	The conjugate transpose operator
$\|.\|_F$	The Frobenius norm of a vector/matrix
$\langle . \rangle$	The inner product in the Hilbert space
$(.)^\dagger$	The pseudo-inverse operation
$\|.\|$	The absolute value
$P(.)$	The probability of an event
$\mathrm{p}_{\mathbf{y}}(.)$	The probability density function (PDF) of a random variable
$Re\{.\}$	The real part of a complex variable
$Im\{.\}$	The imaginary part of a complex variable
$\otimes$	The time convolution operation
$\hat{x}$	The estimated value of x
$Q(.)$	The constellation quantization (slicing) function

List of figures

List of tables

Introduction

Wireless communications is, by any measure, the most rapidly growing sector of the communications industry. As such, it has attracted the attention of the media and the public. Over the last decade, cellular systems have grown exponentially and have approximately two billion users worldwide. In fact, in most developing countries, cellular phones have become an essential business tool and part of daily life, and are rapidly displacing obsolete wireline systems in many homes, businesses, campuses and other modern applications, including wireless sensor networks, automated factories, smart homes and appliances, and remote telemedicine, which are emerging from research ideas to tangible systems. Future generations of wireless communication systems demand higher transmission data rates, which lead up to the use of larger bandwidths. However, the bandwidth of a radio-frequency channel is a scarce and expensive resource. Hence, enhanced resource management and improved transmission techniques are necessary to meet the requirements of higher transmission rates.

Multiple-input multiple-output (MIMO) technology that uses multiple antennas at the transmitter and/or receiver has been demonstrated to be very helpful for providing high-data rate transmission [1], [2].

Multiple antennas can be utilized in order to accomplish a multiplexing gain, a diversity gain, or an antenna gain, thus enhancing the bit rate, the error performance, or the signal-to-noise-plus-interference ratio (SNIR) of wireless systems, respectively. The field of multiple-antenna systems, has developed rapidly, since, an enormous amount of papers were published every year.

Particularly, subjects such as transmitter and receiver structures, channel coding, MIMO techniques for frequency-selective fading channels, diversity reception and space-time coding architectures, beamforming techniques and cooperative diversity schemes, as well as practical aspects influencing the performance of multiple-antenna systems are

addressed. Compared to baseline single-antenna transmissions, MIMO communications obtain higher data rates and improved error performance at the cost of:

- The need for counteracting the interchannel interference emanating from the simultaneous transmission of many data streams from multiple antennas, increased the signal processing complexity at the receiver;
- In order to exploit the benefits of space-time-coded and multi-user MIMO transmissions, more stringent synchronization among the transmit-antennas is required;
- An increased number of multiple RF chains at the transmitter is needed to be able to simultaneously transmit many data streams.

Fueled by these considerations, index modulation (IM) has recently established itself as a promising transmission concept. Compared to traditional communication, IM exploits innovative ways to convey information, and considers as competitive candidates for next-generation wireless networks due to the attractive advantages it offers in terms of spectral and energy efficiency as well as hardware simplicity. IM uses the indices of the building blocks of the corresponding communication systems to convey additional information bits [3], thus, IM is a highly spectrum- and energy efficient yet simple digital modulation technique. In contrast to traditional modulation schemes, IM systems provide alternative ways to transmit information and have the ability to map information bits by altering the on/off status of their transmission entities such as transmit antennas, subcarriers, radio frequency (RF) mirrors, transmit light emitting diodes (LEDs), relays, modulation types, time slots and spreading codes.
Spatial modulation (SM), which considers IM for the transmit antennas of a MIMO system, has attracted tremendous attention over the past few years and introduced new directions for the implementation of MIMO systems. SM have quickly shown their true potential in terms of spectral and energy efficiency and, consequently, have been regarded as possible candidates for next-generation small/large-scale and single/multiuser, full-duplex (FD), cooperative and cognitive radio (CR) systems.

Thesis purpose

The main purpose of this thesis is to study the performance of different solutions provided by SM techniques, that have been the object of hot topics in research. This step,

based on the characteristics of the visited architectures, has allowed us to propose new SM-MIMO scheme. In this context, it is worthy to recall that a tradeoff should be realized between the BER performance, power dissipation, spectral efficiency and complexity of the used schemes. Keeping this in mind, it is interesting to know what would be the performance of SM in extremely critical conditions such as spatial correlations as well as other channel impairments.
According to our knowledge no such study, under the specified scenarios, has been carried out previously. The other novelty of this work is to propose a new multiuser SM-OFDM-based scheme thus suitable for wireless communications over frequency selective channels. We propose to embed the novel spatial modulation technique with code division multiple access (CDMA) architecture in an OFDM framework to ensure a viable communication in in-VIVO frequency selective Nano channels. The immunity of our proposed solution to such an interference is confirmed. This hybrid scheme is shown to efficiently combat the multiple channel-interference (MCI) while enabling a safe retrieval of the useful signal at the very-high data rate communications.

Thesis outline

This thesis is organized as follows: The first chapter discusses the fundamentals of wireless communications, spanning the different generations of mobile communications, then the technical concepts pertaining to transmission in general and MIMO systems in particular are presented, followed by summarizing of the main advantages brought by these systems. The concepts behind multicarrier data transmission techniques and channel environment were also illustrated.

The second chapter is dedicated to the description of the complete framework of index modulation (IM) families where firstly the global SM-MIMO scheme is introduced along with its advantages and disadvantages, and secondly the detection and performance analysis aspects are visited, which obviously, are, a very important aspect in any wireless communication system. The scheme of SM-MIMO introduced in this chapter is extended to the frequency selective channel scenario, giving rise to SM-OFDM alternative. Some concluding remarks are drawn after discussing the simulation results.

In the third chapter, new SM solutions in the presence of multiple users communicating in frequency selective channels should be targeted. To fulfill such a need, a new SM-based architectures incorporating OFDM and CDMA are proposed. In addition, other SM-multicarrier transmission data techniques like (GFDM and OTFS) are also presented. The performance of SM-OFDM architecture is studied over Nakagami-m fading channel when using QAM modulation. In addition to the space correlation encompassed in Nakagami model, the performance is also investigated in the presence of a spatial correlation and the availability of only imperfect channel state information (CSI). Included in the chapter also are some simulations results we run of this novel architectures.

In the last chapter, after analyzing the performance of the most known SM-OFDM-MIMO architectures, we propose a new multiple access scheme based on spatial modulation and code division multiple access in In-VIVO environment which meets the requirements of future generations of health mobile networks. The targeted objective is to address the realistic scenario of the dense deployment of numerous nano-sensors within the human body, and propose a scheme combating the effect of path loss and multiple access interference in THz frequencies while supporting a large number of receive devices, maintaining the required quality of service (Qos) per device, and keeping the hardware complexity as simple as possible. One major problem faced with the deployment of this breakthrough technology, in addition to the very high path loss and molecular absorption noise, is the resulting high level of multiuser interference. As compared with classical designs, the robustness of the resulting architecture to the multiple access and multipath fading interferences has been confirmed.

CHAPTER 1

Chapter 1: Fundamentals of Wireless Communication Systems

1.1 Introduction

Nowadays, wireless communication networks have invaded all the aspects of modern life. A lot of applications illustrate the growth in the use of these technologies, among them the introduction of the android operating system and the iPhone, the adoption of ebook readers such as the iPad, and the social networking. Consequently, the demand for high data-rate transmissions has increased significantly in these last years; leading to new challenges in terms of cellular data traffic quality encompassing high data rates and increased level of security, which have become a critical tools of everyday life.

1.2 History of wireless communication systems

In this section, a brief overview of the history of wireless communication systems is presented.

1. **1G: First Generation networks**
   The main technology of this first generation mobile system was involving FDMA/FDD protocols and analog FM. AMPS was the first U.S. cellular telephone system and was deployed in Chicago in 1983.

2. **2G: Second Generation networks**
   The difference between the first and second generations is the introduction of digital modulation techniques using either the combination TDMA/FDD or CDMA/FDD. The 2G systems introduced three popular TDMA and one popular CDMA standards in the market. These are as follows:

   - **TDMA/FDD standards**
     - *GSM*: global system for mobile communication (GSM) standard was the first digital mobile system utilizing the 900 MHz frequency band that is introduced by Group Special Mobile [4]. In its early version, the initial GSM had a particular amount of resources such as 200 KHz radio channels, 8 full-rate or 16 half-rate TDMA channels per carrier, encryption of speech, low speed data services and support for SMS for which it gained a quick popularity.
     - *IS-136*: known also as North American digital cellular (NADC) system. The objective of using this system was mainly to increase the capacity over the earlier analog (AMPS) system by utilizing 3 full-rate TDMA users over each 30 KHz channel.
     - *PDC*: this technology aimed at improving the spectrum utilization and was created as a counterpart of NADC system in Japan.
     - **CDMA/FDD Standard**
       IS-95: the IS-95 standard, known as CDMA/One, uses 64 orthogonally coded users and code-words are transmitted simultaneously on each of the 1.25 MHz channels. This standard provides many services such as:

short messaging service, slotted paging, over-the-air activation (meaning the mobile can be activated by the service provider without any third party intervention), enhanced mobile station identities etc.

3. **2.5G mobile networks**

   2.5G standard is developed to support modern internet applications, thereby making 2G standards more advanced and compatible with the requirements of increased data rates. The most used services in this standard are:

   - Supporting higher data rate transmission for web browsing;
   - Supporting e-mail traffic;
   - Enabling location-based mobile service.

   The main technologies relying on 2.5G systems were: wireless application protocol (WAP), general packet radio service (GPRS), high speed circuit switched data (HSCSD), enhanced data rates for GSM evolution (EDGE) etc.

4. **3G: Third Generation networks**

   3G networks were developed to obtain more data rates and high speed for internet and video access. Based on IMT-2000 proposal launched by international telecommunication union (ITU), a set of technical requirements were defined in 1997 [5], and can be summarized as:

   - High data rates: 144 kbps in all environments and 2 Mbps in low-mobility and indoor environments,
   - Symmetrical and asymmetrical data transmission,
   - Circuit-switched and packet-switched-based services,
   - Speech quality comparable to wire-line quality,
   - Improved spectral efficiency,
   - Several simultaneous services to end users for multimedia services,
   - Global roaming,
   - Open architecture for the rapid introduction of new services and technology.

Universal mobile telecommunications system (UMTS), based on WCDMA and operating at 2.1GHz [6], was defined by the third Partnership Project (3GPP) organization and it is considered as the most popular technology in third generation standard.

5. **4G: Fourth Generation networks**

   A massive increase in users' mobile number has led researchers and industries to explore the next generation of mobile wireless technology. Thus, high speed, high quality, high capacity and low cost services were the main objectives of 4G technology. 4G, for example, is an all internet protocol (IP) based network for voice, multimedia and internet with the ability of providing high-speed data rates up to 1 Gbits/s in the downlink and 500 Mbits/s in the uplink. It improves the spectral efficiency and reduces the latency, meeting the requirements set by advanced applications like digital video broadcasting (DVB), high definition TV content and video chat. Moreover, through automatic roaming across geographic boundaries of wireless networks, 4G enables mobile terminal to provide wireless services at anytime and anywhere. Long term evolution-advanced (LTE-A) and wireless interoperability for microwave access (WiMAX) are considered as 4G standards [7]. LTE integrates existing and new technologies such as coordinated multiple transmission/reception (CoMP), multiple-input multiple-output (MIMO), and orthogonal frequency division multiplexing (OFDM).

6. **5G: Fifth Generation networks**

   Compared to the current 4G mobile networks, 5G networks are expected to support an enormous system capacity, much less latency, and about 1000 times more devices per squared kilometer, among other specifications. To satisfy these requirements, several new technologies have been suggested and are being developed for 5G networks and beyond. These technologies include but are not limited to: massive MIMO, software-defined networking, mm-Wave, cloud radio access network (cloud-RAN), non-orthogonal multiple access, machine to machine (M2M) communications, mobile edge computing, wireless caching, ultra-dense networks, and full-duplex communications.

7. **6G: Sixth Generation networks**

   Currently, 5G is entering the commercial deployment phase, the researchers of

the worldwide have begun to pay attention to 6G, which is considered to be deployed approximately in 2030. One of the expectations of 6G is to improve the performance of information transmission peak data rates up to 1 Tbps and ensure ultra-low latency in microseconds. It features terahertz frequency communications and spatial multiplexing, providing as much as 1000 times higher capacity than 5G networks. The aim of 6G is to achieve ubiquitous connectivity by emerging satellite communication networks and underwater communications to provide global coverage [8]. The system energy efficiency is improved by the utilization of new materials and energy harvesting technologies, which realize sustainable green networks. Fig. 1.1 illustrates the evolution of mobile networks, elaborating key features of each mobile network generation. Envisaged 6G requirements, vision, enablers, and applications are also highlighted to formulate an overview of the present understanding of 6G.

Figure 1.1 — An overview from 1G to 6G [9].

1.2.1 Why is there a need for 5G and beyond communications?

Fifth generation standard is expected to provide a very high transmitting data traffic and to remove some limitations encompassed in the generations mentioned above. The following are the requirements summarizing the major differences between 5G and other generations [10]:

- More possible interoperability and compatibility between the current global operators and their equipements.

- The utilization of sophisticated, innovative and improved data coding and modulation techniques, within the schemes.
- Feasible use of millimeter wave frequencies.
- One common used platform to make 5G standard more practical for all sorts of radio access technologies.
- Large area coverage with an increased throughput at cell edge.
- Multiple concurrent data transfer paths.
- Possible data rates in mobility up to 1 Gbps and higher.
- More robust; better cognitive radio security.
- Higher system level spectral efficiency.
- World wide wireless web (WWWW), wireless-based web applications that include full multimedia capability beyond 4G speeds.
- More developed applications combined with artificial intelligence (AI) provided by artificial sensors.

1.2.2 5G spectrum and mm-wave Band

In order to reach the Gbps level data rates, the operators need to a aggregate licensed and unlicensed spectrum (via license-assisted access). Indeed, the spectral range 5.15-5.925 GHz (band number 46 B46) is designed to achieve that purpose [11], and for the frequency bands below 6 GHz, 5G has a maximum and limited bandwidth of 100 MHz. Note that large bandwidth can provide an increased data rate, but lower bandwidths can also deliver 5G services. Moreover, the citizens broadband radio service (CBRS) spectrum is utilized as another option besides traditional licensed and unlicensed (5-5.9, 64-71 GHz) spectrum usage. The CBRS spectrum range is 3.55-3.7 GHz (totaling 150 MHz of bandwidth) and is governed by a three-tiered spectrum authorization framework to serve users on a shared basis with incumbent federal and non-federal users of this band. A summary of the issues that need to be considered in using 5G frequency bands is given in Fig. 1.2.

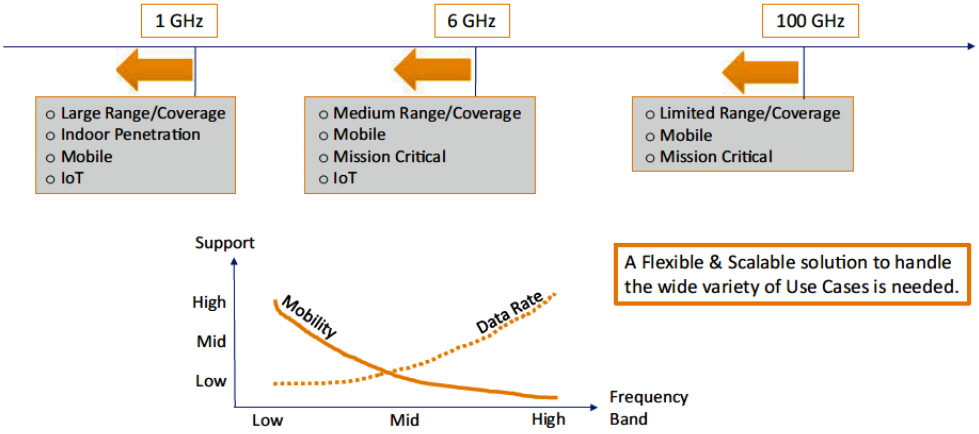

Figure 1.2 — 5G frequency band considerations.

Furthermore, the availability of paired spectrum to support FDD is minimal in this new frequency bands, hence, the industry is constrained to focus more on TDD deployments, and we do not only expect the bandwidth availability to vary across the low (<1 GHz), medium (<6 GHz), and high (>6 GHz) frequency bands, but we should also expect the duplex method to also vary. In the aim to provide high-speed 5G applications (approximately 1Gbps), some operators adopt fixed wireless access, in place of cable/fiber deployments as initial 5G schemes, in mm-Wave bands instead of/in addition to mobile broadband services. This approach will help develop a mm-wave-based ecosystem that will enable 5G technologies, which in their turn, allow the operation of battery operated devices. Some of the new frequency bands being considered in 5G new radio (NR) categorized by region is given in Table 1.1. Operators and equipment manufacturers are faced with various options to identify spectrum (re-farm, acquire new, partner, etc.). We see reasonable convergence (toward global harmonization) around the 3-4 GHz frequency bands around the world and, at the moment, less so in the USA.

Region	Freq.band (<6GHz)	<6GHz bandwidth	Freq.band (>6GHz)	>6GHz bandwidth
Europe	3.4-3.8	400MHz	24.25-27.35	3.1GHz
China	3.3-3.6	300MHz		
Japan	3.6-4.2	800MHz	27.5-29.5	2GHZ
Korea	3.4-3.7	300MHz	26.5-29.5	3GHz
United States	3.55-3.7	150MHz	27.5-28.35	0.85GHz

Table 1.1 — New 5G frequency bands [12]

1.2.3 Six requirements and key performance measures for 6G

The array of modern applications we expect to see by 2030 and beyond will lead to the new requirements that need to be reached by 6G. The 5G key performance indicators (KPIs) will continue to be important measures for 6G performance, the KPI are: data throughput, capacity, latency, reliability, scale and flexibility. Some new features are also important for 6G. We group the requirements for 6G into six categories in figure. 1.3, among which three are similar to the KPIs of 5G and three are new:

- Sensing using communication network and localization will be important features of 6G. Precision and accuracy are considered as the most corresponding performance measures for localization and sensing, respectively. The centimeter level precision is assumed to be reached. On the other hand, object sensing accuracy can be measured in terms of missed detection (MD) and false alarm (FA) probabilities and parameter estimation errors.

- The network will be engineered with distributed artificial intelligence/machine learning (AI/ML) techniques embedded in various nodes, and the speed at which they adapt to new conditions in the network is an important measure. Network automation will be the norm, thus how close a network is to complete automation with zero manual intervention will be another criterion.

- Finally, a major revolution in the end device in the time-frame of 6G is expected. Hence, we introduce few characteristics under the device category to sort out the essential transitions that we target. First, we believe that the end device will be developed in many scenarios to become a network of devices or a sub-network.

1.2.4 6G enabling applications:

Five application scenarios are envisaged to be supported by 6G communications: enhanced mobile broadband plus (eMBB-Plus), big communications (BigCom), secure ultra-reliable low-latency communications (SURLLC), three-dimensional integrated communications (3D-InteCom), unconventional data communications (UCDC). These application scenarios are illustrated in Fig. 1.4.

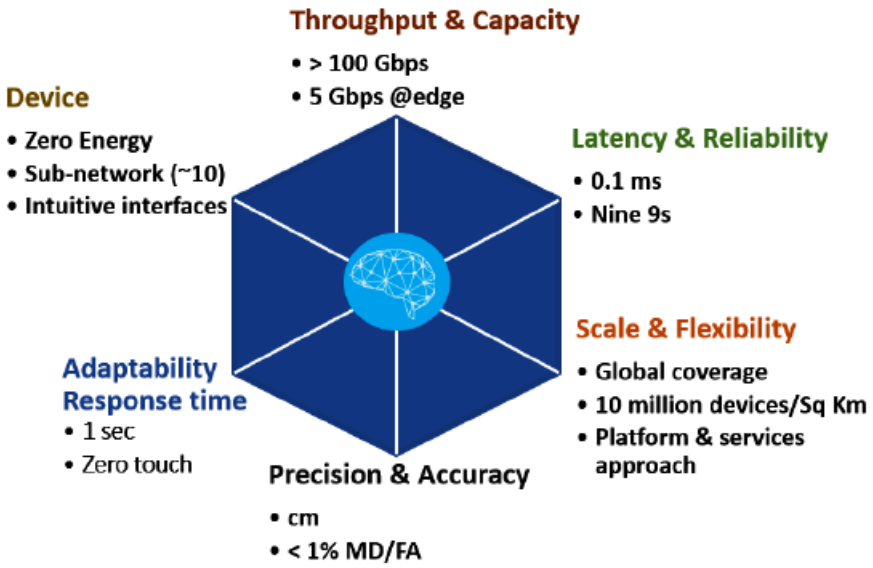

Figure 1.3 — Key requirements and characteristics of 6G [13].

The eMBB-Plus in 6G is the successor of the eMBB in 5G, serving the conventional mobile communications with much higher requirements and standards. In fact, the eMBB-Plus is expected to be more capable of optimizing the cellular networks in terms of interference, hand-over, as well as big data transmission and processing. Additional

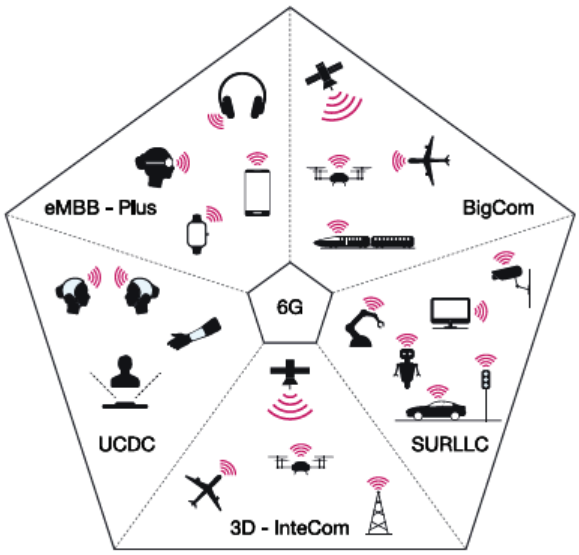

Figure 1.4 — Five application scenarios supported by 6G communications [14].

services will also be furnished to subscribers at a reasonable expense, e.g., accurate indoor positioning and globally compatible connection among diverse mobile operating networks. Note that, special attention to security, secrecy, and privacy must be paid to the eMBB-Plus communication services. Different from 5G which focuses on extremely

good communication services in densely and populated areas but to some extent neglects the service in remote surfaces, the BigCom in 6G takes into consideration the service fairness between dense and remote areas. Nevertheless, the BigCom does not intend to provide the best performance in both areas, but it should maintain a good resource balance to be more feasible. Hence, the BigCom ensures to keep an acceptable data service to cover the area that must be large enough, wherever the communication subscribers are living or moving to. The mMTC in 5G is combined with URLLC to form the SURLLC in 6G, but with higher requirements of reliability (higher than 99.9999999 %), and latency (less than 0.1 ms) [15], , as well as an additional demand on security. The SURLLC has many functionnalities, it serves the industrial and military communications, e.g., a variety of robots, high-precision machine equipments, vehicular communications, and transmission systems in the 6G era.

Features	1G	2G	3G	4G	5G	6G
Period	1980-1990	1990-2000	2000-2010	2010-2020	2020-2030	2030-2040
Maximum rate	2.4 kbps	144 kbps	2 Mbps	1 Gbps	35.46 Gbps	100 Gbps
Maximum frequency	894 MHz	1900 MHz	2100 MHz	6 GHZ	90 GHz	10 THz
Service level	Voice	Text	Picture	Video	3D VR/AR	Tactile
Standards	MTS, AMPS, IMTS, PTT	GSM, IS-95, CDMA, EDGE	UMTS, WCDMA, IMT2000, CDMA2000, TD-SCDMA	WIMAX, LTE, LTE-A	5G NR, WWWW	-
Multiplexing	FDMA	FDMA-TDMA	CDMA	OFDMA	OFDMA	Smart OFDMA plus IM
Architecture	SISO	SISO	SISO	MIMO	Massive MIMO	Intelligent surface
Core network	PSTN	PSTN	Packet N/W	Internet	Internet /IoT	IoE
Highlight	Mobility	Digitization	Internet	Real-time streaming	Extremely high rate	Security-secrecy-privacy

Table 1.2 — Detailed comparisons from 1G to 6G communications [14]

Satellite UAV, and underwater communications can be examples of the three-

dimensional scenario, planning and optimization, which can be supported by the SURLLC. Accordingly, the analytical framework constructed for two-dimensional wireless communications stemmed from stochastic geometry and graph theory needs to be updated in the era of 6G [16]. Considering the node height also enables the implementation of elevation beamforming with full-dimensional MIMO architectures, which provides another direction for network optimization [17]. We give detailed comparisons from 1G to 6G communications in the table. 1.2.

1.3 The wireless channel: propagation and limitations

1.3.1 Radio propagation

The performance of wireless communication systems is mostly dominated by the wireless channel propagation. The wired channel is usually static and predictable; in contrast, the wireless channel is rather dynamic and unpredictable, which makes a precise analysis of the wireless communication system more difficult. In last few years, with the rapid growth of mobile communication and emerging broadband internet access services, the optimization of the performance of the wireless communication systems has become crucial and indispensable. Indeed, the understanding of wireless channels will conduct the foundation for the development of high performance and bandwidth-efficient wireless transmission technology. Radio propagation refers typically to the behavior of radio waves when they are propagated from the transmitter to the receiver side, and affected by three different modes of physical phenomena: reflection, diffraction, and scattering [16, 18].

- Reflection occurs when a propagating electromagnetic wave impinges upon an object with very large dimensions compared to the wavelength, for example, surface of the earth and building. The transmit signal power is constrained to be reflected back to its origin rather than being passed all the way along the path to the receiver.

- Diffraction occurs when the radio path between the transmitter and the receiver is obstructed by a surface with sharp irregularities or small openings. It appears

as a bending of waves around the small obstacles and spreading out of waves past small openings. Moreover, when a line-of-sight path is not present, the secondary waves generated by diffraction established a path between the transmitter and receiver.

- Scattering forces the radiation of an electromagnetic wave to deviate from a straight path with small dimensions compared to the wavelength, induced by one or more local obstacles such as foliage, street signs, and lamp posts, which are referred to as the scatters.
  Furthermore, the propagation of a radio wave is complicated when affected by the three physical phenomenas, which intensity varies with different environments at different instances.

1.3.2 Limitations of wireless communication

1. **Fading and interference**:

   In wireless communication, there are two fundamental aspects that limit their performances. First is the phenomenon of fading: the time variation of the channel strengths due to the small-scale effect of multipath fading, as well as larger-scale effects such as path loss via distance-dependent attenuation and shadowing by obstacles. Second, the significant interference that can be generated since wireless users communicate over the air, it can be between transmitters communicating with a common receiver (e.g., uplink of a cellular system), between signals from a single transmitter to multiple receivers (e.g., downlink of a cellular system), or between different transmitter-receiver pairs (e.g., interference between users in different cells). Figure. 1.5 classifies the types of fading channels. As mentioned above, the fading phenomenon can be broadly classified into two different types: large-scale fading and small-scale fading.

   - **Large-scale fading:** occurs as the mobile moves through a large distance, for example, a distance of the order of the cell size [16]. It is caused by path loss of the signal as a function of distance and shadowing by large objects such as buildings, intervening terrains, and vegetation. In other words,

large-scale fading is characterized by average path loss and shadowing.

- **small-scale fading:** refers to the rapid variation of signal levels due to the constructive and destructive interference of multiple signal paths (multi-paths) when the mobile station moves short distances. Depending on the relative extent of a multipath phenomenon, frequency selectivity of a channel is evaluated (e.g., by frequency-selective or frequency flat) in small-scaling fading. Similarly, depending on the time variation in a channel due to the mobile device speed (characterized by the Doppler spread), short-term fading can be classified as either fast or slow.

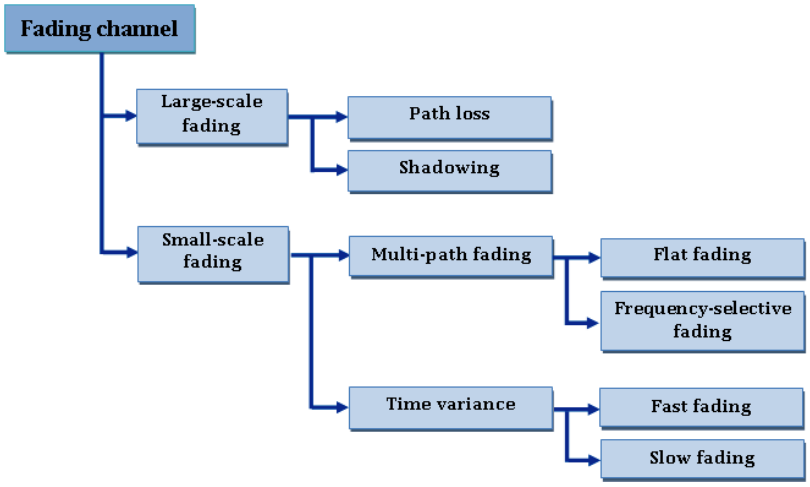

Figure 1.5 — Classification of fading channels.

2. **Path-loss attenuation:**

The radio wave propagation losses taking place on a signal's path from the transmitter to the receiver, this phenomenon is called: path-loss or large-scale fading. The radio link's path-loss value is considered as one of the most important input parameters for a design of any radio communication architecture. Path-loss includes the propagation losses caused by the natural expansion of the radio wave front in free space path-loss includes the propagation losses caused by the natural expansion of the radio wave front in free space (which usually takes the shape of an ever-increasing sphere), absorption losses (sometimes called penetration losses), diffraction losses when part of the radio wave front is obstructed by an opaque obstacle, and losses caused by other phenomena as described in Fig. 1.6.

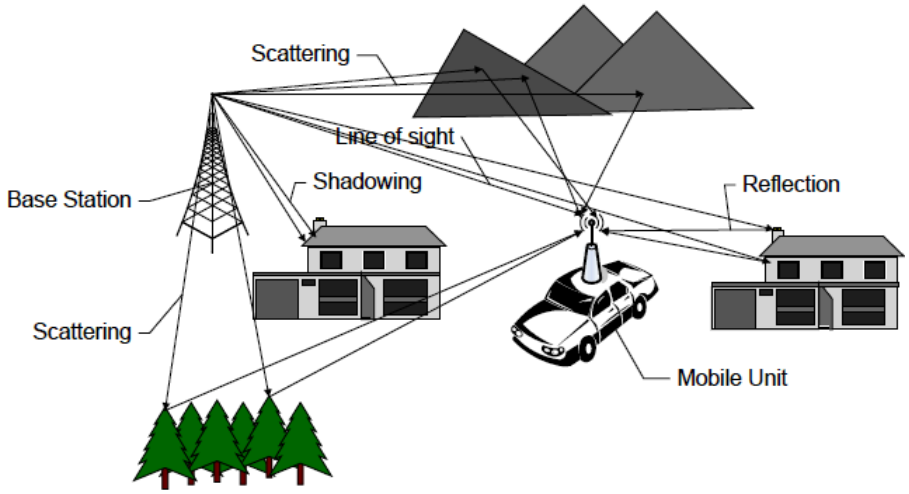

Figure 1.6 — Multipath propagation in a terrestrial mobile radio environment.

The path-loss attenuation between the transmitter and the receiver separated by a distance d is modeled as follows [19, 20]:

$$PL = A + 10\zeta log_{10}\ (d/d_0) + \xi \quad [dB] \tag{1.1}$$

where A is the free space loss measured at a reference distance d_0 and is given by: $A = 20log_{10}(4\pi d_0/\lambda)$, and λ is the wavelength. The quantity ζ is a function of the environment between the transmitter and the receiver. ξ is the log normal shadowing variable and is utilized in practice for the design and analysis of the system as a tool to provide the received powers [20, 21].

1.3.3 Small-scale propagation models

Small-scale fading models describe the rapid fluctuation of the amplitude of the transmitted signal, which is caused by the interference between more than one copy of the transmitted signal, arriving at slightly different times. These copies are called multipath components. Multipath is caused by the presence of reflectors, for example the ground and surrounding structures, and has several effects on small scale MIMO systems [22]:

- Rapid changes in the signal strength.
- Random frequency modulation.

- Time dispersion.

Small-scale fading models are influenced by many factors including,

- **Multipath propagation:** the multipath components are summed constructively and destructively at the receiver, and because of that, the received signal might get distorted or fade.

- **Speed of the mobile:** the relative motion between the transmitter and the receiver causes a shift in frequency to each multipath wave. This shift in frequency is called Doppler shift.

- **Speed of surrounding objects:** the speed of the surrounding objects can vary the Doppler shift in time.

- **The transmission bandwidth of the signal:** as it will be shown later, the bandwidth of the transmitted signal determines if the signal is subject to fast or slow, flat or frequency selective fading.

1.3.4 Parameters of small-scale propagation models

Small-scale propagation models have several parameters. Two of them are needed to determine the type of small scale fading:

- **Doppler shift:** the movement of the transmitter or receiver nodes results in a change in the frequency of the received signal. This change is given by,

$$f_D = \frac{\upsilon}{\lambda} cos\phi \tag{1.2}$$

  where υ is the velocity of the moving node, ϕ is the angle between the signal and the direction of moving node, $\lambda = \frac{c}{f_c}$ is the wavelength where c is the speed of light, and f_c is the carrier frequency.

- **Coherence time:** the coherence time is the time during which the channel impulse response can be considered static, and it is the time domain dual of Doppler spread. Its expression is given by:

$$T_c = \frac{1}{f_{D_{max}}} \tag{1.3}$$

where $f_{D_{max}} = \frac{\upsilon}{\lambda}$ is the maximum Doppler shift.

- **Coherence bandwidth:** it is the range of frequencies over which the channel frequency response can be considered static.

1.3.5 Types of small-scale propagation models

Fading channels can be classified, based on their multipath time delay into flat and frequency selective, and based on Doppler spread into slow and fast. These two phenomena are independent and result in the following fading types [18]:

- **Slow fading:** a channel is classified as slow fading when the coherence time is larger than the symbol period, and the channel impulse response changes at a rate much slower than the transmitted baseband signal, which means that the channel can be considered static during the symbol period. In the frequency domain, this implies that the Doppler spread of the channel is much less than the bandwidth of the baseband signal.

- **Fast fading:** in a fast fading channel, the coherence time is smaller than the symbol period of the transmitted signal. In this case the channel varies within the symbol period. This causes frequency dispersion (also called time selective fading) due to Doppler spreading, which leads to signal distortion. Viewed in the frequency domain, signal distortion due to fast fading increases with increasing Doppler spread relative to the bandwidth of the transmitted signal. Figure 1.7 shows a tree of the two different types of fading.

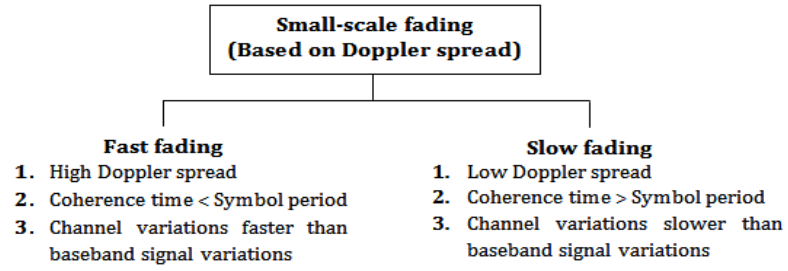

Figure 1.7 — Classification of small scale fading based on Doppler spread.

- **Flat fading:** if the mobile radio channel has a constant gain and linear phase response over a bandwidth (coherence bandwidth) which is greater than the bandwidth of the transmitted signal, then the received signal will undergo flat fading. This type of fading is the most common type of fading. In flat fading, the multipath structure of the channel is such that the spectral characteristics of the transmitted signal are preserved at the receiver.

- **Frequency selective fading:** frequency selective fading is created when the channel possesses a constant-gain and a linear phase response over a bandwidth that is smaller than the bandwidth of transmitted signal. Under such conditions, the channel impulse response has a multipath delay spread which is greater than the reciprocal bandwidth of the transmitted message waveform. When this occurs, the received signal includes multiple versions of the transmitted waveform which are attenuated (faded) and delayed in time, and hence the received signal is distorted. Frequency selective fading is due to time dispersion of the transmitted symbols within the channel. Thus the channel induces intersymbol interference (ISI). Frequency selective fading channels are much more difficult to model than flat fading channels since each multipath component must be modeled and the channel must be considered to be a linear filter. Figure 1.8 summarizes the two different types of fading.

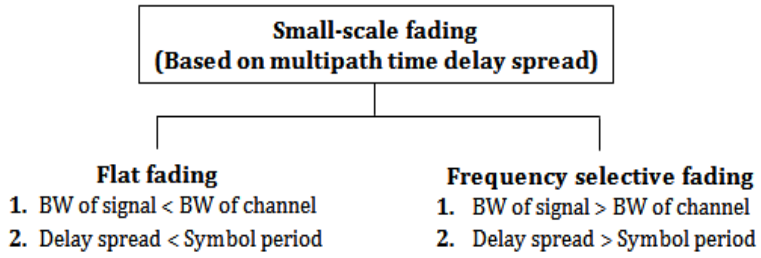

Figure 1.8 — Classification of small scale fading based on time delay spread.

On the other hand, when a channel is specified as experiencing a fast or slow fading, it does not specify whether the channel is flat fading or frequency selective in nature. Fast fading only deals with the rate of change of the channel due to motion. The relation between the various multipath parameters and the type of fading experienced by the signal are summarized in figure 1.9.

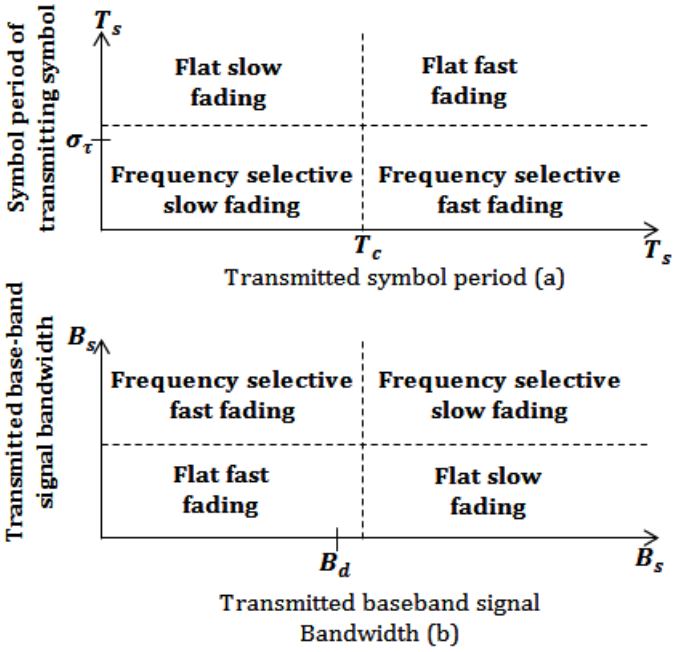

Figure 1.9 — Summarize of the types of fading experienced by the signal.

For the rest of this thesis, we consider slow flat fading MIMO channels, unless mentioned otherwise, such as in chapter (chapter IV).

1.3.6 Slow Flat Fading MIMO Systems

Depending on the nature of the propagation environment, there are different models to describe the behaviour of the MIMO channel.

- **Rayleigh Fading:** the Rayleigh distribution is often used to model non-line of sight (NLoS) channels, where the received signal is visualised as a sum of independent vectors with uniformly distributed phases [23, 24]. Therefore, the entries of the transfer function **H** are modelled as complex, identical and independently distributed (i.i.d.) Gaussian random variables with zero mean and unit variance σ_h^2. In fact, the name Rayleigh fading comes from the distribution of the envelope $\eta = |h(n)|$, which is a Rayleigh distribution:

$$f_\eta(\eta) = \frac{2\eta}{\sigma_h^2} \exp\left(\frac{-\eta}{\sigma_h^2}\right), \eta \geq 0 \tag{1.4}$$

- **Rician Fading:** the channel amplitude gain is characterized by a Rician distribution and exhibited Rician fading if a LOS (line-of-sight) path exists between

the transmit and receive antennas. The Rician fading MIMO channel matrix can be modeled as the sum of the fixed LOS matrix and a Rayleigh fading channel matrix as follows [25]:

$$\mathbf{H}_{Rician} = \sqrt{\frac{K}{1+K}}\bar{\mathbf{H}} + \sqrt{\frac{1}{1+K}}\mathbf{H} \tag{1.5}$$

where $\sqrt{\frac{K}{1+K}}\bar{\mathbf{H}}$ is the LOS component, $\sqrt{\frac{1}{1+K}}\mathbf{H}$ is the fading component, and K is the Rician K-factor, which is defined as the ratio of the LOS and the scatter power components and $\bar{\mathbf{H}}$ is a matrix with all elements being one.

- **Nakagami-m Fading:** Nakagami-m distribution is widely used to describe channels with severe to moderate fading [26]. The main justifications for the use of the Nakagami-m model lie in its appropriateness in fitting the empirical fading data, and in well reproducing the channel when maximum ratio combining (MRC) is used at the receiver [27].

  The few research works addressing the performance of SM-based systems adopt Rayleigh distribution for the channel fading. However, Rayleigh distribution fails to fit the channel behavior over long distances and high frequencies, Nakagami then suggested a parametric gamma distribution-based density function, to describe the experimental data he obtained. Later, it was also shown by different researchers that real-life data was best fitted by the model provided by Nakagami. Basically, Rayleigh distribution is sufficient to model amplitude in urban areas, whereas, Rician distribution suits better sub-urban areas where LOS components exist. By contrast, Nakagami-m distribution is a generalized case which includes different distribution cases. From [28], the envelope of the Nakagami-m fading channel is shown to be distributed according to the law:

$$f_{|\omega_l|}(x) = \frac{2}{\Gamma(m_l)}(\frac{m_l}{\Omega_l})^{m_l} x^{2m_l-1} exp(-\frac{m_l}{\Omega_l}x^2) \quad l = \{1, 2, ..., L\} \tag{1.6}$$

where L is the number of paths, $\Gamma(\cdot)$ is the gamma function defined as $\Gamma(m) = \int_0^\infty x^{m-1}e^x dx$. The parameter $m \geq \frac{1}{2}$ verifies the relation and indicates the fading severity, while $\Omega_l = \varepsilon\{|\omega_l|^2\}$ designates the mean-square value of the l^{th} path signal and ω_l represents the multipath gain. A variety of fading conditions are

generated by varying the fading or Nakagami scale parameter m_l. For critical cases which are represented in Fig. 1.10, we have:

- ⋆ $m_l = \frac{1}{2}$ represents one sided Gaussian channel with PDF $f_{|\omega_l|}(x) = \sqrt{\frac{2}{\pi\Omega_l}} exp(-\frac{x^2}{2\Omega_l})$.
- ⋆ $m_l = 1$ describes equivalent Rayleigh fading channel with PDF $f_{|\omega_l|}(x) = \frac{2x}{\Omega_l} exp\frac{-x^2}{\Omega_l}$, there is no single line-of-sight path for this distribution, it can cause severe distortion or fading.
- ⋆ $m = 1.5$, in this case, a LOS path exists, the fluctuations of the signal strength are reduced compared to Rayleigh fading; hence, Nakagami tends to Rician distribution.
- ⋆ For $m_l = \infty$, the Nakagami-m fading channel converges to a non fading AWGN with a PDF $f_{|\omega_l|}(x) = \delta(x - \Omega_l)$.

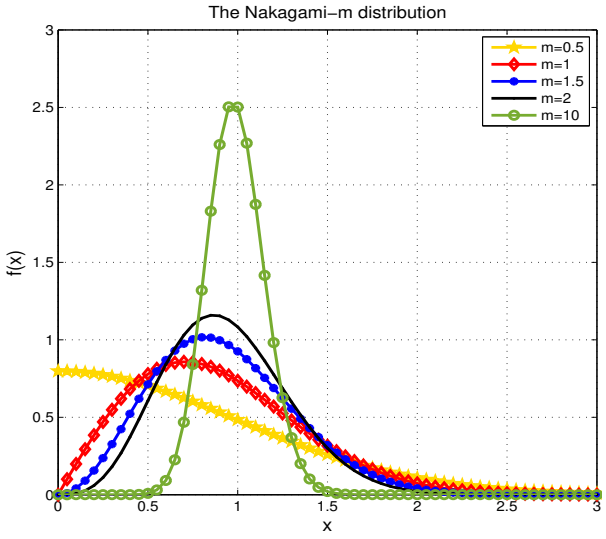

Figure 1.10 — Nakagami-m distribution.

1.4 MIMO communication systems

According to the number of transmit antennas (Tx) and the number of receive antennas (Rx), wireless systems can be classified as single input single output (SISO), single input multiple output (SIMO), multiple input single output (MISO) and multiple

input multiple output (MIMO) systems, where the input and output are with respect to the wireless channel coefficients between the transmitter and the receiver as shown in figure 1.11.

The advantages of employing multiple antennas include:

- **Array gain:** to achieve more effective gain, the copies of the signals received by more than one antenna can be combined coherently using methods such as MRC and equal gain combining (EGC) [29].

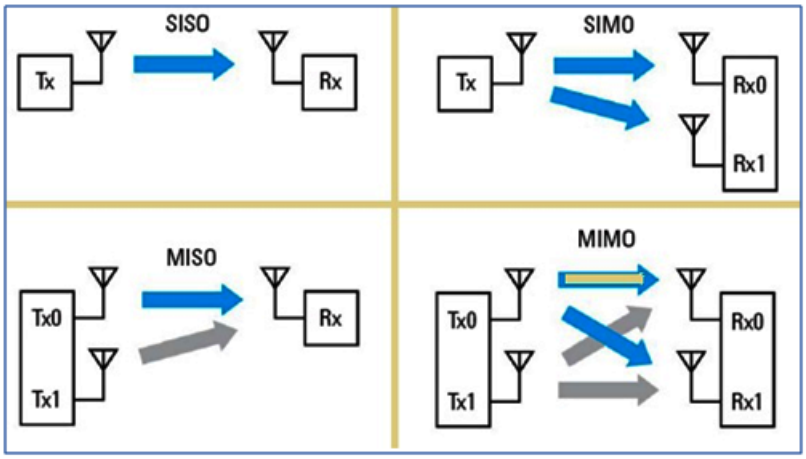

Figure 1.11 — Illustration of transmitters/receivers with different antenna configurations [30].

- **Diversity gain:** the channel fading is combated, and the signals can be transmitted and/or received with diversity when using multiple transmit and/or multiple receive antennas, in contrast, in SISO system and without redundancy, the signals suffer from a deep fading rendering the detection difficult.

- **Capacity gain:** an increase in data rate can be achieved in MIMO transmission techniques by emitting multiple data streams from different antennas. The achieved gain is called spatial multiplexing (SMX) and depends on the number of transmit and receive antennas.

- **Beamforming gain:** transmitting the signals from different angles and combining them at the receiver may create a differentiation in gains for those signals. A beam directed to the receiver along the intended transmitter while suppressing

interference from the other directions can increase the antenna gain and is known as beamforming [31].

Because of the aforementioned provided advantages, the researchers have actively studied MIMO technology, both in theory and in implementation [32].

1.5 MIMO techniques

MIMO systems can be classified as co-located MIMO or distributed MIMO systems, as summarized in figure 1.12.

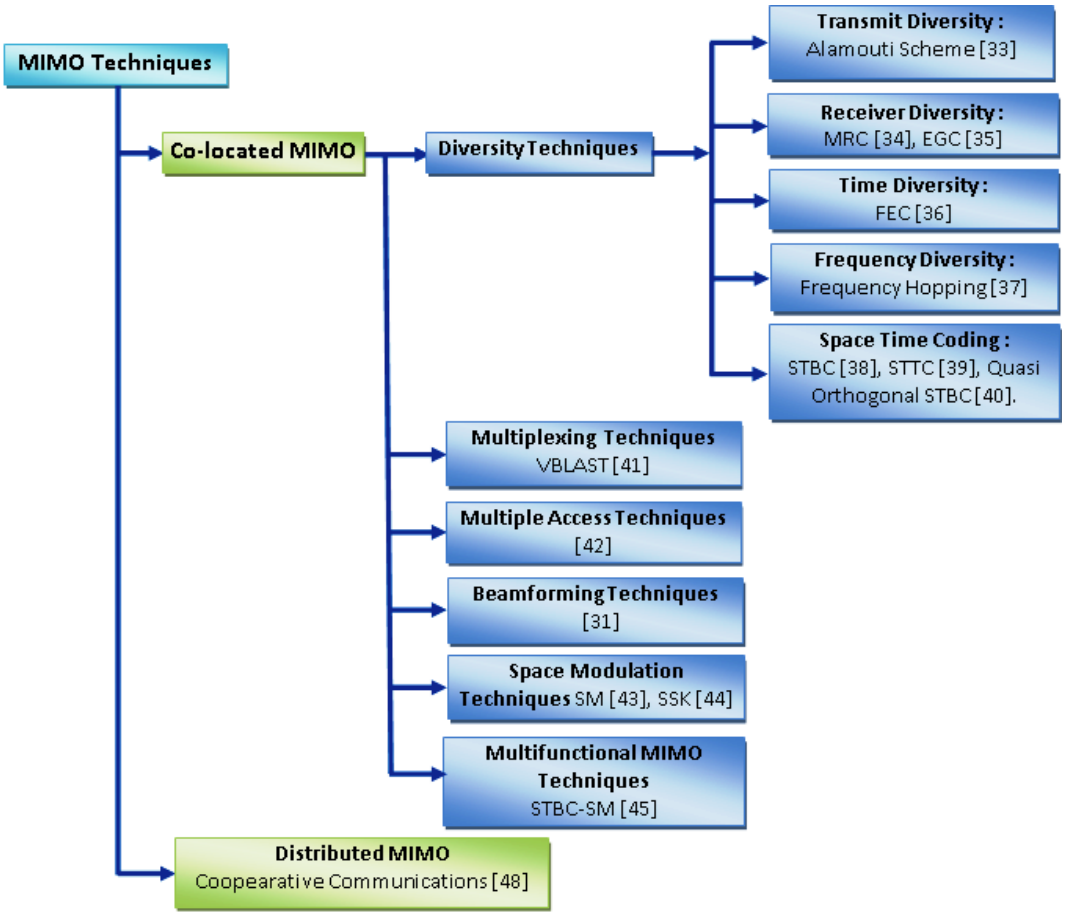

Figure 1.12 — Classification of MIMO systems.

1. **Co-located MIMO systems:** when the multiple antennas are located at the same transmitter or receiver nodes, the scheme is referred as a co-located MIMO system. This latter may be adopted for different purposes which are listed below.

- **Diversity techniques:** in MIMO-based scheme, the diversity occurs when creating independent fading copies of the same transmitted signal in time, frequency, or spatial domains and both at the transmitter and the receiver sides.

  MIMO diversity techniques can be categorized into:

  - ⋆ **Transmit diversity :** transmit diversity is achieved by transmitting copies of the same data symbol over multiple antennas. Alamouti scheme uses this category and is widely adopted [33].
  - ⋆ **Receiver diversity :** receiver diversity is attained by having multiple antennas at the receiver while exploiting techniques such as MRC [34], EGC [35].
  - ⋆ **Time diversity:** time diversity can be achieved by transmitting the same data symbol multiple times, or by adding redundant bits to the original data bits where they are transmitted at different time instances [36].
  - ⋆ **Frequency diversity :** frequency diversity can be reached by emitting the same data symbol at sufficiently separated transmit frequency bands [37].
  - ⋆ **Space time coding (STC):** STC systems diversity is achieved by transmitting the same data from different transmit antennas and different time instances. Typical examples are STBC in [38], STTC in [39], and Quasi Orthogonal STBC [40].

- **Spatial multiplexing techniques (SMX):** the source data sequence is divided into a number of blocks equal to the number of transmit antennas, then transmitting these blocks simultaneously from all antennas using the same carrier frequency. Therefore, the spectral efficiency increases with the increase of the number of transmit antennas. An example of SMX decoders is V-BLAST architecture [41].

- **Multiple access techniques:** multiple access techniques occurs when multiple antennas share the same limited resources efficiently, which means that there is not only a single user for the available bandwidth [42]. Examples of multiple access techniques are: TDMA, FDMA and CDMA.

- **Beamforming techniques:** combining the signals from different antenna elements to form a beam which is directed to a specified direction is called beamforming technique [31].
- **Space modulation techniques:** in this technique, in addition to the emitted symbol, another source of information is also transmitted, which can be the spatial position of the transmitted antenna, and consider that only one transmit antenna is active at each time instant, hence, the spectral efficiency is increased. Examples of space modulation techniques are, spatial modulation (SM) which was first introduced in [43], and which will be described in more details in our thesis, space shift keying (SSK) in [44].
- **Multifunctional MIMO techniques:** combining different MIMO schemes to enhance the system performance is known as multifunctional MIMO techniques. An example of that, is the hybrid space time block coding spatial modulation (STBC-SM) scheme, which results from combing SM with STBC to achieve spatial and diversity gains [45] and the details are given in chapter III.

2. **Distributed MIMO techniques:** referred to as cooperative MIMO, the idea goes back to 1971, when Van de Meulen introduced the classic relay channel [46], and the characterization of the relay channel was visited by Cover and El Gamal [47]. Since then, distributed MIMO has captured much attention [48]. In this technique, the multiple antennas at the front end of the wireless network are distributed among widely separated radio nodes, where each node has only one antenna. As a result, the information is sent to the receiver from different nodes at different locations [48].

1.5.1 Massive MIMO

The term "massive" is used to denote the large number of antenna elements that are used in MIMO architecture. The MIMO system can be considered massive when the number of antennas is greater than 64 elements [49]. Multiple antennas afford two options: first is to provide an array gain by focusing energy in desired directions and nulling in unwanted signal directions (forming a beam). Second, is to provide a spatial multiplexing gain by sending independent data streams on each antenna. Either

technique can be used to increase the overall user or system data rate. The second option is shown in Fig. 1.13 [49]. In first option, when using massive MIMO for beamforming;

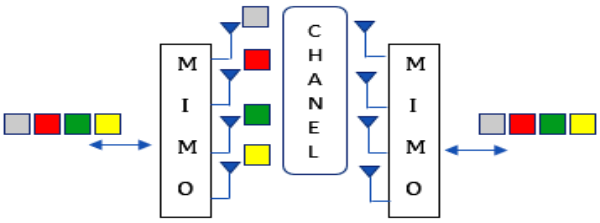

Figure 1.13 — Massive MIMO examples: spatial multiplexing.

the antenna arrays can be arranged and stacked in either linear, rectangular, or circular arrays. Massive MIMO will be deployed for 4G and 5G; in fact, high-frequency bands lead to more compact, large-scale antenna arrays due to the smaller wavelength. It can be also deployed in FDD or TDD duplex methods. When beamforming is considered in massive MIMO architecture, the array gain can be used in a variety of ways: first, to extend the coverage area, then, to reduce the transmit power of devices on the uplink (UL), to improve signal-to-interference-plus-noise ratio (SINR), hence improving the user throughput, and finally, to reduce the transmit power on the downlink (DL), thus improving the overall power efficiency. The number of antenna elements needed depends on the following items:

- Array gain (coverage area, power relief, etc.)
- Multiplexing layers needed
- Multi-users expected to be serviced
- Frequency band used (form factor, etc.)
- Signal processing complexity (CSI estimation, analog vs. digital domain, etc.)
- System performance gains (SINR, capacity, data rate, etc.).

The significant reduction in channel variation is one of the most important benefits of using multiple antenna techniques, for either transmitting or receiving, which is essential in combating multipath fading channel.

1.6 Multicarrier modulation techniques for data transmission

1.6.1 Orthogonal frequency division multiple access (OFDM)

OFDM is a multi-carrier modulation (MCM) technique, in which multiple carriers are used to modulate the information signals. It is used for high data rate transmission and is able to remove inter-symbol interference (ISI) and inter-channel interference (ICI) effects. The available transmission bandwidth is sub-divided into orthogonal and overlapping narrowband sub-channels. For this, the data streams are transmitted in parallel over multiple subcarriers where the peak of one sub-carrier occurs at the zero of the other sub-carriers, when using iFFT formula. Figure 1.14 illustrates this principle, where, $1/NT_s$ is the sub-carrier spacing.

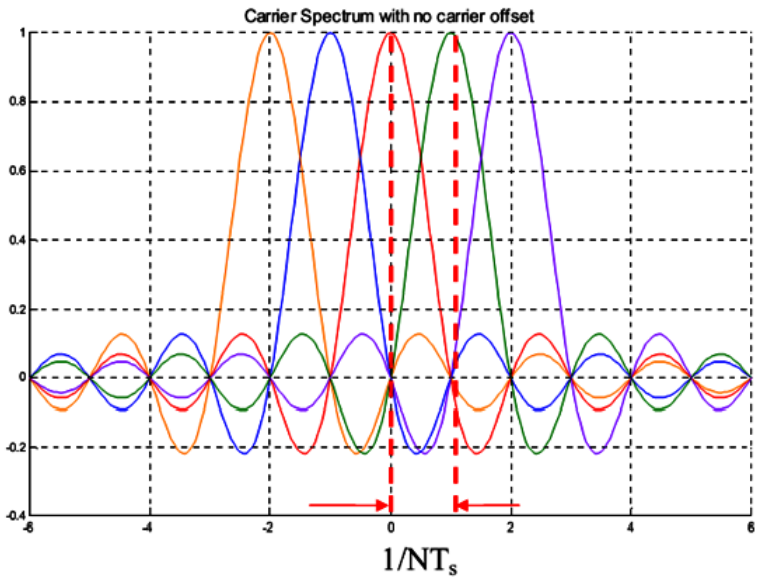

Figure 1.14 — Frequency Spectrum for 5 Orthogonal Subcarriers [50].

System design

The general block diagram of an OFDM transceiver is shown in Fig. 1.15. The digital data is first modulated, and then the symbols are parallelized and converted from the frequency to time domains. Afterwards, the resultant signals are emitted over the wireless channel after an addition of an appropriate cyclic prefix (CP). At the receiver

side, the cyclic prefix is first removed, and the FFT is applied in the second stage. Subsequently, the output signals are transformed from parallel to serial transmission and are finally demodulated to retrieve our original data streams.

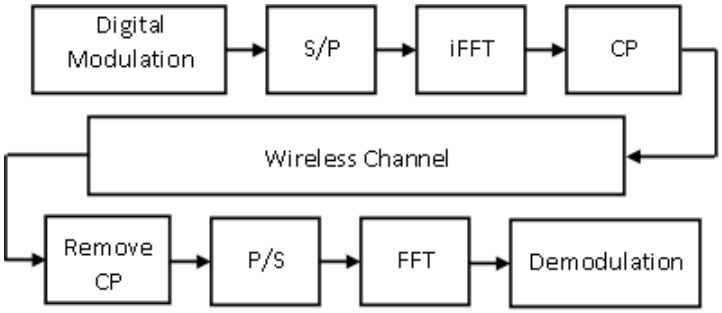

Figure 1.15 — OFDM Transmitter-Receiver Model.

OFDM transmission over time varying channels

1. **Addition of Guard Band:**
   The delay spread of multipath channel causes ISI in OFDM symbols. To remove ISI entirely, a guard band interval with no signal transmission can be used. The guard interval can be used in two ways, either by resorting to zero padding (ZP) or cyclic extension. Cyclic extension itself can be extended in two ways: cyclic prefix (CP) or cyclic suffix (CS).

   - **Cyclic prefix:** the cyclic prefix introduces the use of a guard time which allows reducing the interchannel interference (ICI) caused by the dispersive channel. CP principle depicts the copying of the tail part of the OFDM symbol to the front of the block to obtain a new OFDM symbol cyclically extended as presented in Fig. 1.16 . CP has three benefits:
     - First, it acts as a guard space between sequential OFDM symbols, and helps to avoid inter-symbol-interference (ISI);
     - Second, it allows ensuring the orthogonality between the sub-carriers; hence avoiding inter-carrier-interference.
     - It facilitates the equalization mechanism by creating a circular matrix.
   - **Cyclic suffix:** cyclic suffix is the opposite case of cyclic prefix; it consists in removing the upper portion of the OFDM symbol and copying it to the tail

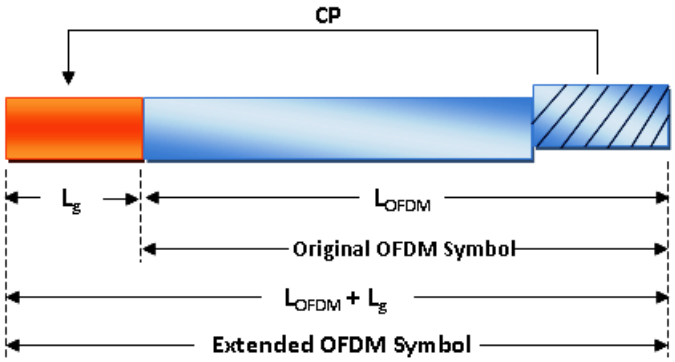

Figure 1.16 — Cyclic prefix principle.

part of the block as we can see in Fig. 1.17

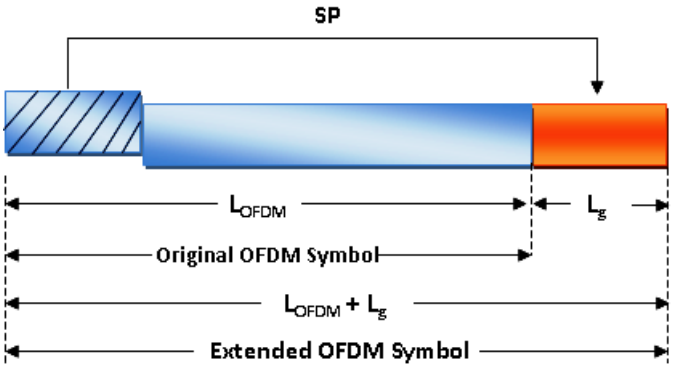

Figure 1.17 — Cyclic suffix principle.

- **Zero padding:** in zero padding (ZP) top and bottom portion of the transmitted symbols are filled with zeros as shown in Fig. 1.18.

Figure 1.18 — Zero padding principle.

Advantages of OFDM systems

OFDM-based system holds the following benefits:

- **Saving of bandwidth:** in OFDM system, the sub-carriers overlap each other by exploiting the orthogonality features at sampling time instants, which allows to more efficiently use the bandwidth compared to frequency division multiplexing (FDM), as shown in Fig. 1.19.

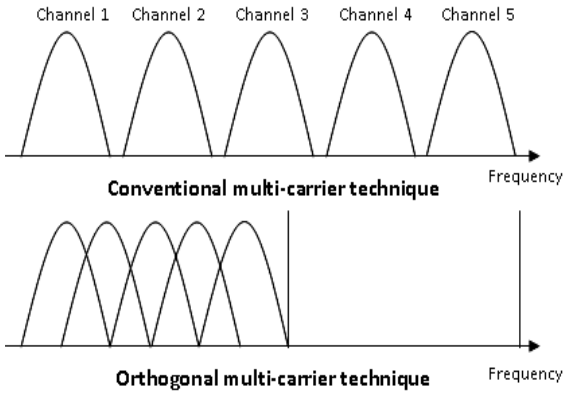

Figure 1.19 — Comparison of conventional and orthogonal multi-carrier techniques.

- **Facility to implement modulation and demodulation:**
  The concept of "Data transmission" can be efficiently implemented using iFFT and FFT instead of bank of modulators at the transmitter side and demodulators at the receiver side, respectively which, is a challenging problem in multicarrier modulation (MCM) system.

- **Susceptibility to frequency selective fading:**
  OFDM converts a frequency selective fading channel into several flat fading channels.

- **Protection against ISI:**
  The use of cyclic prefix between consecutive OFDM symbols renders the signal immune to ISI.

- **Facility of channel equalization:**
  Equalization is the process of measuring the channel response and using this information to correct the received signal. The insertion of cyclic prefix facilitates the channel equalization.

Major problems of OFDM systems

Despite several advantages, OFDM systems have some major problems such as:

- **High peak to average power ratio (PAPR) of the transmitted signal:** The RF power amplifiers should be operated in general in a very large linear region. However, for OFDM-based scheme, the signal peaks get into non linear region of the power amplifier, which is one of its major drawbacks. Subsequently, a signal distortion is produced by the resulting inter-modulation products among the sub-carriers. Hence, to reduce the PAPR, the power amplifiers should be operated with large power back-off, which leads to very inefficient amplification and expensive transmitters. The back-off of the power amplifier is a very important aspect for a wireless uplink as the terminal is likely to be battery powered, it determines the power efficiency of the transmitter.

- **Synchronization (timing and frequency) at the receiver**- At the receiver side, it is required to correct the timing between FFT and iFFT because OFDM approach is very sensitive to Doppler shifts that affect the carrier frequency offset (CFO), generating a high level of ICI.

- **Frequency Errors**- caused by frequency differences between the local oscillators in the transmitter and the receiver sides.

1.6.2 Generalized frequency division multiplex (GFDM)

GFDM is considered as a block-based multicarrier filtered modulation scheme, utilized to address the challenges in the vast usage applications of the fifth generation by providing a flexible wave-form [51]. GFDM allows the reuse of techniques that were originally deployed for OFDM, for example, the individual subcarriers are filtered by using circular convolution, hence, the GFDM frame is considered as a self-contained in a block structure. GFDM is more suitable multicarrier waveform for tactile internet scenarios, since, it has a good robustness over highly mobile channels. This is done via exploiting the benefit of the transmit diversity delivered by the easy way in generating the impulse responses resulted from circularly shifting the single prototype filter in time and frequency. The GFDM waveform can be combined with the Walsh-Hadamard transform for increased performance in single-shot transmission scenarios in order to

enhance the reliability and latency features. Also, when GFDM is combined with offset quadrature amplitude modulation mapping, GFDM can avoid self-generated interference if non-orthogonal filters are used for next generation multiple accessing.

OFDM has been successfully utilized in many systems such as LTE and Wi-Fi due to its several benefits such as low complexity implementation with FFT and its robustness against multipath channels. Nevertheless, OFDM suffers from the distortions caused by the non-linearity of the power amplifier (PA), and severe adjacent channel interference is caused due to the block nature of OFDM, which may result in a high out-of-band (OOB) leakage. Subsequently, GFDM offers some advantages over OFDM. However, backward compatibility of OFDM with the existing technologies along with the other advantages makes the enhancement of OFDM more suitable for the industry than the generation of a new waveform, as far as seen in the current standard discussions [52]-[53].

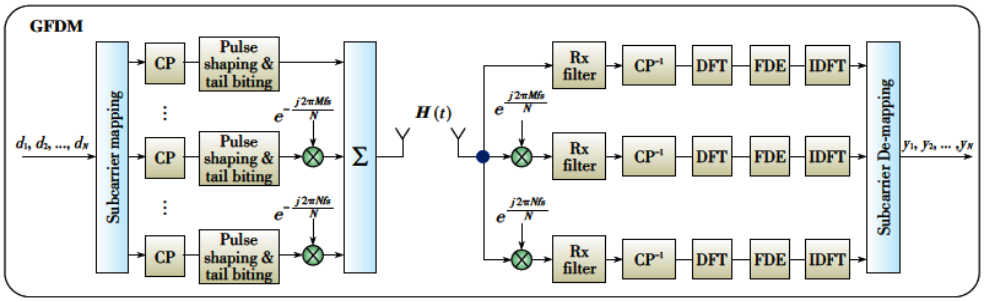

Figure 1.20 — Block diagrams of multicarrier scheme GFDM.

1.6.3 Orthogonal time frequency space (OTFS)

Orthogonal time frequency space (OTFS) modulation is a recently proposed two-dimensional (2-D) modulation technique which uses the delay-Doppler domain for multiplexing information symbols. Compared to the conventional multicarrier techniques, the bit error performance is improved by OTFS due to the adoption of pre- and post-processing operations. Also, a rapidly time-varying multipath channel will induce slow variations in the delay-Doppler domain. In fact, delay-Doppler representation of a multipath channel makes it time invariant for a longer duration compared to that in time-frequency representation. Therefore, the design of the equalizer will be simple, which allow the channel to be estimated less frequently in OTFS, thereby reducing the

channel estimation overhead in a rapidly time-varying channel. OTFS modulation was first introduced in [54], where it was shown that, for vehicle speeds as high as 500 km/h, OTFS yields a better error performance, as compared to OFDM alternative.

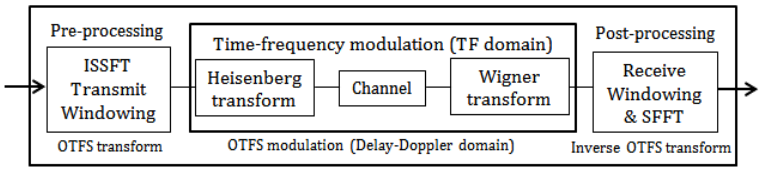

Figure 1.21 — OTFS modulation scheme.

Figure 1.21 shows the block diagram of OTFS modulation architected over a general multicarrier modulation system. At the OTFS transmitter, the information symbols (e.g., QAM/PSK symbols) are treated as points in two dimensional delay-Doppler grid and are mapped to the time-frequency (TF) plane through the 2D inverse symplectic finite Fourier transform (ISFFT). The TF signal so obtained is then passed through a multicarrier modulation system and transformed to a time domain to be transmitted using Heisenberg transform. The output of the Heisenberg transform is transmitted over the linear time variant channel. At the receiver, the received time domain signal is transformed to TF domain using Wigner transform (inverse of Heisenberg transform) to be afterwards mapped back to delay-Doppler domain using symplectic finite Fourier transform (SFFT). At the transmitter, the time domain signal obtained as the output of Heisenberg transform has to be amplified before it is transmitted through the wireless channel.

1.6.4 Advantages of OTFS

OTFS operates in the delay-Doppler coordinate system and when this scheme is coupled with equalization, all modulated symbols experience the same channel gain by extracting the full channel diversity. As a result of its operating principle, OTFS has the following important advantages:

1. No need for channel adaptation, since OTFS provides a stable data rate. This is especially important in systems with high mobility, where feedback of CSI to the transmitter becomes impossible, or afflicted with large overhead.

2. Better packet error rates (for the same SNR) or reduced SNR requirements (for the same PER) in the presence of high mobility (V2V, high-speed rail), or high phase noise (mm-wave systems).

3. Improved PAPR, in particular for short packet transmission.

4. Improved MIMO capacity when using finite-complexity receivers.

1.7 Nano communications

Nano-communication has captured much attention as an emerging building block for many novel services in the health care field. Indeed, the coordination and the control of nano machinery becomes the crucial challenge to be solved. Nowdays, nano-technologies has introduced incredible improvements, that enabled nano-scale machines to afford new solutions for many applications in biomedical, industry and military fields. Some of these applications exhibit to exploit the potential advantages of communication, especially, cooperative behavior of these nano-scale machines to reach a common and challenging objective that exceeds the abilities of a single device.

1.7.1 Recent development in nano-communication

In general, a set of nano-scale devices is called nono-networks, allow nano-machines to communicate and share any sort of information required by wide range of applications such as biomedical engineering, biological and chemical defense technologies, and environmental monitoring. Akyildiz et al. [55, 56] essentially established the domain of nano-networks by categorizing application and communication requirements. More specifically, the function of the nano-networks is to spread information signals among nano-devices in similar way like in sensor networks. hence, nano-networks can be considered as next generation sensor networks [57], but, with unbelievable reduced communication and computation abilities. Taking into account the large number of nano-devices composing the nano-networks, where all the individual nodes and devices constitute a massively distributed system, self-organization will become the dominant control mechanism [58].

Depending on the mean used to transmit the information, the following communication mechanisms can be distinguished [55]:

- **Electromagnetic waves**, e.g., using classical wireless radio transmission but now using nano-scale antennas and frequencies in the terahertz band,

- **Acoustic communication**, e.g., ultrasonic communication that is based on what is currently successfully used for imaging methods,

- **Nano-mechanical communication**, that is based on physical contact between sender and receiver, and

- **Molecular communication** that can be classified into short-range communication using calcium signaling, medium-range communication using molecular motors, and long-range communication using pheromones. Other options include, e.g., information transport using flagellated bacteria.

The motivation behind nano-scale communications comes from the research in biological systems and processes [55, 57]. Indeed, nano-networks are novel artifacts of bioinspiration in terms of both their architectural elements, e.g., nano-machines, and their principle communication mechanism, i.e., molecular communication [59]. In fact, many biological entities whitin organisms conduct as nanomachines since they have similar structures, i.e., cells, and the same interaction mechanism and vital processes, e.g., cellular signaling [60]. Furthermore, through the exchange of biochemical transmitters over the surface or the diffusion of soluble molecules that bind to specific receptor molecules on other cells [60–62], the cells can easily communicate with each other. Otherwise, the In-Body nano communication research community has been coined recently, initial works date back about ten years ago, focusing on adapting molecular communication principles [63, 64], which helped to constitute the bio-inspired networking community in which nature-inspired solutions such as the capability of cells to offer robust communication in rather harsh environments have been investigated for their use in artificial networks [61, 65]. An overview on the field of bio-inspired and its potential use in nano communication networks can be found in [57, 59]. Moreover, the nano communication community now does not only investigates molecular communication as a primitive, but focuses also on In-Body networks and the utilization of electromagnetic waves for terahertz radios or acoustic ultrasonic communication. More details on the state of the art of In-Body networks and nano communication can be found in [56].

1.7.2 Nano-communication concepts

In general, communication techniques can be classified into two aspects: in first, **digital communication**, identical to what we know from sensor networks, however, it adopts different kinds of media and trasmitters. In second, **novel communication paradigms**, based on biological systems for encoding information, where, the complex proteins are utilized as information carrier and the symbols are not necessarily required to be converted into digits. In addition, molecular communications rely on using anorganic chemicals (e.g., calcium signaling) or on complex molecules (e.g., proteins). RF radio communication operating on the terahertz band is an example of the proposed technical realizations of digital nano-communication [66]. More specifically, miniature radios are used based on carbon nano-tubes as antenna technology. Larger devices on the micro scale may even use acoustic communication. Digital communication may also be deployed with bio-signaling based, e.g., on the calcium level in cellular environments [55]. When we study the category of molecular communication, we see proposals relying on similar biological signaling mechanisms [67], but also more exotic forms like nanomotors and even flagellated bacteria [68]. Generally, the information is encoded in form of complex bio molecules such as proteins that intrinsically support an extremely high information density. Furthermore, all common communication designs, which use these transmission schemes, and known from ordinary communication networks are supported, from simple undirected broadcast communication, e.g., radio broadcast or undirected diffusion in fluids, to obviously targeted unicast communication basing on biological means of node addressing.

1.8 NANO-sensors and networks

Nano-sensors are very small integrated devices, made of nanomaterials or biological materials, and are utilized to detect and respond to a physical phenomenon of the environment. Nano-sensors are considerably small than conventional sensors, however, they work in similar way as conventional ones. They can implement a range of simple functions to manipulate signals to detect, edit, and record measurements. They have different sizes and shapes ranging from the size of a macromolecule to that of a bio-cell (i.e., dimensions of 1-100 nm) [69]. For example, in biomedical applications, the nano-

sensors used for taking invasive measurements are extremely small than the one used to record noninvasive measurements. The measurement and the application of area play a crucial role in determining the size and material of a nanosensor. In healthcare field, different aspects such as monitoring, detection, and treatment can be ensured by nano-sensors. For example, nano-sensors can detect the presence of different infectious agents such as virus or harmful bacteria [69]. An example of such a nano-sensor is biotransferrable graphene wireless nano-sensor [70] illustrated in Fig. 1.22. This proposed architecture has a satisfactory response in sensing the most sensitive chemicals and biological compounds up to single bacterium. There is also a wireless remote power and readout functionality. Therefore, nano-sensors with thier computation, communication,

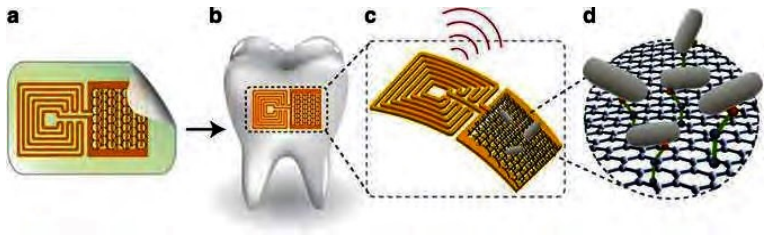

Figure 1.22 — Bio-transferrable graphene wireless nano-sensor [70].

and action components are miniaturized and fabricated into a single box called nano-machine [71]. Several nano-machines can be connected together through nanorouters that rout measured data to other nano-devices or external devices such as mobile phones [73]. The interconnected cluster of such nano-machines is called a nano-network. An example of such nano-network is given in Fig. 1.23.

1.9 Applications of NANO-sensors

Nano-sensors have great potential and incredible applications in all domains of life including, healthcare, environmental monitoring, consumer products, robotics, transportation, security, surveillance, defense, and agriculture etc. Currently, biomedical and healthcare are rapidly growing sectors for nano-sensors due to increasing demand for rapid, compact, accurate and portable diagnostic sensing systems. In biomedical and healthcare area, these devices can offer revolutionary personal healthcare solutions by providing continuous monitoring. The applications of nano-sensors can be divided into the following broad groups: biomedical, environmental, industrial, smart office

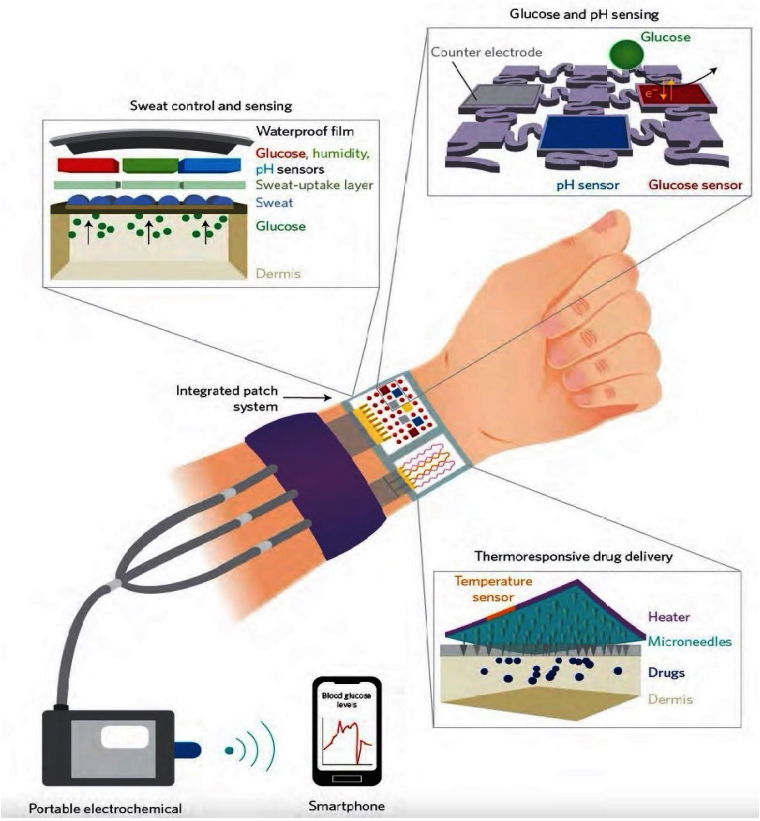

Figure 1.23 — Nano-network: glucose graphene skin sweat sensor and drug delivery chip [72].

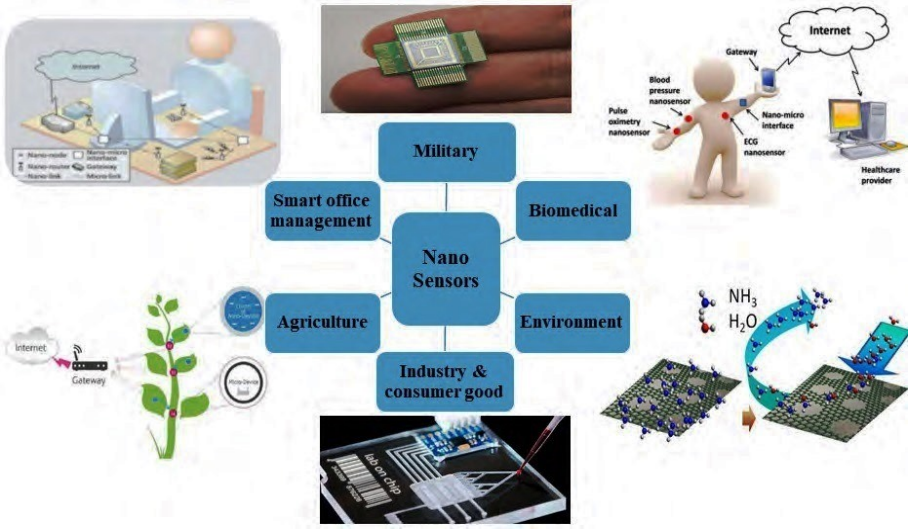

Figure 1.24 — Application fields of nano-sensor networks.

management, agricultural, and military applications as shown in Fig. 1.24.

1.10 In-VIVO Communication

Wireless body area networks (WBANs) are new generation of wireless sensor networks (WSNs) dedicated for healthcare monitoring applications. The aim of these applications is to ensure continuous monitoring of the patients' vital parameters, while giving them the freedom of moving thereby resulting in an enhanced quality of healthcare [74]. In fact, a WBAN is a network of wearable computing devices operating on, in, or around the body. It consists of a group of tiny nodes that are equipped with biomedical sensors, motion detectors, and wireless communication devices [75]. In-VIVO networking is considered as an important application platform for WBANs, that facilitates continuous wirelessly-enabled healthcare, internal health monitoring, internal drug administration, and minimally invasive surgery are examples of the pool of applications that require communication from in vivo sensors to body surface nodes. However, the study of in vivo wireless transmission, from inside the body to external transceivers is still at its early stages. Fig. 1.25 shows a modified network organization for interconnecting the

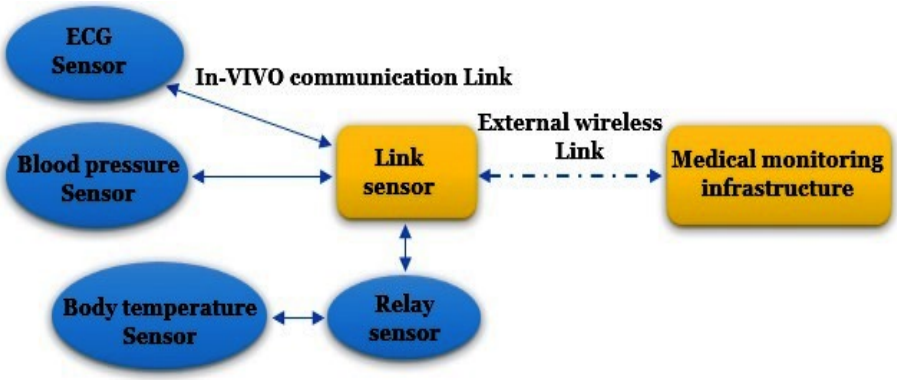

Figure 1.25 — Simplified overview of the In-VIVO communication network.

biomedical sensors. The data is basically not directly transferred from the biomedical sensors to the hospital infrastructure. Indeed, sensors send their data via a suitable low-power and low-rate in-VIVO communication link to the central link sensor (located on the body like all other sensors). Any of the sensors may act as a relay between the desired and the central link sensor if a direct connection is limited. An external wireless link enables the data exchange between the central link sensor and the external hospital infrastructure [76]. Wireless in-VIVO communication creates a wirelessly-networked cyber-physical system of embedded devices. In-VIVO communication is a genuine signal

transmission field which utilizes the human body as a transmission medium for electrical signals. The body becomes a vital component of the transmission system. Electrical current induction into the human tissue is enabled through sophisticated transceivers while smart data transmission is provided by advanced encoding and compression.

1.11 Summary

In this chapter, the fundamentals of wireless communication systems were investigated; the concepts behind MIMO transmission techniques and channel environment were also illustrated. Multiple antenna configurations introduce a new space dimension to wireless signals so that MIMO systems can provide array gain, diversity gain and capacity gain. A detailed description of multicarrier data transmission is carried out. Furthermore, stating all these concepts, the up-to-date overview and operation principle of SM will be discussed in next chapter to justify the proposition of this novel architecture as an alternative to conventional MIMO schemes.

CHAPTER 2

Chapter 2: Design guidelines of IM and performance analysis of SM-MIMO

2.1 Introduction

Index modulation (IM) has captured much attention as an emerging modulation concept and is identified by sparse symbol mapping. More precisely, beyond that of the traditional amplitude and phase shift keying modulation schemes, an additional information is sent by the IM transmitter, due to the activation of a subset of indices. In this chapter, we shed light on the potential and implementation of index modulation (IM) technique for MIMO and one of the multicarrier techniques (OFDM), which are expected to be two of the key technologies for 5G systems and beyond. Specifically, we focus on the promising applications of IM: spatial modulation (SM), which can offer significant data rates with a low hardware complexity. This technique has brought a new concept in the communication paradigm for MIMO systems, by proposing to transmit both the signal and spatial informations in a whole symbol.

2.2 Principles and richness of index modulation families

Index modulation (IM) is considered as a family of modulation techniques that activates states of some resources/building blocks for information embedding. The nature of the resources/building blocks can be physical, e.g., antenna, subcarrier, time slot, and frequency carrier, or virtual, e.g., virtual parallel channels, signal constellation, space-time matrix, and antenna activation order. IM is distinguished from the other techniques by the fact that part of the information is implicitly incorporated into the transmitted signal. Subsequently, for a massive MIMO configuration, a small number of radio frequency (RF) chains is used, caused by the random selection of transmit antennas according to the information bits [3, 77, 78]. Application of IM is applicable in several domains, which enables an attractive tradeoff among spectral efficiency (SE), energy efficiency (EE), transceiver complexity, interference immunity, and transmission reliability [79]- [80]. Hence, new research opportunities are opened for 5G and beyond wireless communication systems. On the other hand, the performance of 1-D IM types, such as SM and OFDM-IM, leads to the creation of the multidimensional IM concept, which possessed a set of various combinations of 1-D IM options and has been introduced in recent studies. Otherwise, the following key questions remain unanswered within the context of emerging IM solutions: how can IM solutions accomplish the broad range of user and application demands and how can the flexibility of IM be used for 5G and beyond systems?
Fig. 2.1 shows the most applied multidimensional domains IM in the literature and described their dimensional-based categorization in detail.

2.2.1 1-D Index modulation

The 1-D IM corresponds to the fundamental IM techniques that form multidimensional IM types. As illustrated in Fig. 2.1, space, frequency, time, code, channel, and polarization domains are regrouped under this category.

1. **Space-Domain IM:** two different physical entities consisting of antennas and radio intelligent surfaces (RISs) are evaluated in the context of space-domain IM.

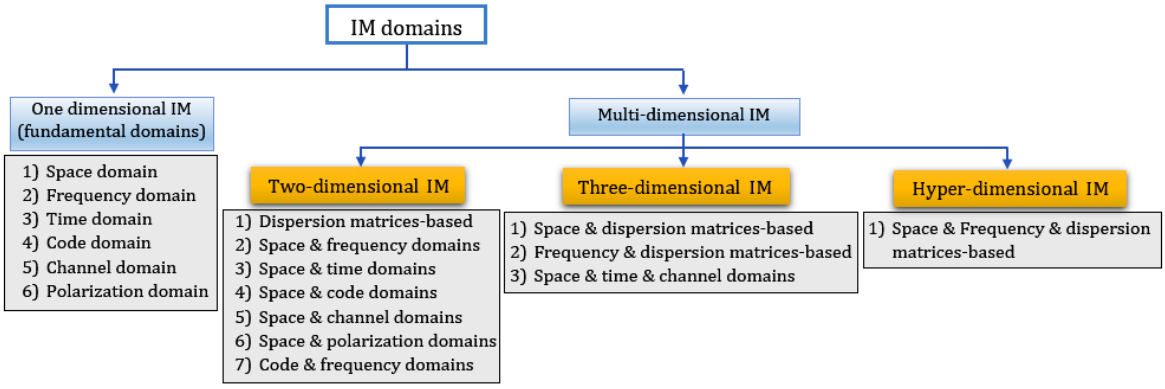

Figure 2.1 — Dimensional-based categorization of the existing IM domains in the literature.

- **IM via antennas:** the space-domain IM is introduced via space shift keying (SSK) modulation that uses a single antenna out of a number of Tx antennas. [44]. The integration of SM in MIMO communication scheme is an important breakthrough that not only allow emerging the general IM concept to the wireless communication designs but also sheds light on its development [77], [43, 81, 82]. Furthermore, SM performs the transmission of the conventional M-ary modulated information symbols via the active Tx antenna index.
- **IM via RISs:** RIS consist of small, low cost, and a high number of passive elements that control the reflection aspects of the incoming signals. RIS concept has been widely investigated in the past few years. For more details, interested readers are referred to [83–85]. RIS-based IM concept is introduced in [86]. It is shown that IM can be applied to Tx and Rx antennas, as well as the passive elements.

2. **Frequency-Domain IM:** in the aim to improve the SE as well as the EE of the conventional OFDM systems, indexing of the subcarriers in the frequency domain is proposed. An example of this category is subcarrier index modulation (SIM-OFDM), where the incoming data bits are divided into two parts [87]. First part is the ON-OFF keying data bits which are used to decide the status of a number subcarriers in an OFDM block, and the remaining bits are emitted through the subcarriers whose status is ON.

3. **Time-Domain IM:** inspired by the frequency-domain IM, single carrier IM

(SC-IM) is proposed in the time domain [88]. SC block is divided into subblocks. Data transmission is performed at the time intervals corresponding to active symbols, and the remaining symbols are set to zero. SC subblocks are grouped to generate an SC block, and then, CP is added before its transmission to the receiver over a multipath channel.

4. **Code-Domain IM:** code index modulation spread spectrum (CIM-SS) has been proposed in [89] by taking the benefits of direct sequence spread spectrum (DS-SS) technology. The information-bearing unit is the spreading code which can be found in a predefined table of spreading codes. Two orthogonal Walsh codes are stored in the lookup table in [89]. The incoming two bits are concatenated to generate a subblock, and one bit in each subblock selects a code to spread the remaining bit over a time duration.

5. **Channel-Domain IM:** in media based modulation (MBM) technique, the information bits are conveyed via different channel realizations created by the ON-OFF status of the available RF mirrors, which are located in the vicinity of the Tx antenna [90], [91], [92–94]. Moreover, each channel realization corresponds to a different point in the constellation diagram at the Rx. No additional energy is required to transmit the bits by MBM. On the other hand, it is shown that SIMO systems with MBM can gain the same energy as MIMO systems [90].

6. **Polarization-Domain IM:** higher multiplexing gain and an inreased SE for the single RF MIMO systems, can be achieved by using polarization shift keying (PolarSK) [95]. In order to convey the incoming data bits as in SSK, polarSK uses the available P polarization states, that is, linear polarization, circular polarization, and elliptic polarization. As an example and in a recent study, a new IM scheme, which is, polarization modulation (PM), utilizes polarization characteristics to carry extra information bits along with the complex data symbols. More precisely, not only vertical and horizontal polarizations but also the axial ratio and tilt angle of elliptic polarization are used for transmitting the extra information bits through IM [96].

Table. 2.1 illustrates the available IM options in the literature regarding their application domains.

1-Dimensional IM	**Space domain:** SSK[44], SM[77], GSM[97], QSM[98], ESM[99], STBC-SM[100], RIS-IM[86].
	frequency domain: SIM-OFDM[87], OFDM-IM[101], GFDM-IM[102]
	Time domain: SC-IM[88], FTN-IM[103], DM-SCIM[104].
	Code domain: CIM-SS[89], IM-OFDM-SS[105].
	Channel domain: MBM[90], STCM[106], ST-MBM[107]
	Polarization domain: PolarSK [95], PM [96]
2-Dimensional IM	**Dispersion matrices-based:** DSM[108], STSK[109], OFDM-STSK[110]
	Space and frequency domains: OFDM-STSK[110], [107]
	Space and time domains: TI-SM[111], TI-SM-MBM[112].
	Space and code domains: CIM-SM[113].
	Space and channel domains: SM-MBM[113], SM-MBM[112], QCM[114].
	Space and polarization domains: SPSK[115], DP-SM[116], [117]
	Code and frequency domains: CF-IM[118]
3-Dimensional IM	**Space and dispersion matrices-based:** MS-STSK[119], JA-STSK[120]
	Frequency and dispersion matrices-based: MSF-STSK[119]
	Space, time and channel domains: TI-MBM[112], TI-SM-MBM[112]
Hyper-Dimensional IM	**Space, frequency and dispersion matrices-based:** OFDM-STSK-IM[121]

Table 2.1 — Summary of the available IM variants in the literature.

2.3 Enabling IM techniques for next-generation services

The presented IM techniques are categorized considering the requirements of three main services, figure. 2.2 presents the most promising IM variants for 5G and beyond communications.

1. **Enhanced mobile broadband (eMBB):** the efficient use of spectrum is the key issue for eMBB. Accordingly, IM patterns are evaluated based on their SE performance.

2. **Massive machine-type communications (mMTC):** Academic and industrial researchers are looking for technologies that can cover a wide area, low power

consumption, and low cost for mMTC services, where, latency, data rate, and reliability are not the main concerns. In summary, IM provides high EE due to the energy-free carried information bits identified by the indices of the transmit entities.

3. **Ultra-reliable low-latency communication (URLLC):** Due to the simultaneous and conflicting demands of ultra-reliability and low-latency, URLLC is considered as the most challenging service. In the aim to achieve the block error rate (BLER) values given in table 2.2, IM schemes that provide diversity gain, interference immunity, and robustness against hardware impairments, such as carrier frequency offset (CFO), which is one of the promising solutions for URLLC.

Service type	KPIs	Definitions
eMBB	Data rate	Supporting peak data rates of 10 Gbits/s and 20 Gbits/s for UL and DL transmission respectively
	Mobility	Achieving desired data rate for a given mobility class $10km/h \leq V \leq 500km/h$
mMTC	Connection capability	number of mMTC UEs per cell (1.000.000 UEs per km^2)
	Power consumption	at least 10 years of life time for a device by sending 20 bytes and 200 bytes for UL and DL transmission, respectively
	Coverage	Maximum coupling loss that corresponds to total loss including antenna gain, path loss and shadowing for baseline data rate of 160 bit/s
URLLC	Latency	The elapsed time for successful transmission end reception of a packet $0.25ms \leq latency \leq 1ms$
	Reliability	Successful reception of a packet with the reliability range of $10^{-5} \leq BLER \leq 10^{-9}$

Table 2.2 — Key performance indicators (KPIs) of next-generation services.

In a given IM domain, to reach a high reliability via IM, a sufficient selectivity between the active entities is necessitated. Hence, for space-domain IM techniques, a separation distance of $(\lambda/2)$ between Tx antennas, is required to improve the detection performance at Rx.

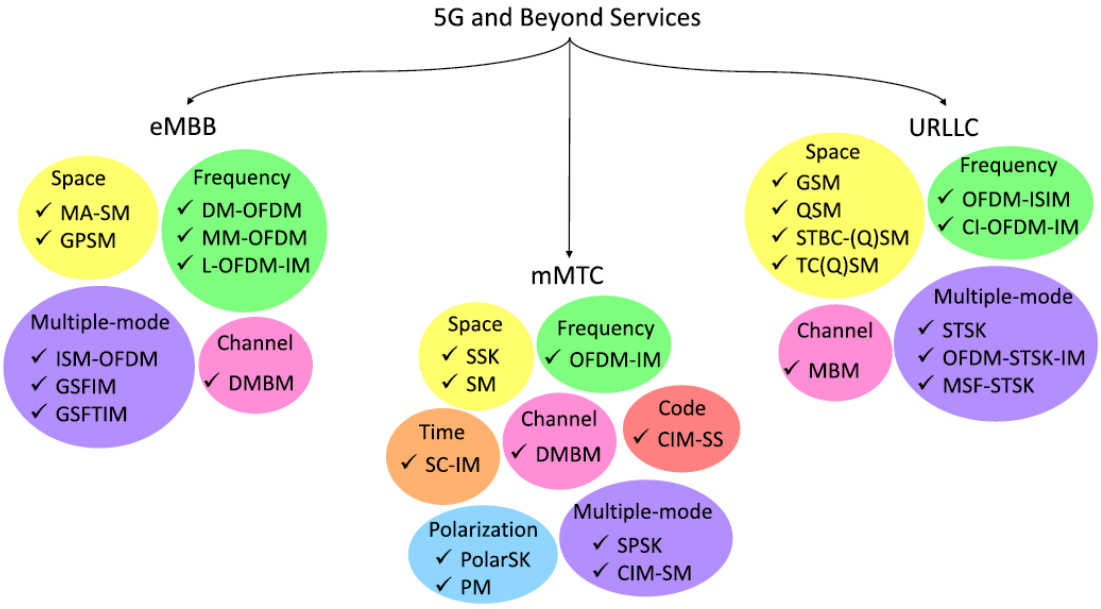

Figure 2.2 — Promising IM variants for 5G and beyond services.

2.4 From MIMO to SM-MIMO: One-D IM in the space domain

In conventional MIMO schemes, multiple data bits are conveyed simultaneously over all the available antennas at the transmitter, which are in active state at any time instant. Compared to SISO schemes, MIMO communications provide higher data throughputs and enhanced spectral efficiency but with the following drawbacks:

- To avoid the interference caused by simultaneously transmitting many data streams, more signal processing complexity at the receiver is required;
- To exploit the benefits of multi-user MIMO transmission techniques, additional and hard synchronization is required;
- To transmit the data streams at the same time instance, multiple RF chains will be used at the transmitter resulting in increasing the complexity of MIMO-based scheme;

Fueled by these considerations SM has been recently proposed as a new transmission concept [43].

2.5 State of the art of SM-MIMO

2.5.1 Historical perspective

In the last few years, SM-MIMO based scheme has captured a great attention from the research community. In this section, we describe the main historical perspectives of SM-MIMO based on some pioneering papers: SSK principle was firstly introduced in 2001 [122] and known as "space modulation" technique, where, the concept of exploiting the differences between the received signals to recover the transmitted information sequence is investigated. However, more than one antenna is activated at each time instant requiring inter-antenna synchronization (IAS) and multiple RF chains [122]. One year later in 2002 in [123], orthogonal space division multiplexing (OSDM) is proposed as multi-antenna modulation scheme, where the spatial position of the activated transmit antenna in every channel utilization was exploited for the first time, by multiplexing a number of bits which is equal to the number of transmit antenna elements. Information-guided channel-hopping (IGCH) modulation was proposed in two years later in 2004 [124], and shared the same principle with the technique proceeded in [122], with an exception in [124], where it was applicable to any number of transmit-antennas. Afterwards, basing on [124], and relying on the idea of switching one transmit antenna at every channel use and encoding some information bits using this transmit antenna, an inter carrier interference (ICI)-free multi-antenna modulation architecture is created [125]. One year later in 2006, Mesleh et al. exploit the scheme presented in [125] and proposed a new scheme [43], [126], [127], where the spatial position of the activated antenna is used as an additional source of information, in the purpose to reduce the complexity while achieving a high spectral efficiency and an enhanced BER performance compared with conventional MIMO scheme. To estimate the antenna index and retrieve the transmitted data, a simple MRC algorithm was applied at the reception side of the SM architecture [128]. An optimal detector (OD) was developed in [81] and was proved to be able to provide a significant performance gain at a high complexity cost when compared with other detectors such as zero forcing (ZF) and MRC. Moreover, the hard-decision ML-optimum decoding in [81], is generalized to soft-decision ML detector in [129] which is applied over orthogonal frequency division multiple access (OFDM) systems, allows to avoid IAS and ICI by activating only one antenna for each

sub-channel. Afterthat, an analytical framework of SM based on optimal detector with partial state information (CSI) was derived in [130]. It was shown that partial CSI at the receiver leads to a sub-optimal receiver design; yet has to be considered because more representative of practical cases. The effect of channel estimation errors on the performance of SM and space modulation has been studied in [131, 132]. Clearly, it appears that SM is robust to channel estimation errors. Furthermore, in [133, 134], SM is applied to optical wireless communications (OW), a scheme which was referred to as optical spatial modulation (OSM). It was shown to offer a power and bandwidth efficient pulse modulation technique for OW communications. In OSM only one LED for an array of LEDs is active and radiating a certain intensity level at each time instant. The different SM techniques described in this section are summarized in the following table 2.3.

Modulation Type	Modulation Techniques
Space Modulation	SSK [122] IGCH [135]
Spatial Modulation	SM-MRC [128] SM-ML optimum detector [81] Soft-decision ML detector [129] Partial State Information detector [130]
Optical Wireless SM	OSM [133, 134]

Table 2.3 — Summary of the different SM techniques

2.5.2 Design guidelines for SM-MIMO systems

SM is a new modulation concept that aims to offer some benefits in terms of:

- **Rate:** due to the adoption of the three-dimensional constellation diagram and to the introduction of the spatial-constellation, SM-MIMO can offer a high throughput and an increased SE, which is higher than that of single antenna transmission. Hence, this design should be tuned accurately since the data rate could further enhanced by a proper data streams encoding ensuring ICI mitigation, but at the cost of an additional receiver complexity [136].

- **Capacity:** mutual information of SM-MIMO systems configured with a single-RF chain ($N_{RF} = 1$) and Gaussian input signals depends on the number of transmit antenna elements (N_t) [135].

- **Error performance :** it was shown in most of research papers that SM-MIMO can offer a better BER performance than SISO counterpart, especially, when the number of transmit antenna elements is higher than four and the number of receive antenna elements is more than one [137]. Hence, BER is proportional to the number of receive antennas (the higher the number of receive antennas, the better the BER performance).
- **Channel fading:** the distribution of the wireless channel fading influences on the BER performance of SM-MIMO based scheme [137]. Thus, more bits can be encoded and transmitted if there is less channel fading or equivalently a higher Nakagami fading parameter [137].
- **Channel state information:** based on the assumption that adequate channel estimators are used, it has been shown that SM-MIMO is robust to imperfect channel state information (CSI) [131, 132].
- **Demodulation:** the choice of the best demodulator depends on the BER performance and the detection complexity imposed at the receiver, ranging from the matched filter that provides the worst performance at the lowest complexity [128], to the ML-optimum detector that offers the best performance at the highest complexity [81].
- **Energy-Efficiency:** SM-MIMO scheme uses one RF chain at each time instant, thus providing a better energy efficiency and minimizing the complexity and the total power dissipation of the power amplifiers [138].

2.6 SM-MIMO: Operating principle

2.6.1 System model

The general system model of SM-MIMO-based scheme as shown in Fig. 2.3 and which will be described later on, includes a MIMO wireless links with N_t transmit and N_r receive antennas [43, 126]. Therefore, the signal model of SM-MIMO, can be simply written as follows:

$$\mathbf{y} = \mathbf{H}\mathbf{x} + \mathbf{w} \tag{2.1}$$

where: $\mathbf{y} \in C^{N_r \times 1}$ is the complex received vector; $\mathbf{H} \in C^{N_r \times N_t}$ is the complex channel matrix; $\mathbf{w} \in C^{N_r \times 1}$ is the complex AWGN at the receiver; and $\mathbf{x}$ is the complex modulated transmitted vector.

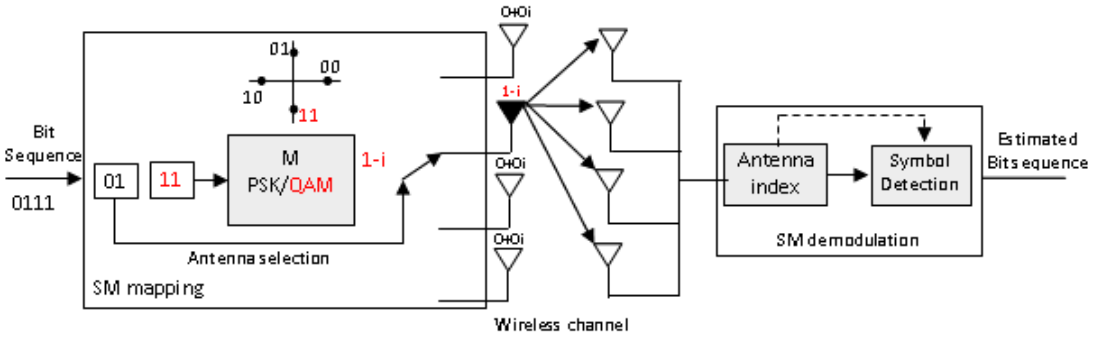

Figure 2.3 — Spatial Modulation System Model.

2.6.2 SM-MIMO: How It Works?

1. **The transmitter:** spatial Modulation proposed for MIMO systems adopts a new mapping paradigm allowing a high spectral efficiency, while eliminating ISI and ICI [125]. This is reached by considering just one activated antenna at the transmitter at each time instant, thereby exploiting the spatial position of this activated antenna as an additional source of information for conveying data. At the transmitter, the incoming data bits are divided into blocks, each one of them has the length:

$$b_{SM} = log_2(N_t) + log_2(M) \tag{2.2}$$

with $log2(N_t)$ being the number of bits used to indicate the activated transmit antenna among the possible ones in the antenna-array which are kept silent meanwhile, and $log_2(M)$ is the number of bits needed to identify the symbol in the signal constellation emitted by the selected antenna as shown in Fig. 2.4. This idea was introduced for the first time in [43].

Figure 2.4 shows an example of SM with $N_t = 2$ that uses $4QAM$ modulation, thereby using 3bits/symbol for each transmitted SM symbol. Let us assume that the input data sequence is $[1 \quad 0 \quad 0]^T$, which corresponds in SM mapping as shown in Fig. 2.4, to the transmission of the symbol $-1.0000 + 1.0000i$ from the second

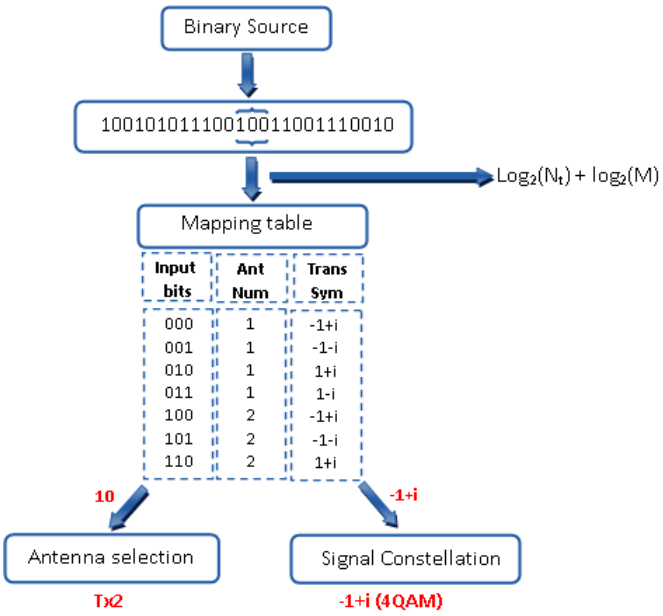

Figure 2.4 — SM: How it works "The Transmitter".

transmit antenna. As a result, the modulated signals belong to a tridimensional constellation since using the spatial position of the activated antenna as a source of information introduces one additional dimension. A simple example is shown in figure 2.5 when adopting a linear antenna array with $N_t = 2$, and a $4QAM$ modulation.

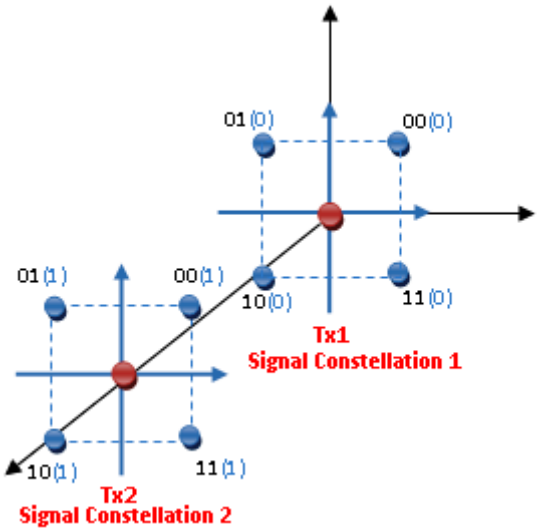

Figure 2.5 — Tridimensional constellation diagram of SM when using "4QAM" and two transmit antennas.

2. **The wireless channel**

The signal proceeded by the transmitter is conveyed through the wireless channel environment in which different propagation phenomenons, caused by different interacting environmental objects, occur. Based on the fact that in SM communication mechanism, only one transmit antenna is concerned at each time instant, ICI is hence inexistant and the signals emitted by distinct transmit antennas are distinguishable at the receiver. Figure 2.6 shows the wireless links between the transmitter and receiver designs.

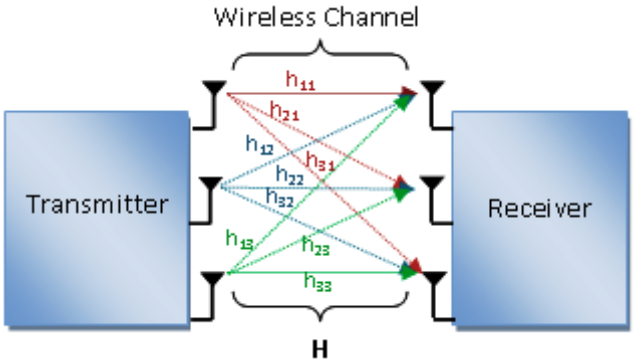

Figure 2.6 — Wireless channel.

Recall that the channel model $\mathbf{H}(k)$ can be written as a set of complex coefficients between the transmit and receive antennas as illustrated in the following equation:

$$\mathbf{H} = \begin{pmatrix} h_{11} & h_{12} & \dots & h_{1N_t} \\ h_{21} & h_{22} & \dots & h_{2N_t} \\ \vdots & \vdots & \ddots & \vdots \\ h_{N_r1} & h_{N_r2} & \dots & h_{N_rN_t} \end{pmatrix} \tag{2.3}$$

3. **The receiver**

The receiver exploits the random attenuation introduced by the wireless channel for signal detection. By applying one of the detectors that will be described later in this chapter, the receiver should estimate the activated antenna index at the transmitter; and assuming that the impulse channel response is known, the receiver evaluates Euclidean distance between the received signal and the set of possible modulated signals to recover the original transmitted bit stream. In summary, the working principle of SM is based on the following facts:

- Each transmit-to-receive wireless link has a different channel,
- The receiver employs in general the a priori channel knowledge (or an estimation of that) to detect the transmitted signal.

2.6.3 Advantages and disadvantages of SM

In this section, we summarize the main advantages and disadvantages of SM with respect to other MIMO architectures.

1. **Advantages**

   - Compared with conventional MIMO solutions, such as V-BLAST and Alamouti schemes, transmitting over only one RF chain and switching to one transmit antenna at each time instant allows SM to eliminate ICI and IAS.
   - Compared with conventional MIMO solutions, SM can provide a high SE and an important multiplexing gain in the spatial domain by resorting to the so-mentioned tridimensional constellation diagram. Spectral efficiency increases logarithmically with the number of transmit antennas without any bandwidth and power loss.
   - Compared with conventional MIMO systems, SM avoids ICI and attains ML decoding at a simpler receiver design, unlike V-BLAST which adopts complex interference cancelation algorithms.
   - One receive antenna is sufficient to exploit SM paradigm, since incorporating multiple receive antennas aims only at providing the receive diversity gain. Thus, SM is suitable for downlink settings with low complexity mobile units which is not the case of conventional MIMO solutions.
   - Compared with conventional MIMO systems, SM offers a high capacity due to the multiplexing gain achieved by exploiting the spatial position of the transmit antenna as an additional index.

2. **Disadvantages**

   - At least two transmit antennas are required to exploit the SM concept.

- The SM mechanism might not offer adequate BER performance if the wireless spatial subchannel links are not sufficiently different, which is similar to conventional spatial multiplexing techniques that require a rich scattering environment to achieve a significant data rate.
- For data recovering, perfect channel knowledge is required at the receiver, which may impose complexity constraints on the channel estimation unit. In the space-time coding literature, an advanced well-known differential encoding/decoding modulation scheme appropriate for single-antenna systems has been proceeded to avoid the knowledge of the wireless channel at the transmitter and at the receiver. Since the wireless channel is a part of the actual modulation unit in SM, the development of such receiver structures poses some design challenges.
- SM can provide only a logarithmic increase (depending on the number of transmit antennas) in data rate, hence, SM might not achieve very high data rate. The above list of SM advantages and disadvantages explicitly indicates that SM appears to be a promising candidate for low-complexity MIMO implementations.

2.7 SM-OFDM based scheme

Spatial modulation-OFDM (SM-OFDM) is an alternative multiple antenna-OFDM transmission approach, that entirely avoids ICI at the receiver input while maintaining high spectral efficiency, particularly in frequency selective channels. Traditionally, modulation techniques such as $BPSK$, $QPSK$, $16QAM$ map a fixed number of information bits into one symbol (b/s). Each symbol represents a constellation point in the complex, two dimensional signal plane. SM extends this two dimensional plane to a third dimension: the spatial dimension. Hence, if the channel and interference environment do not allow the use of $64QAM$ and one transmit antenna, the same spectral efficiency can be achieved with $16QAM$ and four transmit antennas. In fact, the information is not only included in the transmitted symbol, but also in the actual physical location of the antenna, a combination with OFDM transmission is not straightforward. The proposed solution is as follows: The output block of symbols from the spatial modulation is grouped into N_t vectors, where N_t is the number of transmit antennas. This is done

by grouping the mapped symbols at the output of the spatial modulator in vectors corresponding to their assigned transmit antenna number and setting all other symbols in that vector to zero. The OFDM modulator is applied to each vector; thus, resulting in N_t OFDM blocks to be transmitted simultaneously from the N_t transmit antennas. However, at each instant of time and for each sub-carrier only one transmit antenna will be active and all other transmit antennas are off. As a result, ICI is completely avoided at the receiver input. Therefore, the symbol duration in SM is unchanged even though the transmitted symbol carries different number of information bits due to the described working mechanism. Subsequently, the bandwidth occupied is unchanged which effectively results in the desired increase in SE.

2.7.1 Operating principle

OFDM converts a frequency-selective channel into a parallel collection of frequency flat-fading subchannels, allowing SM-OFDM to be more efficient in using the available bandwidth [139]. Furthermore, this mechanism increases the symbol duration and thus reduces or eliminates the ISI caused by the multipath fading [43], [126–129].

Let us consider an $N_r \times N_t$ MIMO SM-based system as illustrated in Fig. 2.7, where N_t and N_r are the number of transmit and receive antennas, respectively.

Thus, as shown in Fig. 2.7, after insertion of error correction codes in the original interleaved data to fight against channel errors, the bit stream is divided into blocks. The key feature of SM is that each block is divided into two sub-blocks, one indicating the transmit antenna index, and the other one dedicated to the constellation symbol transmitted over the activated antenna. In general, the number of bits/symbol/sub-carrier or sub-channel b_{SM} that SM-OFDM based scheme can transmit for each block is given earlier in eq. (2.2).

Then, the output vectors from the SM mapping $\mathbf{R}(t)$ are transformed to the time domain by using the inverse fast Fourier transform ($IFFT$). Afterwards, a cyclic prefix is inserted, to avoid the ISI between the OFDM symbols.

After that, the resultant vectors $\mathbf{R}(t)$ are transmitted simultaneously from the N_t transmit antennas over the MIMO channel, denoted $\mathbf{H}(t)$, using the following equation:

$$\mathbf{Y}(t) = \mathbf{H}(t) \otimes \mathbf{R}(t) + \mathbf{W}(t) \tag{2.4}$$

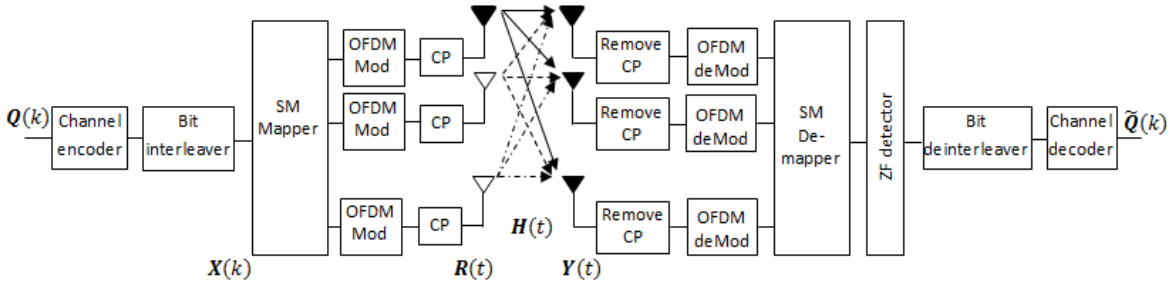

Figure 2.7 — SM-OFDM System model.

where $\mathbf{Y}(t)$ is the received matrix, $\mathbf{W}(t)$ is the additive white Gaussian noise (AWGN) matrix, $\mathbf{H}(t)$ is a block matrix containing a set of $N_r \times N_t$ vectors each of length L, $\mathbf{H}(t)$ sets to:

$$\mathbf{H}(t) = \begin{pmatrix} \mathbf{h}_{1,1}(t) & \mathbf{h}_{1,2}(t) & \dots & \mathbf{h}_{1,N_t}(t) \\ \mathbf{h}_{2,1}(t) & \mathbf{h}_{2,2}(t) & \dots & \mathbf{h}_{2,N_t}(t) \\ \vdots & \vdots & \ddots & \vdots \\ \mathbf{h}_{N_r,1}(t) & \mathbf{h}_{N_r,2}(t) & \dots & \mathbf{h}_{N_r,N_t}(t) \end{pmatrix} \tag{2.5}$$

Each vector of $\mathbf{H}(t)$ corresponds to the multipath channel gains between each transmit ν and receive ϱ antennas as follows:

$$\mathbf{h}_{\varrho\nu}(t) = \left[h_{\varrho\nu}(t)^1 \; h_{\varrho\nu}(t)^2 \cdots h_{\varrho\nu}(t)^L \right] \tag{2.6}$$

where L is the number of paths.

After that, the received signal vectors at each antenna are demodulated using an OFDM demodulator resulting in the matrix $\mathbf{Y}(k)$ of size $N_r \times N$, where N is the number of sub-carriers, and each column vector in $\mathbf{Y}(k)$ includes the received data for each sub-carrier. The active transmit antenna index and the emitted symbol can be recovered using one the detectors that will be described in the next section.

2.8 SM-OFDM detectors

The transmit antenna index is combined with the symbol index by the SM mapper. Hence, only these parameters have to be estimated at the receiver. The detection techniques of SM-MIMO system could be divided into four fundamental categories as

described in [140]: matched filter (MF) based detection in [128], maximum likelihood (ML) detection in [81, 129], sphere decoding (SD) [141, 142], and hybrid detection which combines the modified MF concept, the reduced complexity exhaustive ML search of [143, 144], and other detectors as signal vector based list detection (SVD) in [145]. An overview of the various detection techniques conceived for SM-related schemes is seen in Fig. 2.8.

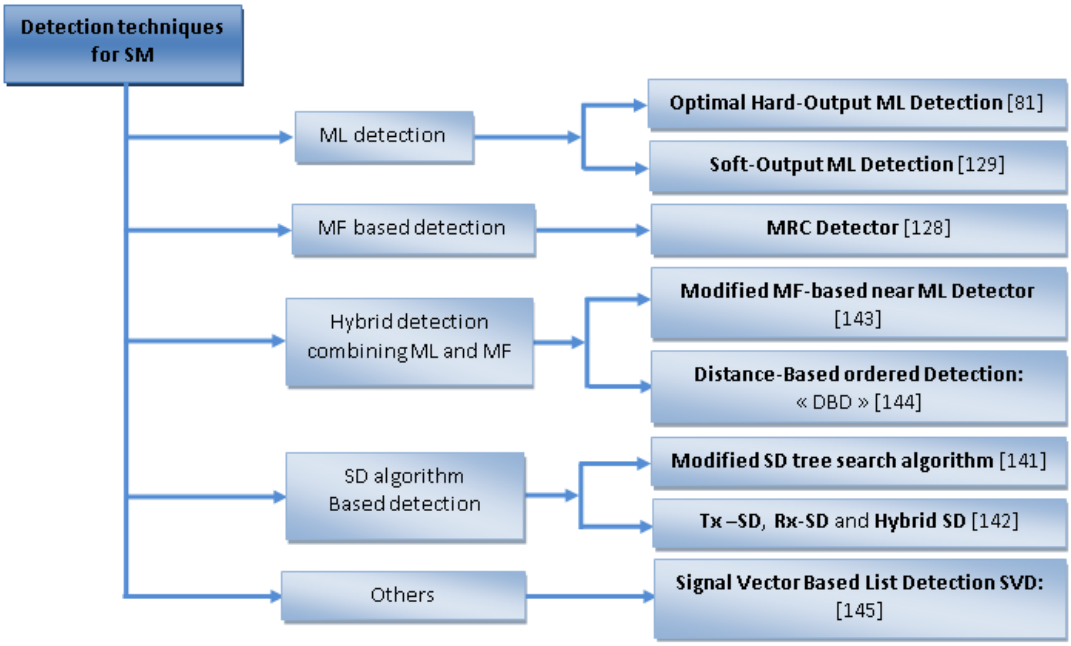

Figure 2.8 — Overview of SM detectors.

2.8.1 Zero Forcing (ZF) equalizer

An equalizer is a digital filter that is used to mitigate the effects of ISI that is introduced by a time dispersive channel. OFDM modulation could be used for this purpose but, zero forcing (ZF) equalizer is viewed as an element-wise division of the OFDM demodulated signal by the transfer function of the discrete frequency channel response. The so-mentioned channel transfer function is computed by a DFT of the zero-padded discrete time channel impulse response. It follows that the per-carrier ZF is performed as:

$$\tilde{\mathbf{z}}^c(k) = \frac{\mathbf{y}^c(k)}{\mathbf{h}_j^c(k)} \tag{2.7}$$

However, for SM, spatial location of the transmit antenna index, from which the symbol was transmitted, needs to be estimated. This is done by finding the location of the maximum absolute value of the output vector from the ZF equalizer $\tilde{\mathbf{z}}(k)$ for each sub-carrier c, which is described in the following equation:

$$\hat{j}^c = arg\max_j |\tilde{\mathbf{z}}^c(k)| \quad for \quad j = \{1, 2, ..., N_t\}, \quad c = \{1, 2, ..., N\} \tag{2.8}$$

where $\hat{j}$ denotes the estimated value of the antenna index for each sub-carrier c. Then, the symbol is detected using the following equation:

$$\hat{q}^c = Q(\tilde{\mathbf{z}}^c(k)_{(j=\hat{j})}) \tag{2.9}$$

Assuming correct estimates for $\hat{j}$ and $\hat{q}$, the receiver can straightforwardly de-map the original information bits.

2.8.2 Minimum Mean Square Error (MMSE) detection

A minimum mean square error (MMSE) algorithm describes the approach which minimizes the mean square error (MSE) between two entities. MSE, refers to the estimation in a quadratic cost function in a Bayesian setting. The MMSE algorithm provides a balanced solution to the problem of reducing the effects of both interference and channel noise enhancement plaguing the ZF equalizer, whereas the ZF receiver removes only the interference components in the output. Therefore, our pair of transmit antenna index and the transmitted symbol are obtained by following these steps:

First, the MMSE-based equalizer is applied to the received signal as follows:

$$\tilde{\mathbf{z}}^c(k) = (\mathbf{h}_j^c(k))^H[(\mathbf{h}_j^c(k))^H * \mathbf{h}_j^c(k) + \sigma_w^2\mathbf{I}]^{-1}\mathbf{y}^c(k) \tag{2.10}$$

Then, the estimate of the transmit antenna index is computed by:

$$\hat{j}^c = arg\max_j |\tilde{\mathbf{z}}^c(k)| \tag{2.11}$$

Finally, the transmitted symbol is computed using the quantization function, in a similar way as described in eq. (2.9).

2.8.3 Maximum likelihood sequence estimation (MLSE)

The ML detection, which is based on maximum likelihood sequence estimation (MLSE), is a detection scheme that calculates the minimum Euclidean distance between the received signal and all possibly transmitted sequences. An example of such a detection scheme and the search for the closest lattice point is performed in [146] for general MIMO case and is carried out in [147] for SM-MIMO case. ML estimates the combination of antenna index and transmit symbol at one shot, given by the expression:

$$[\hat{j}^c, \hat{q}^c] = arg \min_{j,q} \|\mathbf{y}^c(k) - \mathbf{h}_j^c(k)\mathbf{x}_q\|_F^2 \tag{2.12}$$

2.8.4 Optimal detection (OD)

This detector follows a different rule compared to the detectors mentioned above. Let us assume that the transmitted signals are equally likely, as in [81], the optimal detector based on ML is given as:

$$[\hat{j}, \hat{q}] = arg \max_{j,q} p_y(\mathbf{y}|\mathbf{x}_{j,q}, \mathbf{H}) \tag{2.13}$$

$$= arg \min_{j,q} (\|\mathbf{g}_{jq}\|_F^2 - 2Re\{\mathbf{y}^H \mathbf{g}_{jq}\}) \tag{2.14}$$

where $\mathbf{g}_{jq} = \mathbf{h}_j \mathbf{x}_{j,q}$, $1 < j < N_t$, $1 < q < M$, M being the modulation order and $p_y(\mathbf{y}|\mathbf{x}_{j,q}, \mathbf{H}) = \pi^{-N_r} exp(-\|\mathbf{y} - \mathbf{H}x_{jq}\|_F^2)$ is the PDF of $\mathbf{y}$, conditioned on $\mathbf{x}_{jq}$ and $\mathbf{H}$. It can be seen that optimal detection requires a joint detection of the antenna indices and symbols, as opposed to the schemes outlined in ZF and MMSE techniques, where the problem is decoupled.

2.8.5 Signal vector-based detector (SVD)

The SVD principle is based on the observation that the received vector $\mathbf{h}_j \mathbf{x}_q$ has the same direction of $\mathbf{h}_j$, without consideration of the noise, as described in [145]. Based on the assumption that the entries of the channel vectors are distributed independently, we can conclude that the index of channel vector with the smallest-included angle with $\mathbf{y}$ corresponds to the expected one. The direction is found by estimating the angle θ_j^c

between $\mathbf{h}_j^c$ and $\mathbf{y}^c$, as follows:

$$\theta_j^c = arccos \frac{\|\langle \mathbf{h}_j^c(k), \mathbf{y}^c(k) \rangle\|_F}{\|\mathbf{h}_j^c(k)\|_F \|\mathbf{y}^c(k)\|_F} \tag{2.15}$$

Then, the transmit antenna index is estimated by:

$$\hat{j}_{SVD}^c = arg \min_j \theta_j^c \qquad j = \{1, ..., N_t\} \tag{2.16}$$

Finally, assuming that the traditional QAM demodulation is performed to recover the constellation symbol, the transmitted symbol can be estimated as:

$$\hat{q}_{SVD}^c = arg \min_q \|\mathbf{y}^c(k) - \mathbf{h}_{jSVD}^c(k) x_q\|_F^2 \quad q = \{1, ..., M\} \tag{2.17}$$

2.8.6 Distance-Based ordered Detection (DBD)

The distance-based ordered detection algorithm achieves an ordered sequence of antenna indices based on the distances between the estimated symbols and their demodulation constellations [144]. First, for DBD algorithm, the received vector $\mathbf{y}$ is multiplied by the pseudo-inverse of $\mathbf{h}$ as:

$$\mathbf{z}^c(k) = (\mathbf{H}^\dagger)^c(k) \mathbf{y}^c(k) \quad j = \{1, 2, ..., N_t\} \quad c = \{1, 2, ..., N\} \tag{2.18}$$

Then the estimated symbol $\hat{x}_q$ is obtained by the demodulator as described in the following expression.

$$\hat{x}_q^c = Q(z^c(k)) \tag{2.19}$$

Let $d_{j,q}^c$ denotes the distance between $\hat{x}_q$ and all possibly values of the transmitted sequences x_q by applying this following equation:

$$d_{j,q}^c = \|\mathbf{h}_j^c(k)\| |\hat{x}_q^c - x_q| \tag{2.20}$$

Hence the estimated antenna index $\hat{j}$ and the corresponding modulated symbol x_q are obtained by:

$$[\hat{j}^c, \hat{q}^c] = \min_{j,q} (d_{j,q}^c) \tag{2.21}$$

2.8.7 Multiple stage detection

1. **Multiple stage-scheme using ZF equalizer:**
   The transmit antenna index is estimated in the first stage by using ZF equalizer followed by the symbol estimation using OD principle in the second one.

   - **First stage**: The transmit antenna index is estimated by applying eq. (2.7), followed by the eq. (2.8) respectively.
   - **Second stage**: The OD criterion is then employed in order to obtain a symbol estimate based on the asumption that the transmit antenna index found in the first stage is the one activated.

$$\hat{q}^c = \min_{j,q}(\|\mathbf{h}^c_{(j=\hat{j})}(k)\mathbf{x}_q\| - 2Re\{\mathbf{y}^H\mathbf{h}^c_{(j=\hat{j})}(k)\mathbf{x}_q\}) \tag{2.22}$$

2.8.8 Sphere decoder (SD)

Sphere decoding (SD) method consists on searching the transmitted signal vector that has the minimum ML metric. Hence, a sphere that contains a set of vectors among all possible transmitted signal vectors is considered [148]. This technique is based on adjusting the sphere radius until there exists a single ML solution vector within this sphere. Otherwise, when there is no vector within the sphere, the radius is subsequently increased.

Therefore, SM-SD focused on finding the paths that lead to point $(\hat{j}, \hat{q})$ which has an error less than or equal to the sphere radius R.

The initial radius is a function of the noise variance as expressed in eq. (2.23) and depicted in [141].

$$R^2 = \eta N_r \sigma_n^2 \tag{2.23}$$

where σ_n^2 is the noise variance and η is a constant based on experience, chosen to maximize the probability $1 - \epsilon$, of having at least one point inside the sphere. Hence, in the aim to avoid the exhaustive search of ML and for the seek of a lower detector complexity, an appropriate value of η should be chosen, from the ones pre-defined by a computer search, as depicted in Table. 2.4.

η	1.1	1.2	1.3	1.4
$1-\epsilon$	0.9755663	0.9861741	0.9923018	0.9957736
η	1.5	1.6	1.7	1.8
$1-\epsilon$	0.9977082	0.9987707	0.9993470	0.9996562
η	1.9	2.0	2.1	2.2
$1-\epsilon$	0.9998204	0.9999068	0.9999520	0.9999754
η	2.3	2.4	2.5	2.6
$1-\epsilon$	0.9999874	0.9999936	0.9999967	0.9999983
η	2.7	2.8	2.9	3.0
$1-\epsilon$	0.9999991	0.9999995	0.9999998	0.9999999

Table 2.4 — Values of η based on the probability $1-\epsilon$ [149].

Several algorithms of SD exist in literature; one of them is the RX-SD algorithm, which is especially suitable when the number of receive antennas N_r is very large, and reduces the size of the search space related to the multiple antennas at the receiver (we refer to this search space as "receive search space").

The detector can formally be written as follows:

$$[\hat{j}^c, \hat{q}^c] = \min_{j\in\{1,2,...,N_t\} q\in\{q_1,q_2,...,q_M\}} \{ \sum_{r=1}^{\tilde{N}_r(j,q)} \mid \mathbf{y}_r^c - \mathbf{h}_{j,r}^c \mathbf{q} \mid^2 \} \tag{2.24}$$

More specifically, the receiver calculates the set of optimal $\tilde{N}_r(l,s)$ for $j \in \{1,2,...,N_t\}$ and $\mathbf{q} \in \{q_1, q_2, ..., q_M\}$ as follows:

$$\tilde{N}_r^c(j,q) = \min_{n\in\{1,2,...,N_r\}} \{ \sum_{r=1}^{n} n \mid \mathbf{y}_r^c - \mathbf{h}_{j,r}^c \mathbf{q} \mid^2 > R^2 \} \tag{2.25}$$

In other words, the receiver keeps combining the signals for each $j \in \{1,2,...,N_t\}$ and $q \in \{q_1, q_2, ..., q_M\}$ until the Euclidean norm in (2.24) gives a point that lie inside a sphere of radius R and centered around the received signal itself.

2.8.9 Simulation results

We consider the following parameters in the simulation: Rayleigh channel model with $L = 7$ taps configuration is retained, the FFT size is set to 128 and 4 antennas are considered at the transmitter and the receiver sides, BPSK modulation is retained. First, the receiver is assumed to have full channel knowledge and perfect time and frequency synchronization are considered. The receive antennas are assumed separated sufficiently

such that to avoid spatial correlation. Fig. 2.9 demonstrates the BER performance of the system when considering MIMO channel model. As expected, the performance of SM is operated by ZF, MMSE, MLSE, DBD, OD, SVD and SD. ZF and MMSE are suboptimal detection schemes, which performances are inferior to MLSE, OD, DBD, SVD and SD detectors, mainly because antenna indices are not accurately estimated. The channel matrices in this case are not orthogonal and a linear detection, such as ZF scheme, has a limitation to estimate antenna indices accurately, as compared to OD and DBD detectors.

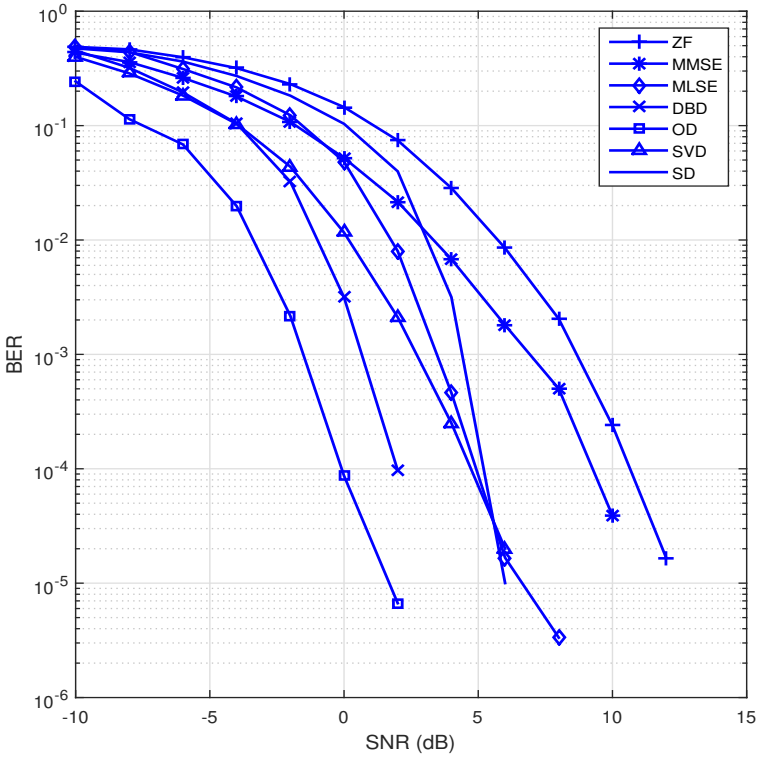

Figure 2.9 — Performance of SM-OFDM detectors.

2.9 Performance of SM-OFDM Detectors over Adverse Nakagami-m Fading

2.9.1 Channel impairments

1. **Spatial correlation**

   In a practical multipath wireless communication environment, the wireless channels

perceived by the antenna elements are not independent from each other due to scatterings in the propagation paths. This kind of correlation is called spatial correlation. One possible model for $\mathbf{H}$ that takes the spatial fading correlation into account, splits it into two independent components namely the receive $\mathbf{R}_r$ and the transmit correlations $\mathbf{R}_t$ .Thus $\mathbf{H}$ is modelled as follows:

$$\mathbf{H} = \mathbf{R}_r^{1/2}\mathbf{H}_w\mathbf{R}_t^{1/2} \tag{2.26}$$

where $\mathbf{H}_w$ is a matrix with independent Gaussian elements, and the superscript $(.)^{\frac{1}{2}}$ stands for the Hermitian square root of a matrix. The diagonal entries of $\mathbf{R}_t$ and $\mathbf{R}_r$ are constrained to be equal to unity. The correlation matrices $\mathbf{R}_t$ and $\mathbf{R}_r$ can be measured or computed by assuming the scattering distribution around the transmit and receive antennas. For uniform linear array at the transmitter and the receiver sides, $\mathbf{R}_t$ and $\mathbf{R}_r$ can be calculated according to [150]. Because of the adopted SM modulation scheme, one transmit antenna is concerned at each time instant. Therefore the transmit correlation is not of interest. It follows that the correlated channel becomes:

$$\hat{\mathbf{H}} = \mathbf{R}_r^{1/2}\mathbf{H} \tag{2.27}$$

where $\mathbf{R}_r \in R^{N_r \times N_r}$ is a matrix that has the following Toeplitz structure correlation:

$$\mathbf{R}_r = \begin{bmatrix} 1 & \alpha & \dots & \alpha^{N_r-1} \\ \alpha & 1 & \dots & \alpha^{N_r-2} \\ \vdots & \vdots & \ddots & \vdots \\ \alpha^{N_r-1} & \alpha^{N_r-2} & \dots & 1 \end{bmatrix} \tag{2.28}$$

where $\alpha = exp(-\beta)$, with β being the correlation decay coefficient set to $\frac{2\pi}{\lambda}dsin\phi$, with λ being the wavelength, d the inter-element spacing and ϕ describing the angle of arrival (AOA) offset. The channel coefficients are said to be perfectly correlated when $0 < \alpha << 1$.

2. **Imperfect channel state information (I-CSI)**

Most of research works assume that the channel estimation errors are mitigated, thereby adopting error free (perfect) or erroneous (imperfect) CSI. In practice, this should be considered by formulating the estimated channel matrix as follows [151]:

$$\hat{\mathbf{H}} = \rho\mathbf{H} + (1-\rho)\lambda^{N_r \times N_t} \tag{2.29}$$

where λ is a normal distributed random variable with zero mean and unit variance. The coefficient $0 < \rho < 1$ is a factor that determines the similitude of the estimated CSI to the actual one. Perfect CSI estimation is achieved when $\rho = 1$.

3. **Correlated and erroneous channel**
   We assume that we combine both spatial correlation at the receiver and the erroneous CSI, rendering equations (2.27) and (2.29) as follows:

$$\hat{\mathbf{H}} = \rho\mathbf{R}_r^{1/2}\mathbf{H} + (1-\rho)(\lambda)^{N_r \times N_t} \tag{2.30}$$

where the overall channel model in eq. (2.30) is obtained by the variation of the two parameters α and ρ.

2.9.2 Simulation results

For the results depicted in Fig. 2.10, the used error correction codes, are half rate convolutional codes obtained with the generator polynomial (7,5). Furthermore, for simplification purposes, each frame comprises one OFDM block, the bit interleaver is random and the evaluated coded BER performance is the one reached by adopting 8 bits per subcarrier and 64 QAM modulation scheme. Fig. 2.10 compares the achieved BER performance for different values of m, and different correlation and CSI conditions, when adopting the three presented detectors. Rayleigh channel scenario, obtained when $m = 1$, is compared against purely Nagakami channel, simulated with $m = 10$. Furthermore, uncorrelated ideally estimated channels are herein taken as a reference and are obtained by setting the values of ρ and α to one and zero, respectively. From this figure it can be seen that, in ideal channel conditions, Nagakami channel is more favorable to communication than Rayleigh channel, whatever is the used detector. This

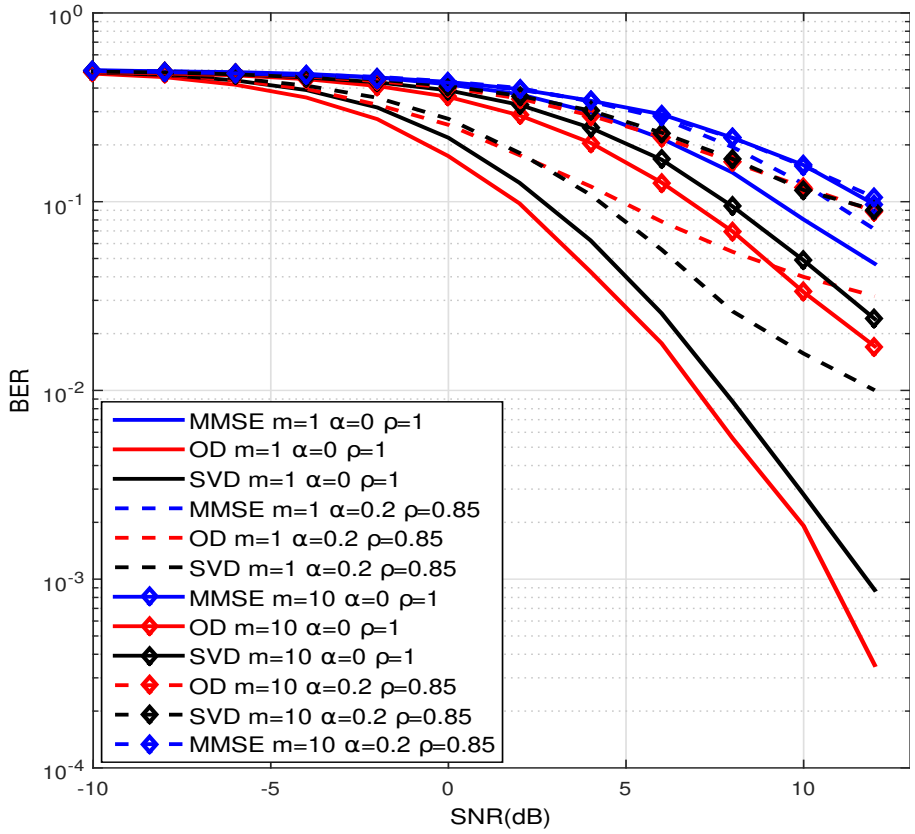

Figure 2.10 — Comparison of the achieved BER performances of three different SM-OFDM architectures in Nakagami channel with different CSIs and correlations.

was expected because of the high scattering level characterizing propagation in Rayleigh channel (uncorrelated perfectly known channel). Performance gain in Nakagami channel is negligeable when opting for a given detector over the others, unlike in Rayleigh channel where OD exhibits the best performance and MMSE is the least performing, which cosolidates the observations reported in different references [151]. This is mainly due to the lack of accuracy in estimating the values of antenna indices in MMSE. The attained data reliability is quite interesting since low BER values are provided at reasonable SNR levels. However, as shown in this figure, increasing slightly the receive spatial correlation and CSI imperfection levels, has a drastic degradation effect on the data reliability, more particularly in purely Nagakami channel.

2.10 Summary

This chapter has presented the recent research progress on 1-D and multidimensional IM techniques. Moreover, considerations regarding the utilization of these IM schemes for next-generation wireless communication are provided. Especially, IM schemes presented in the literature have been first grouped regarding their application scopes. Later, we have discussed the operating principle of SM-MIMO and SM-OFDM-based schemes. The performance of SM-OFDM modulation over Nagakami-m fading channel of different detectors is also investigated in this chapter. In addition to the space correlation encompassed in Nakagami model, the performance is depicted under the constraints of a spatial correlation and the availability of only imperfect channel state information. It was found that, in ideal correlation and CSI conditions, and assuming Rayleigh fading, SM-OFDM with OD detector outperforms MMSE and SVD alternatives. Nakagami channel offers a more favorable propagation scenario, and the attained BER performance is quite viable. Moreover, SM-OFDM was shown to be quite sensitive to the increase of spatial correlation and CSI imprecisions, regardless of the used detector and the considered channel.

CHAPTER 3

Chapter 3: Performance analysis of multiuser SM architectures

3.1 Introduction

One of the techniques which are likely to be adopted in the forthcoming wireless communication standards is the so-called spatial modulation (SM). However, the wireless channels pertaining to such standards will mostly be frequency selective because of the involved high data rates, and SM technique alone can not overcome the resulting signal distorsion. In this context, orthogonal frequency division multiplexing (OFDM) has been used as an efficient solution to combat this impediment. Obviously, new SM solutions in the presence of single/multiple users communicating in frequency selective channels should be targeted. To fulfill such a need, a new SM-based architectures incorporating OFDM and CDMA are proposed in this chapter. In addition, other SM-multicarrier transmission data techniques like (GFDM and OTFS) are also presented.

3.2 SM-GFDM based scheme

For SM multicarrier schemes, one transmit antenna is active and the other kept silent at each subcarrier. Therefore inter-antenna interference (IAI) and inter-antenna synchronization (IAS) are efficiently avoided and significant complexity reduction is provided. Resulting from these improvements, SM-GFDM system has a potential to bring all of the advantages of GFDM scheme to MIMO setups without increasing the system cost and complexity. The proposed SM-GFDM system is presented in Fig. 3.1.

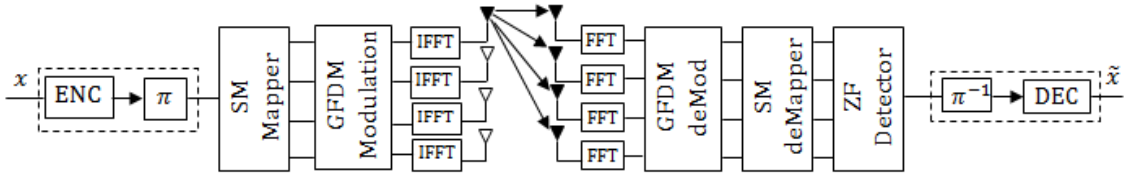

Figure 3.1 — SM-GFDM bloc transceiver

3.2.1 SM-GFDM transmitter side

At the transmitter side, as described earlier, spatial modulator processes the incoming bits in blocks of size $b_{SM} = log_2(N_t) + log_2(M)$, and arranges each in a matrix $\mathbf{X}$ of size $N_t \times NM$, where each row vector $\mathbf{x}_j$ contains the symbols to be transmitted from the transmit antenna j and each column vector contains the symbols to be transmitted on the c^{th} subcarrier and m^{th} subsymbol. First $log_2(N_t)$ bits of the block identify the row of the matrix and the $log_2(M)$ bits select the symbol from the signal constellation diagram. Then, selected symbol is placed in an empty column on the corresponding row. When a symbol is placed in a column, all other elements in that column are set to zero. As a result, the matrix $\mathbf{X}$ has one non-zero element in each column. Therefore, at each GFDM subcarrier, only one antenna transmits the information symbol selected from signal constellation and all other antennas remain silent. Then, each row vector $\mathbf{x}_j$ is modulated using a GFDM modulator. GFDM is a circularly-filtered multicarrier communications scheme, which consists of N subcarriers, each filtered with a circular transmit filter, and each block contains M subsymbols on each subcarrier. The total number of symbols becomes $N \times M$. The system is modeled in the digital baseband and the overall GFDM transmit signal $\mathbf{x}(n)$ is given by:

$$\mathbf{x}(n) = \sum_{c=0}^{N-1} \sum_{m=0}^{M-1} d_{c,m} g_{c,m}[n] \quad n = \{0, ..., (N \times M) - 1\} \tag{3.1}$$

where n denotes the sampling index, $d_{c,m}$ denotes the complex valued data sub-symbol, taken from an MPSK or MQAM constellation, and $g_{c,m}[n] = g[(n - mN)_{mod\,(N \times M)}] \exp\left(j2\pi \frac{cn}{N}\right)$ is the transmit filter circularly shifted to the m^{th} sub-symbol and modulated to the c^{th} subcarrier, where *mod* stands for the modulo function. The collection of the filter samples in a vector $\mathbf{g}_{c,m} = [\ g_{c,m}[0] ... g_{c,m}[(N \times M) - 1]]^{\ T}$ allows to formulate (3.1) as:

$$\mathbf{x} = \mathbf{A} \times \mathbf{d} \tag{3.2}$$

where $\mathbf{d}$ is a column vector containing $d_{c,m}$ as its $(mN + c)^{th}$ element and $\mathbf{A}$ is a $NM \times NM$ transmitter matrix [152] with the following structure:

$$\mathbf{A} = [\ \mathbf{g}_{0,0} \cdots \mathbf{g}_{N-1,0} \quad \mathbf{g}_{0,1} \cdots \mathbf{g}_{N-1,1} \cdots \mathbf{g}_{N-1,M-1}] \tag{3.3}$$

The figure 3.2 shows how each bit block of size b_{SM} is mapped to each transmit symbol according to signal constellation. The mapping mechanism is designed for 4-QAM constellation where each transmit symbol is assigned to a particular transmit antenna which is 4 in number for this case. The transmit symbol selected according to the mapping table is spread by a vector of ones, $[1 \quad 1 \quad 1 ..... 1]^T$ of a size equal to the number of time-slots in each GFDM subcarrier. The spread data vector is then allocated to a subcarrier corresponding to a specific transmit antenna as determined by the mapping table. All the other subcarriers of that particular transmit antenna are loaded with zeros. Afterwards, GFDM modulation steps are applied on this set of subcarriers, while the other transmit antennas perform the same transmit side GFDM processing on a set of subcarriers which contain zero data in the time slots. So, output from the other transmit antennas corresponding to this particular symbol instant is zero. This procedure is repeated for all the incoming symbols in the mapped symbol stream. As a consequence, if transmit antenna 1 transmits a 64 sample length GFDM data stream with $N = 4$ subcarriers and $M = 16$ time-slots corresponding to incoming symbol $1 + j$, then the antennas 2, 3 and 4 transmit a stream of zeros of length 64 samples corresponding to the data block transmitted by the 1^{st} antenna. The same holds true for antennas 2, 3 and 4 which, later, transmit a GFDM data stream corresponding

to symbols $1-j$, $-1+j$ and $-1-j$, respectively. Moreover, this scheme also avoids self-ICI between time-slots of adjacent subcarriers because, at any symbol instant, only one subcarrier corresponding to the particular mapped transmitter antenna is active.

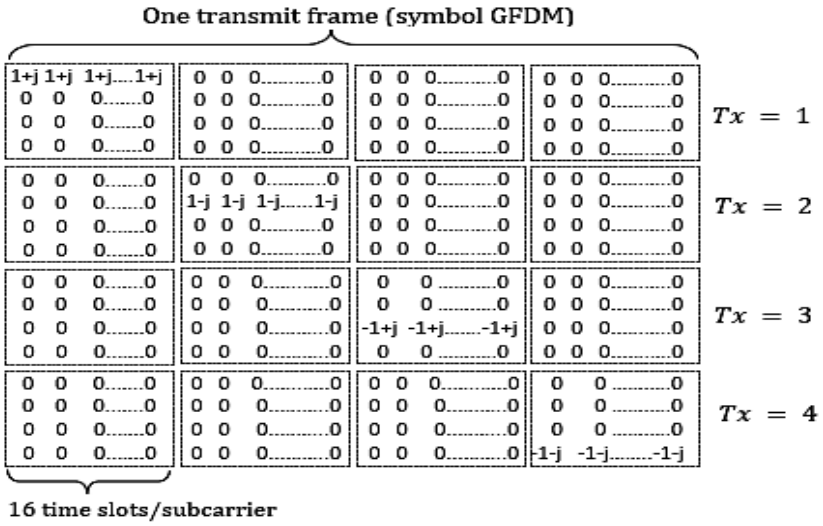

Figure 3.2 — Antenna Index Selection, Transmit Symbol Spreading and specific subcarrier allocation

3.2.2 SM-GFDM receiver side

At the receiver side, first, OFDM demodulation is performed by FFT transform, since GFDM demodulation must be performed before the spatial demodulation. After that, and in the aim of limiting the receiver complexity, a suboptimal detection approach (ZF, for instance) is preferred, hence, allowing to recover the original symbol at the reception.

3.3 SM-OTFS system architecture

3.3.1 System model

A number of system improvements incorporating OTFS were proposed in literature, since the first paper in [54]. All these works have studied OTFS over time-variant (high Doppler) wireless channels, a formal analysis and claim on the performance achieved by SM-OTFS is yet to appear. Filling this gap, our contribution in this section provides a formal study of the benefits achieved by coupling spatial modulation and OTFS and compare the resulting scheme with SM-OFDM and SM-GFDM alternatives. Let us consider an $N_r \times N_t$ MIMO SM-OTFS-based system, as illustrated in Fig. 3.3. As

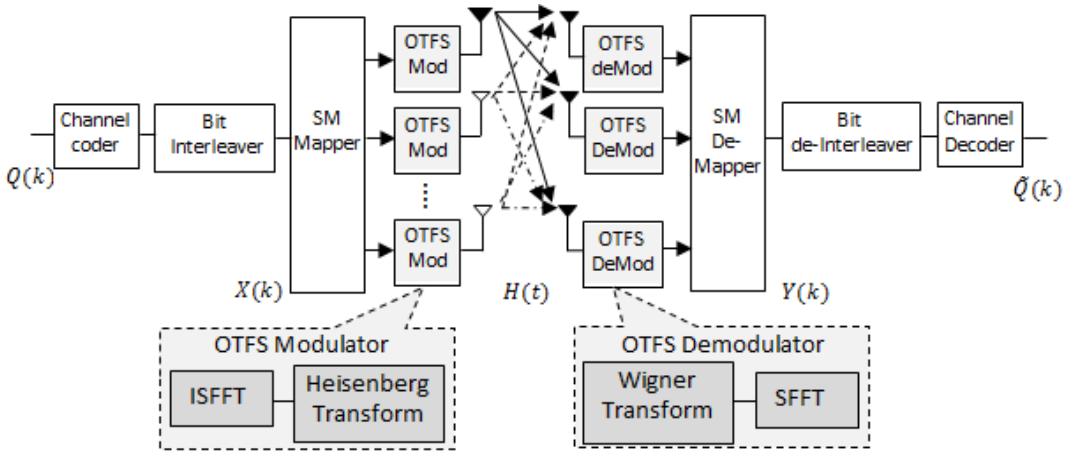

Figure 3.3 — SM-OTFS System architecture.

discussed earlier, the key feature of SM is that each block is divided into two sub-blocks, one indicating the activated transmit antenna index, and the other one dedicated to the constellation symbol taken from the total number of symbols M, and transmitted over the activated antenna. Thus, as shown in Fig. 3.3, after insertion of error correction codes in the original data and its interleaving, SM mapping is applied on the resulting signal, as explained above, and the SM block is transformed to the time domain by applying OTFS modulation. This latter is produced by a cascade of two 2D transforms at both the transmitter and the receiver. The modulator first maps the SM information symbols in the delay-Doppler domain to symbols in the time-frequency domain using inverse symplectic finite Fourier transform (ISFFT). Next, the Heisenberg transform is applied to time-frequency symbols to create the time domain signal transmitted over

the wireless channel. The multipath signal received at the ϱ^{th} antenna element from the ν^{th} transmit antenna could be written as:

$$\mathbf{y}_{\varrho}(t) = \mathbf{h}_{\varrho\nu}(t) \otimes \mathbf{x}_{\nu}(t) + \mathbf{w}(t) \tag{3.4}$$

where $\mathbf{x}_{\nu}(t)$ is the signal emanating from the ν_{th} activated antenna, $\mathbf{w}(t)$ is the additive white gaussian noise vector with $CN(0, \sigma^2)$ elements, $\otimes$ denotes the time convolution operator and $\mathbf{h}_{\varrho\nu}(t) = \left[h_{\varrho\nu}(t)^1 \; h_{\varrho\nu}(t)^2 \cdots h_{\varrho\nu}(t)^L)\right]$ is the $L \times 1$ channel vector between each pair of transmit-receive antennas containing the L multipath channel gains.
At the receiver, the resulted signal is mapped to the time-frequency domain through the Wigner transform (the inverse of the Heisenberg transform), and then to the delay-Doppler domain using SFFT, for symbol demodulation. A conventional OTFS zero-forcing (ZF) detection is considered. Channel decoding and de-interleaving are carried-out and the transmit antenna index and symbol are finally recovered.

3.3.2 Simulation results

This section investigates the BER performance of the proposed scheme, when convolutional codes with half rate with the generating polynomial (7,5) are retained, the bit interleaver is the random one, and the selected modulation scheme is $8QAM$, and

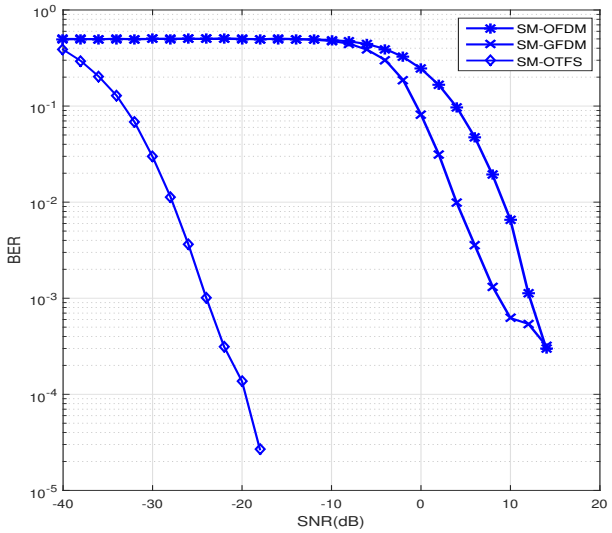

Figure 3.4 — BER performance analysis of SM-OTFS compared with SM-OFDM and SM-GFDM at T=16, K=4, FFT=64, $N_t = N_r = 4$ and 8QAM modulation.

the FFT size is equal to 64. For comparison purposes, SM-OFDM architecture is investigated and taken as reference. The number of transmit and receive antenna is 4, respectively, and $L = 7$, and for simplification purposes, each frame comprises one OFDM and GFDM block. Furthermore, Fig. 3.4 illustrates the BER performance in terms of SNR in such a setting. It is shown that SM-OTFS technique yields a better error performance, as compared to SM-OFDM and SM-GFDM alternatives. We observe that OTFS outperforms OFDM by approximately 18 dB at a BER of 10^{-3}. This is probably due to the achieved constant channel gain over all transmitted symbols in OTFS, unlike OFDM-based case, where, the error performance is limited by the subcarrier with the lowest gain.

3.4 SM-STBC architecture

Space-time coding (STC) is a well-known technique to enable transmit diversity, and the Alamouti scheme is the most famous example. Alamouti presents a remarkably simple scheme to achieve transmit diversity with two transmit antennas without any loss of bandwidth efficiency [33]. Figure 3.5 depicts how the Alamouti scheme transmits two symbols, x_1 and x_2, over two symbol intervals (time periods). In the first symbol interval, the scheme transmits x_1 from antenna 1 and x_2 from antenna 2. In the next symbol interval, symbol $-x_2^*$ is transmitted from antenna 1 and x_1^* is emitted from antenna 2, where the superscript $*$ represents complex conjugate operation. The transmitted codeword is thus given as:

$$\mathbf{X} = \begin{pmatrix} x_1 & -x_2^* \\ x_2 & x_1^* \end{pmatrix} \tag{3.5}$$

Here, it is assumed that the channel gains are quasi-static (i.e., they are constant during two time slots). Then, the received signals at the single-antenna receiver over two time slots are presented as:

$$\mathbf{y} = [\mathbf{y}_1, \mathbf{y}_2]^T = \mathbf{h}\mathbf{X} + \mathbf{w} \tag{3.6}$$

where $\mathbf{y} = [y_1, y_2]^T$ is the complex received vector, $\mathbf{h} = [h_1, h_2]^T$ is the channel vector; and $\mathbf{w}$ is the complex AWGN noise vector. The case of having two active antennas (i.e., two RF chains) in SM is of great practical interest since it is only slightly more complex than the conventional SM scheme, while it offers both increased spatial diversity as

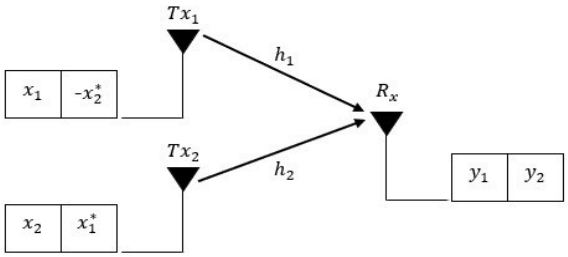

Figure 3.5 — Spatial diversity provided by using multiple transmit antennas.

well as higher transmission rate. The scheme proposed in [100], called space-time block coded spatial modulation (SM-STBC), makes use of the famous Alamouti STBC as a core. Based on this architecture, our proposed scheme presented in the figure. 3.6 extends the study to the more realistic frequency selective channels, where see, the transmit diversity is increased and high data rate can be achieved.
At the transmitter side, the input data sequence, is first encoded by a convolutional encoder, which consists of a concatenation of error correction, preceding an interleaving π module.

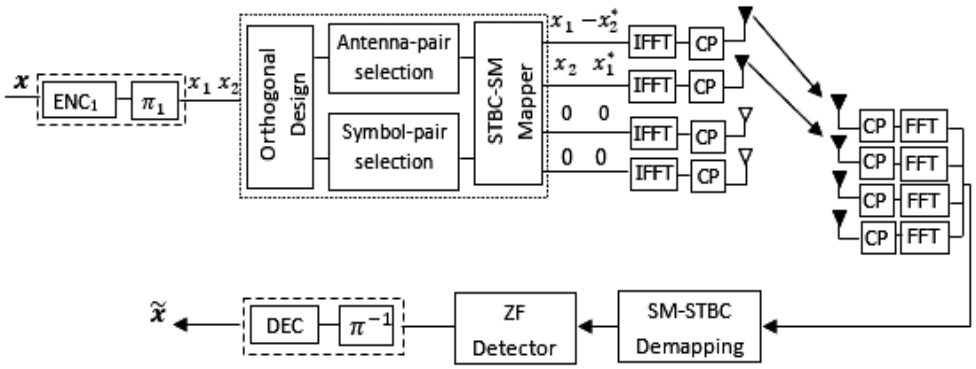

Figure 3.6 — SM-STBC-OFDM System block diagram

In the SM-STBC scheme, both STBC symbols and the indices of the transmit antennas from which these symbols are transmitted, carry information. Without loss of generality, we assume in the upsequent discussions that $N_t = N_r = 4$. In the proposed SM-STBC mapping, two complex information symbols (x_1, x_2), drawn from a MPSK constellation, are sent from two transmit antennas among four, in two symbol intervals in an orthogonal manner by the codeword $\mathbf{X}_j$, which corresponds to one component of

the mapping matrix represented by the codeword $\mathbf{X} = \{\mathbf{X}_1, \mathbf{X}_2, \mathbf{X}_3, \mathbf{X}_4\}$:

$$\{\mathbf{X}_1, \mathbf{X}_2\} = \left\{ \begin{pmatrix} x_1 & -x_2^* \\ x_2 & x_1^* \\ 0 & 0 \\ 0 & 0 \end{pmatrix}, \begin{pmatrix} 0 & 0 \\ 0 & 0 \\ x_1 & -x_2^* \\ x_2 & x_1^* \end{pmatrix} \right\} \tag{3.7}$$

$$\{\mathbf{X}_3, \mathbf{X}_4\} = \left\{ \begin{pmatrix} 0 & 0 \\ x_1 & -x_2^* \\ x_2 & x_1^* \\ 0 & 0 \end{pmatrix}, \begin{pmatrix} x_1 & -x_2^* \\ 0 & 0 \\ 0 & 0 \\ x_2 & x_1^* \end{pmatrix} \right\} \tag{3.8}$$

j refers to the transmit antenna index that indicates the pair of activated antennas, and rows and columns of the mapping matrix, correspond to the transmit antennas and the two time slots of the STBC coding, respectively.

Table.3.1 corresponds to the matrices of the proposed SM-STBC mapping. Note that during the two time slots, the channel is assumed constant.

Table 3.1 — Mapping table of SM-OFDM-STBC.

j	I/bits	Matrix	j	I/bits	Matrix
1	0000	$\begin{pmatrix} 1 & 1 & 0 & 0 \\ -1 & 1 & 0 & 0 \end{pmatrix}^T$	3	1000	$\begin{pmatrix} 0 & 1 & 1 & 0 \\ 0 & -1 & 1 & 0 \end{pmatrix}^T$
	0001	$\begin{pmatrix} 1 & -1 & 0 & 0 \\ 1 & 1 & 0 & 0 \end{pmatrix}^T$		1001	$\begin{pmatrix} 0 & 1 & -1 & 0 \\ 0 & 1 & 1 & 0 \end{pmatrix}^T$
	0010	$\begin{pmatrix} -1 & 1 & 0 & 0 \\ -1 & -1 & 0 & 0 \end{pmatrix}^T$		1010	$\begin{pmatrix} 0 & -1 & 1 & 0 \\ 0 & -1 & -1 & 0 \end{pmatrix}^T$
	0011	$\begin{pmatrix} -1 & -1 & 0 & 0 \\ 1 & -1 & 0 & 0 \end{pmatrix}^T$		1011	$\begin{pmatrix} 0 & -1 & -1 & 0 \\ 0 & 1 & -1 & 0 \end{pmatrix}^T$
2	0100	$\begin{pmatrix} 0 & 0 & 1 & 1 \\ 0 & 0 & -1 & 1 \end{pmatrix}^T$	4	1100	$\begin{pmatrix} 1 & 0 & 0 & 1 \\ -1 & 0 & 0 & 1 \end{pmatrix}^T$
	0101	$\begin{pmatrix} 0 & 0 & 1 & -1 \\ 0 & 0 & 1 & 1 \end{pmatrix}^T$		1101	$\begin{pmatrix} 1 & 0 & 0 & -1 \\ 1 & 0 & 0 & 1 \end{pmatrix}^T$
	0110	$\begin{pmatrix} 0 & 0 & -1 & 1 \\ 0 & 0 & -1 & -1 \end{pmatrix}^T$		1110	$\begin{pmatrix} -1 & 0 & 0 & 1 \\ -1 & 0 & 0 & -1 \end{pmatrix}^T$
	0111	$\begin{pmatrix} 0 & 0 & -1 & -1 \\ 0 & 0 & 1 & -1 \end{pmatrix}^T$		1111	$\begin{pmatrix} -1 & 0 & 0 & -1 \\ 1 & 0 & 0 & -1 \end{pmatrix}^T$

Simulation results

Figure. 3.7 illustrates the BER performance in terms of SNR in such a setting. It can be observed that, SM-STBC-OFDM technique yields a better error performance, as compared to the two remaining alternatives, regardless of the SNR level. Indeed, the former offers a SNR gain of 8 dB relative to SM-OFDM and of 15 dB relative to conventional SM, at a required BER of 10^{-2}. This is obviously due to the additional diversity offered by STBC configuration in the proposed solution. The impact of multi-path interference is observed to be important on the SM-scheme, since the performance gap between SM and SM-OFDM is considerable.

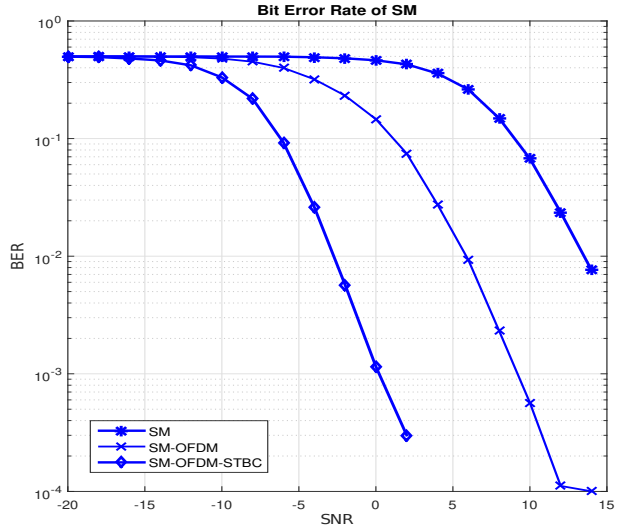

Figure 3.7 — BER performance of SM-STBC-OFDM at FFT=128, $N_t = N_r = 4$ and BPSK modulation.

3.5 Multiuser spatial modulation

Many SM-MIMO schemes have been studied by implicitly assuming a single-user transmission. However, this operating scenario is quite restrictive for typical cellular deployments, where many users may simultaneously transmit over the same resource block, aiming at maximizing the aggregate throughput at the cost of increasing the interference. Motivated by this consideration, the focus of this section is to investigate SM for multiuser communications. In the context of multiuser communications, the performance of both optimal and suboptimal receivers designed for SM-MIMO com-

munications has been investigated in the presence of multiple-access interference [153]. The authors in [154] study the error probability of SSK-MIMO by considering two receivers: (1) the single-user receiver, which is of low complexity, but it is oblivious to the interference; and (2) the optimum ML multiuser receiver, which is of high complexity, and has the benefit of being interference aware. In [155], the precoding-aided SM is applied to multiuser downlink transmission to resist a multiple-antenna eavesdropper. In particular, the authors design the signal precoding matrices to cancel the multiuser interference and modulate partial information bits on the indices of receive antennas (RAs). For uplink transmission, the achievable uplink spectral efficiency of a multicell massive SM-MIMO system relying on linear combining schemes is investigated in [156]. Motivated by the papers listed above, this section is concerned with uplink multiuser transmission between a base station and multiple users.

3.5.1 Code division multiple access (CDMA)

Code division multiple access (CDMA) is a concept using channel access method through a form of multiplexing that allows multiple signals occupying single transmission channel and optimizing the available bandwidth. This allowed for dramatic development of wireless communication in this century and gained a wide spread international use by cellular radio system [157]. CDMA is a form of spread-spectrum communications. The spread is done through pseudo random or orthogonal codes which are independent from the data. Consequently, multiple users can access the same frequency band at the same time [158], [159]. Unlike TDMA and FDMA, a completely different approach, realized in CDMA systems, does not attempt to allocate disjoint frequency or time resources to each user. Instead the system allocates all resources to all active users.

Types of Spread Spectrum Communications

Three ways to spread the bandwidth of the signal:

1. **Direct sequence spread spectrum (DSSS)**: The digital data is coded at a much higher frequency. In direct sequence (DS) CDMA systems, the narrowband message signal is multiplied by a very large-bandwidth signal called the spreading signal, where, the same carrier frequency is used by all users and can convey coded data simultaneously. Each user has its own spreading code, which is orthogonal

to the spreading sequences of the other users. Moreover, to detect the message addressed to a given user, a correlation operation is performed at the receiver. Hence, due to the decorrelation of the spreading signals, the resulted sequences from other users are considered as noise. In order to retrieve the data stream, the receiver utilizes the same spreading sequence used for coding at the transmitter. Each user operates independently with no knowledge of the other users (uncoordinated transmission). More specifically, the code is generated pseudo-randomly and the receiver generates the same code, correlates the received signal with that code to extract the data through the following steps:

- Signal transmission through: pseudo-random code generated differently for each channel and each successive connection, the information data modulates the spreading code, the resulting signal modulates a carrier, the resulted signal is amplified and transmitted.
- Signal reception through: the carrier is received, the received signal is mixed with a local carrier to retrieve the spread digital signal, a pseudo-random code is generated matching the one generated at the transmitter, the resulted signal is then correlated with the generated code, thereby extracting the information data.

2. **Frequency hopping spread spectrum (FHSS):** within this category, the signal switches rapidly between different hopping frequencies pseudo-randomly, the receiver knows in advance which frequency is of concern at any given time, and tunes the received signal accordingly to retrieve the original signal.

3. **Time hopping:** the signal is transmitted in short bursts pseudo-randomly, and the receiver knows in advance when to expect the burst.

Based on the concepts presented in this chapter, the following subsections introduce our proposed SM-based architectures along with the simulation results associated with them.

3.5.2 Multiuser SM scheme combining OFDM and CDMA

We consider a single-cell multiuser uplink MIMO system, in which the base station (BS) is equipped with N_t antennas serving K users. At the transmitter side, the input

data sequence $\mathbf{d}^k$ corresponding to the k^{th} user is first encoded by a convolutional encoder, which consists of a concatenation of error correction, preceding an interleaver $\pi^{(k)}$ module, from which the sequence $\mathbf{q}^{(k)}$ is generated. Let us consider the k^{th} user's encoding

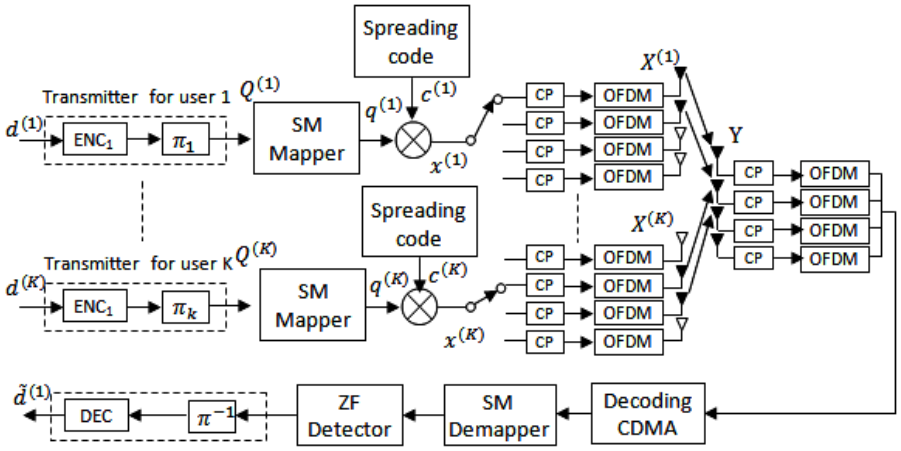

Figure 3.8 — SM-CDMA-OFDM system transceiver block diagram

procedure. The modulated signal $\mathbf{x}^{(k)}$ results from the Hadamard product between an array of the signal $\mathbf{q}^{(k)}$ repeated N_t times and the spreading code $\mathsf{c}^{(k)} \in \mathbf{C}^{N_t \times P}$. Mathematically expressed, the spread signal $\mathbf{x}^{(k)}$ is thus CDMA encoded through the following expression:

$$\mathbf{x}^{(k)} = \mathbf{q}^{(k)}. \quad \mathbf{c}^{(k)} \in \{-1, +1\}^{1 \times P} \tag{3.9}$$

$\mathbf{x}^{(k)}$ is the CDMA-modulated signal for the k^{th} user, $\mathbf{q}^{(k)}$ and is $\mathbf{c}^{(k)}$ are the transmit data and the spreading code, and P is length of the spreading code. Afterwards, in each transmitter, the input sequence is transformed to the time domain by applying the inverse fast Fourier transform (IFFT). Subsequently, a cyclic prefix (CP) is inserted to eliminate the inter-symbol interference (ISI) between OFDM symbols, and the resulting signals are transmitted over the channel. The multipath signal received at the ϱ^{th} antenna element from the ν^{th} transmit antenna could be written as:

$$\mathbf{y}_{\varrho}(t) = \sum_{i=0}^{K} \mathbf{h}_{\varrho\nu}^{k}(t) \otimes \mathbf{x}_{\nu}^{k}(t) + \mathbf{w}(t) \tag{3.10}$$

where $\mathbf{x}_{\nu}^{k}(t)$ is the signal emanating from the ν_{th} activated antenna of the k^{th} user, $\mathbf{w}(t)$ is the additive white Gaussian noise vector with $CN(0, \sigma^2)$ elements, $\otimes$ denotes the time convolution operator and $\mathbf{h}_{\varrho\nu}^{k}(t) = \left[h_{\varrho\nu}(t)^1 \; h_{\varrho\nu}(t)^2 \cdots h_{\varrho\nu}(t)^L)\right]$ stands for the

$L \times 1$ channel vector between each pair of transmit-receive antennas encompassing the L significant multipath channel components. At the receiver side, the stages are simply the reverse ordered operations of the transmitter side.

Simulation results

This section investigates the BER performance of the proposed SM-OFDM-CDMA scheme, when the number of users is varied. The channel of interest in this work is experiencing Rayleigh fading, in which omnidirectional antennas are adopted, despite the fact that opting for directional ones would have improved the performance [160]. $L = 7$ taps are present, the number of subcarriers in OFDM is set to 128, and convolutional codes with half rate with the generating polynomial (7,5) are retained. Furthermore, each frame comprises one OFDM block for simplicity, the bit interleaver is the random one, the selected modulation scheme is $8QAM$, and the length of the spreading code is $N_c = 128$. Fig. 3.9 illustrates the BER performance in terms of SNR

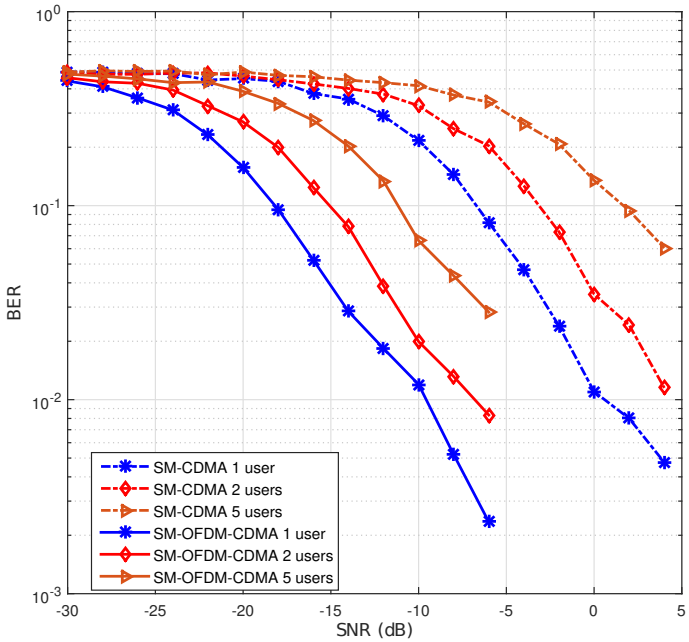

Figure 3.9 — Comparison of BER performance with the variation of the number of users.

in such a setting. As observed, the reliability of the data is altered by the users number increase, which is what was expected. However, the immunity of our proposed solution to such an interference is consolidated, since less than -2 dB in SNR level is required to

support 5 users simultaneously communicating with a BER which is inferior than 10^{-3} . By contrast, even though SM-CDMA alternative is taking in charge multiple access mitigation through the CDMA feature, it is shown to exhibit a lower performance than our proposal, because of the critical effect of multipath fading. Indeed, this architecture is not able to reach a BER of 10^{-3}, even in the presence of only one user.

3.5.3 Multiuser SM scheme combining STBC-OFDM and CDMA

Incorporating STBC in SM architectures has been envisaged lately for the improvement of the quality of reception [161]. Source information in that case is taken from the two STBC-coded symbols and the antenna indices. To the best of our knowledge, the performance of SM-STBC configurations has been investigated in the literature only in quasi-static Rayleigh channel. In frequency selective channels, orthogonal frequency division multiplexing modulation (OFDM) and its variants have been widely adopted. Very recently, STBC-OFDM design was used to yield a viable data link quality in such channels. However, no system has been proposed to support SM-STBC mapping in multiple access scenario and frequency selective channels. This section introduces a new architecture which aims at aligning with the future standard requirements, by encompassing STBC-OFDM structure in SM-CDMA design, thereby providing a data reliability per user. We consider in the proposed architecture presented in Fig. 3.10, a

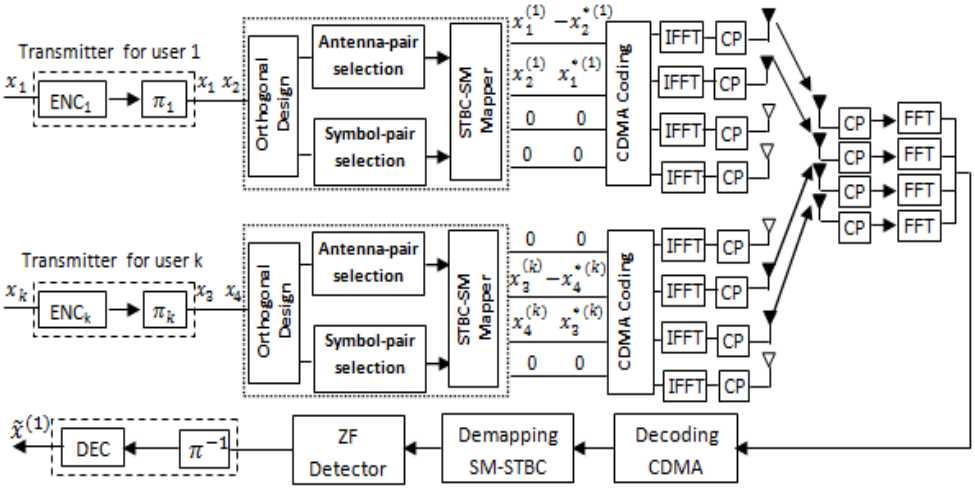

Figure 3.10 — SM-STBC-OFDM-CDMA System block diagram

single-cell multiuser uplink MIMO system, in which the base station (BS) is equipped with N_t antennas serving K users. At the transmitter side, the input data sequence corresponding to the k^{th} user, is first encoded by a convolutional encoder, which consists of a concatenation of error correction, preceding an interleaving $\pi^{(k)}$ module.

The encoded signal is then mapped with SM-STBC mapping and coded using CDMA multiple access technique as explained earlier. Afterwards, the resulted signal is transmitted over the channel to the receiver. At the receiver side, the stages are simply the reversed ordered operations of the transmitter side: first, OFDM demodulation is carried out, then, the resulting signal is despread via its multiplication by its corresponding user synchronized CDMA code. A decoding algorithm for SM is subsequently performed, then ZF decoding is adopted to recover the transmit antenna index and the transmitted signal. Finally, the channel decoding and de-interleaving operations are applied.

Simulation results

This section investigates the BER performance of the proposed scheme, when convolutional codes with half rate with the generating polynomial (7,5) are retained. Furthermore, each frame comprises one OFDM block for simplicity, the bit interleaver is the random one, and the selected modulation scheme is $BPSK$. For comparison

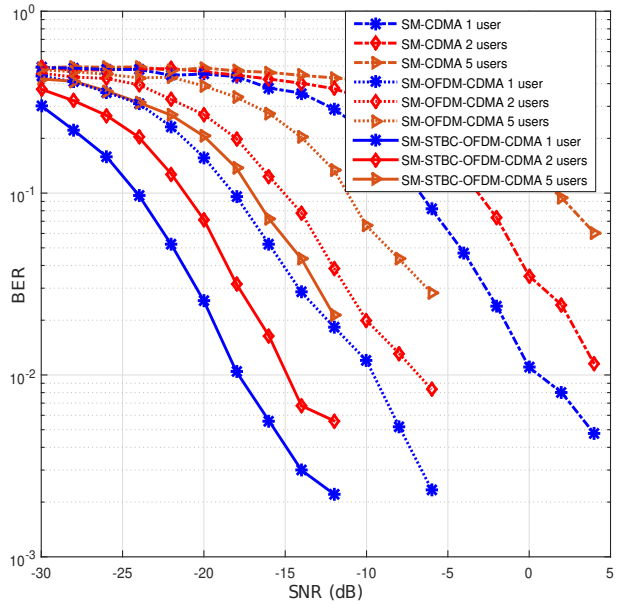

Figure 3.11 — Comparison of BER performance of SM-STBC-OFDM-CDMA with the variation of the number of users.

purposes, SM-CDMA and SM-OFDM-CDMA architectures are investigated. The number of users is varied $k = 1, 2, 5$, $P = 128$, $L = 7$, and $N_c = 128$. Fig. 3.11 illustrates the BER performance in terms of SNR in such a setting. It can be observed that, SM-STBC-OFDM-CDMA technique yields a better error performance, as compared to the two remaining alternatives, regardless of the number of users and SNR level. Indeed, the former offers a SNR gain of 8 dB relative to SM-OFDM-CDMA and of 18 dB relative to SM-CDMA, at a required BER of 10^{-2}. This is obviously due to the additional diversity offered by STBC configuration in the proposed solution. The impact of multipath interference is observed to be important on the SM-scheme, since the performance gap between SM-CDMA and SM-OFDM-CDMA is considerable. Despite the fact that the reliability of the data is altered by the increase of the multiple access interference, with the proposed solution, the performance is viable, even in adverse channel conditions, where the SNR is quite low.

3.5.4 Multiuser SM-scheme Combining STBC-OFDM and CDMA over Nakagami-m fading channel.

The performance of SM-STBC configurations has been investigated in the literature only in quasi-static Rayleigh channel. In frequency selective channels, OFDM and its variants have been widely adopted. Indeed, no system has been proposed to support SM-STBC mapping in multiple access scenario and frequency selective Nakagami-m channels. It is worthy to recall that Nakagami model is one of the most adopted to reflect different channel conditions, since it encompasses a wide range of models, from the pure Rayleigh to the one approaching deterministic behavior. This section introduces a new architecture which aims at aligning with the future standard requirements, by incorporating STBC-OFDM structure in SM-CDMA design, thereby providing a data reliability per user. The performance of the resulting SM-STBC-OFDM-CDMA system is investigated in Nagakami channel fading, more particularly in the presence of imperfect channel estimates. We investigate the same transceiver bloc as described in Fig. 3.10. Fig. 3.12 compares the achieved BER performance for different values of m, and different CSI conditions, when adopting SM-STBC-OFDM-CDMA scheme over Nakagami-m fading channel. Rayleigh channel scenario, obtained when $m = 1$, is compared against Rician and Gaussian cases, simulated with $m = 1.5$ and $m = 0.5$

respectively. Furthermore, ideally estimated channels are herein taken as a reference and are obtained by setting the value of ρ to 1. The selected modulation scheme is

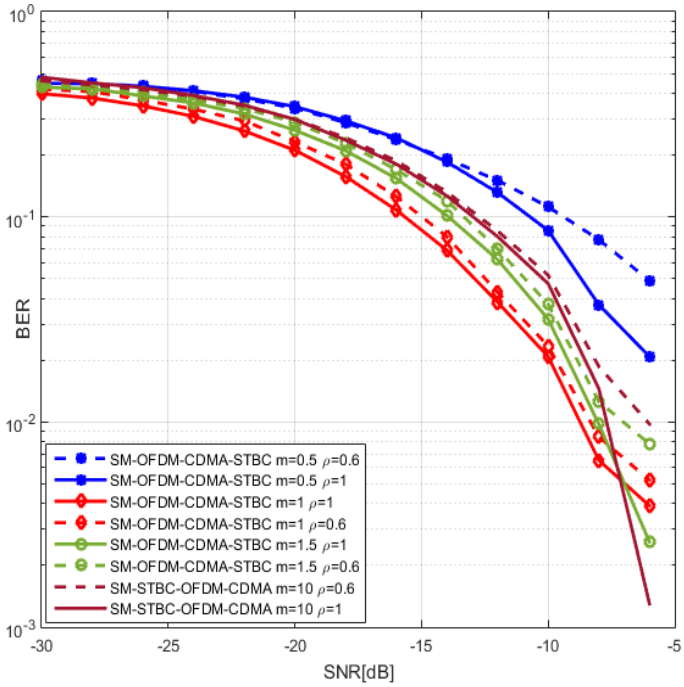

Figure 3.12 — Comparison of BER performance with the variation of the channel estimation accuracy and Nakagami parameters.

$BPSK$. The simulation parameters are fixed as follows: the number of users is $k = 2$, $P = 128$, $L = 3$, and $N_c = 128$. It can be observed from Fig. 3.12 that, in this particular SNR range where the noise power is higher than the desired signal, in ideal channel conditions, Rayleigh channel is more favorable to communication than the general Nagakami channel where $m = 10$. Gaussian channel exhibits the lowest performance. The attained data reliability in all channel conditions remains quite interesting since low BER values are provided at low SNR range. However, as shown in this figure, increasing slightly the imperfection levels, has a drastic degradation effect on the data reliability, more particularly in Gaussian channel.

3.5.5 Hybrid cooperative spatial modulation scheme with CDMA multiple access using DF relaying protocol

Cooperative communication is an impressive technique that uses multiple nodes as relays to help the transmission of information. The destination receives not only

the information from the source but also the transferred one from other collaborating nodes. The adoption of the cooperative relaying results in increasing network coverage, improving transmission reliability and extending communication range [162]. In cooperative communications, a source (S) transmits its own data to a relay (R) and a destination (D) in the first time slot and (R) forwards the received signal either by decoding (decode-and-forward, DF) or amplifying it (amplify-and-forward, AF) in the second time slot. This forwarding concept forms a virtual MIMO system to combat fading and provides a larger coverage area [163]. Combining the advantages of SM and cooperative communications has been recently studied in the literature [164, 165]. The first study is performed by Serafimovski et.al in [164] in which a dual-hop SM system is proposed (where there is no direct link between the source S and the destination D). A real cooperative scenario in which the source S sends its information to the relay R and the destination D in the first time slot is considered in [166]. In this system, the source S transmits its data using SSK to N relays and D (all nodes have single transmit and receive antennas) in the first time slot and N relays amplify the incoming signal and retransmit to D in the following N time slots. In the same study, the use of DF strategy is investigated when the relays which correctly detect the source symbol are permitted to forward. Since the relays have single antenna, communication between R and D can not be performed with SSK. In [167], the dual-hop SSK system in [168] is enhanced to N-relay system using opportunistic relaying to increase the spectral efficiency. The performance of SM with multiple decode and forward (DF) relays in which the relays that correctly detect the source signal forward the decoded message to the destination is investigated in [169]. The first cooperative system in which all nodes have multiple transmit and receive antennas is introduced in [170], where space shift keying (SSK) modulation is used and an incremental relaying (IR) scheme with selection combining (SC) at the destination is considered.

System model

A cooperative SM-CDMA system that combines DF relaying with SM in the presence of multiple relays is shown in Fig. 3.13. The system contains one source, multiple relays and one destination. With the DF protocol at each relay, the transmission process is divided into two phases. In the first phase, the source transmits the signal to the relays and the destination. Considering the N_t antennas at the source, the SM mapper assigns

$log_2 N_t$ and $log_2 M$ bits to determine the active transmit antenna index j, $j \in \{1, ..., N_t\}$, and the q^{th} symbol of M-ary constellation diagram x_q, $q \in \{1, ..., M\}$, respectively. Therefore, the output of SM mapper is given by $\mathbf{x}_{j,q} = [0\,0 ... x_q ... 0]^T$, where $\mathbf{x}_{j,q}$ is an N_t-dimensional column vector, and the unique non zero element is in the j^{th} row. In the study we are proposing, the relay node $r_k, k = \{1, 2, ..., K\}$ and the destination node D are equipped with multiple antennas. First, the input sequence is encoded and interleaved to fight against channel errors and transmitted after that over the channel to the relays and the destination according to the following equations:

$$\mathbf{y}_r^{(k)} = \mathbf{H}_{rs}^{(k)} \mathbf{x}_{j,q} + \mathbf{w}_r^{(k)} \tag{3.11}$$

$$\mathbf{y}_d = \mathbf{H}_{ds} \mathbf{x}_{j,q} + \mathbf{w}_d \tag{3.12}$$

where, for the k^{th} relay, $\mathbf{y}_r^{(k)} \in C^{N_r \times 1}$ is the complex received vector at the relay; $\mathbf{H}_{rs}^{(k)} \in C^{N_r \times N_t}$ is the complex channel matrix; $\mathbf{w}^{(k)} \in C^{N_r \times 1}$ is the complex AWGN; and $\mathbf{x}_{j,q}$ is the complex SM-modulated transmitted vector.

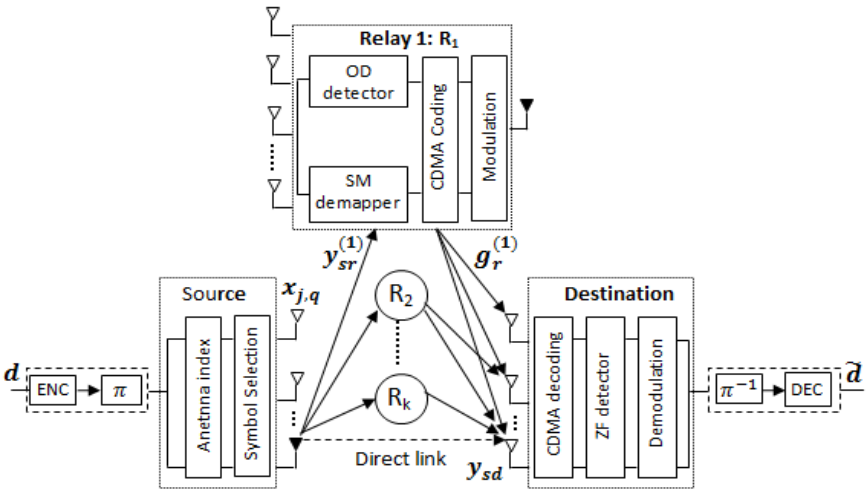

Figure 3.13 — Cooperative SM-OFDM-based CDMA system transceiver block diagram

In the second phase of DF relaying process, a decoding algorithm for SM is subsequently performed at each relay, then optimal detector (OD) is adopted to recover the combination of the transmit antenna index and the emitted symbol.

After the SM-demapping, the data symbols of the K relays are multiplied by their specific orthogonal spreading code. Mathematically expressed, the spread signal $\mathbf{g}_r^{(k)}$ is

thus CDMA encoded through the following expression:

$$\mathbf{g}_r^{(k)} = \mathbf{q}^{(k)}. \quad \mathbf{c}^{(k)} \in \{-1, +1\}^{1\times P} \tag{3.13}$$

$\mathbf{g}_r^{(k)}$ is the modulated signal for the k^{th} relay, $\mathbf{q}^{(k)}$ and is $\mathbf{c}^{(k)}$ are the transmit data and the spreading code, and P is length of the spreading code. Furtheremore, each relay signal is equipped with a unique code which can be used to distinguish between the set of the relay signals at the receiver. Afterwards, the resulting signals $\mathbf{g}_r^{(k)}$ are transmitted over the channel to the destination, which gives birth to the following equations:

$$\mathbf{y}_{rd}^{(k)} = \sum_{i=0}^{K} \mathbf{H}_{dr}^{(k)} \mathbf{g}_r + \mathbf{w}_d \tag{3.14}$$

$$\mathbf{y}_G = \mathbf{y}_{rd} + \mathbf{y}_d \tag{3.15}$$

where $\mathbf{y}_{rd}$ is the received signal at the destination d emanating from the relays, $\mathbf{y}_d$ is the one at the destination originating from the source node, $\mathbf{w}_d$ is the additive white Gaussian noise vector with $CN(0, \sigma^2)$ elements at the destination.

At the destination side, the stages are simply the reverse ordered operations of the relay side. First, the resulting signal is multiplied by its corresponding relay synchronized replica of CDMA code, such that to despread the data. A combination of the two received signals $\mathbf{y}_{rd}$ and $\mathbf{y}_{sd}$ is computed as expressed in Eq. 3.15 and a demodulation is subsequently performed, to retrieve the emitted signal from the source (S). Using this demapping rule, the combination of the transmit antenna index and the emitted symbol can be obtained.

Simulation results

In this section, we present computer simulation results for the BER of cooperative SM-OFDM-CDMA scheme considering DF protocol with four transmit antennas at the source, one receive and transmit antenna used at each DF relay, and eight receive antennas at the destination, considering $4PSK$ constellation. We assume that the relays are randomly distributed between the source and the destination. $L = 7$ taps are present, the number of subcarriers in OFDM is set to 16, and the length of the spreading code is $N_c = 128$. For comparison purposes, cooperative SM-OFDM-CDMA architecture for one relay is chosen as a reference. Fig. 3.14 investigates the BER performance in terms

of SNR in such a setting. It can be observed that the reliability of the data is altered by the increase of the number of relays. Indeed, the performance of the proposed scheme is quite viable, even in using a very high number of relays since 10 relays offers a BER performance of 10^{-3} when the SNR gain is low (8 dB).

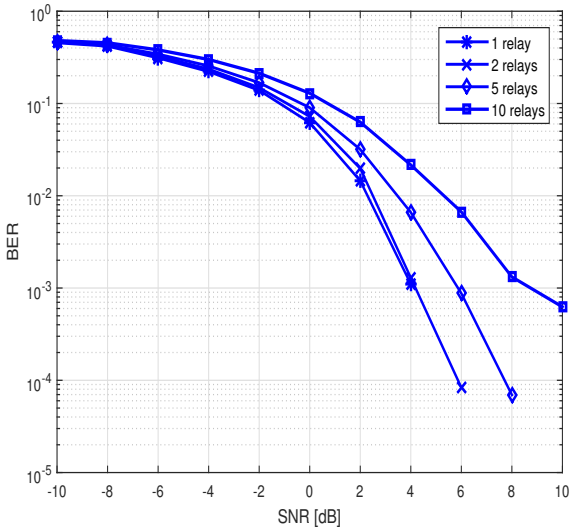

Figure 3.14 — BER performance with the variation of the number of DF relays of cooperative SM-OFDM-based CDMA system

3.6 Summary

In this chapter, we have proposed novel multi-carrier based SM configurations, namely SM-GFDM and SM-OTFS and studied their performances in Rayleigh channels. We have also proposed multiuser SM-OFDM schemes, which are well adapted for 5G and beyond systems, more particularly for massive MIMO. These are mostly the result of a combination of SM, STBC, OFDM, and CDMA capabilities for offering a highly reliable low complexity multiple access communication in frequency selective channels. The resulting robustness and improved performance of the proposed schemes have been confirmed. The performances of the proposed multi-access SM-OFDM architectures were investigated in Nakagami channels, where they were shown to be quite sensitive to the increase of spatial correlation and CSI imprecisions, regardless of the used detector. Relaying mechanisms were also tackled in such configurations and the data reliability improvement yield by the cooperative diversity was highlighted.

CHAPTER 4

Chapter 4: Integration of SM Scheme with CDMA for VIVO-based Frequency Selective Nano Sensor Networks.

4.1 Introduction

Due to their suitability for human-body based communications, in-VIVO nano sensor networks are envisioned to use the promising Terahertz signals in order to ensure the forthcoming high-rate communication needs of the modern medicine, while being fully protected from interferences. However, the propagation losses at these frequency bands are quite significant and dependent on the operation frequency as well as on the physiological characteristics, thus impeding the use of Terahertz rates to their utmost benefit. Using numerous emitting elements is likely to improve the quality of the received signal, but gives rise to multi-channel interference (MCI) emanating from multi-antenna signaling reception, which necessitates a relatively complex signal processing to mitigate it. When multiple physiological signals are of interest, detecting them necessitates to mitigate multiple-access interference (MAI). In this perspective, orthogonal frequency division multiplexing (OFDM) allows to combat the channel frequency selectivity, whereas code division multiple access (CDMA) scheme cancels MAI. In this chapter, we propose to embed the novel spatial modulation technique with CDMA architecture in an OFDM framework to ensure a viable communication in

in-VIVO frequency selective Nano channels. The immunity of our proposed solution to such an interference is confirmed, since less than -2 dB in SNR level is required to support 5 MIMO systems simultaneously communicating with a BER which is inferior to 10^{-3}, when the operating frequency is equal to 1THz. This hybrid scheme is shown to efficiently combat the MCI, while enabling a safe retrieval of the useful signal at the very-high data rate communications.

4.2 Related work

It has become obvious that, unless the frequency resources allocation policy is totally reviewed to encompass the cognitive radio paradigm, in which the primary users share their bands with the secondary users, the frequency resources in low and medium bands are used to their extreme, and can no more support additional subscribers. Under this perspective, the free terahertz (THz) systems are considered as the alternative to allow the ultra-high data rates communications foreseen for the forthcoming sixth generation (6G) of wireless systems.

Incorporating technological tools in the biomedical field has allowed the consolidation of the medical care quality, the decrease of care costs and the increase of human life expectancy. In-VIVO Wireless body area networks (WBANs) and technologies, such as wireless capsule endoscopes and nerve simulators, are no exception, and are likely to be widely adopted in future biomedical services and infrastructures. Indeed, they are oriented towards the same trend of ensuring ubiquitous health monitoring, assisting the doctors in delivering reliable and accurate diagnosis and analysis, screening early critical diseases, and offering the patients a seamless physiological data collection and the comfortable idea that the surgery will be avoided unless it becomes the ultimate solution.

In monitoring a patient's real-time vital signs through WBAN technology, rich data sources are communicated to medical practitioners. Beyond clinical use, professional disease management environments, and private personal health assistance scenarios (without financial reimbursement by health agencies/insurance companies), WBAN enables a wide range of health care applications and related services. In [171], the authors propose a non-intrusive breathing monitoring system using the C-Band sensing technique. In [172], cooperative techniques are exploited to enhance the coverage and the reliability of WBANs. Interference cancellation in WBANs is targeted in [173], while [174] introduces an FPGA-based realistic solution to reduce the implementation complexity by recoursing to compressed sensing tools. Recently, the nanotechnology and the subsequent possibilities it opens for the reduction of the devices size to the nanoscale dimension, in addition to the research community interest for the adequate nano materials for such devices, such as the graphene, have made conceivable the adoption of the nano-networks for the THz communication within the human body.

However, one major problem faced with the deployment of this breakthrough technology, in addition to the very high path loss and molecular absorption noise, is the resulting high level of multiuser interference. This latter comes from the very high density of in-body sensors; in the order of hundreds per square millimeter, which needs to be deployed in order to compensate the reduced coverage range, pertaining to the operation at the THz band. The signals emanating from the co-communicating transmitters at the reception side are superimposed with the signal of interest, leading to the degradation of the communication quality. The investigation of the body-supported networks has been thouroughly carried out in the last two decades, at the ISM and UWB frequencies [173, 175–181]. The characterization of the propagation and the channel modeling of the THz in-VIVO networks have been recently conducted in [182–185]. According to the authors knowledge, only few studies have been accorded to these particular networks, when evolving in multi-user scenario. The authors in [186],[187] proposed a pulse communication-based statistical interference model which is adapted to THz-band in a very specific setting. The weakness of that work lies in the fact that the presented interference model, relying on the polynomial approximation of the received signal, is parametrized by the power and shape of the transmitted signal and the channel molecular distribution, hence varies with the variation of the communication medium or the signal features. Interference and signal-to-noise-plus-interference ratio (SINR) was also analyzed in [188–190] when considering the effect of antenna radiation pattern and directivity. In [191], a network level analysis was carried out by extracting the interference model and the SINR of the in-VIVO nano-networks when adopting time spread ON-OFF keying (TS-OOK) modulation scheme was derived. Various communication conditions were investigated to highlight the interference impingement on signal degradation. According to the discussion above, it appears clearly that the previous studies have solely been concerned with assessing the effect of interference on the THz communication of the nano networks. Surprisingly, no work has been dedicated to overcoming this undesirable effect. Motivated by this limitation, in this chapter, a solution is proposed to mitigate interference in this particular environment, by recoursing to a scheme which combines index modulation and code division multiple access. The adoption of the index modulation is consolidated by the current communication trend in its incorporation in massive multiple-input multiple-output (MIMO) systems. Indeed, a key challenge of future mobile communications research is to strike an attractive compromise between the

two wireless network's areas: spectral-efficiency and energy-efficiency. This necessitates a clean-slate approach to wireless system design, embracing the rich body of the existing knowledge on MIMO technologies to its extension to massive MIMO paradigm [192], [193]. However, conventional MIMO systems design would need an RF chain at each transmitting and receiving element side, rendering the integration of massive MIMO, practically unfeasible due to the high hardware complexity and the prohibiting energy consumption. To alleviate such constraints, index modulation, which in spatial domain holds the name of spatial modulation (SM), has emerged as a viable solution in 5G and beyond-communication systems, and proposed to include within the transmitted signal block, a part dedicated to the activated antenna index, in addition to the usual data part [128, 194]. This allows to circumvent in the uplink single user scenario, and without resorting to successive interference cancellation (SIC) schemes, the inter-channel interference (ICI) emanating from multiple transmitting antennas to the same receiver. This is achieved in the conventional SM scheme by randomly activating only one antenna at the transmit side, and retrieving from the signal block at the multiple-antennas receive side both the index of the activated antenna and the associated transmitted data. Most of the SM-related contributions have addressed point-to-point communication systems, i.e. the case of the single-user, and the investigated channels were undergoing mostly either flat Gaussian or flat Rayleigh fading [195]. According to the best of our knowledge, the sole work incorporating index modulation for in-VIVO nano networks has targeted a single device scenario [196]. Furthermore, a very little research interest has been dedicated to the investigation of SM architectures in multiple user access context, and the ones which have reported related works, have only dealt with flat fading channels [197],[198]. The objective of this work is to address the realistic scenario of the dense deployment of numerous nano-sensors within the human body, and propose a scheme combating the effect of path loss and multiple access interference in THz frequencies. Obviously, in upcoming communication multipoint-receive systems, in addition to the challenging targeted types of applications where high data rates and mobility are involved, the pertaining solutions should support a large number of receive devices, while maintaining the required quality of service (QoS) per device, and keeping the hardware complexity as simple as possible. Due to the involved large communication frequency band and high data rates, the associated in-body channel will be shown to be frequency-dependent. In this direction, we have retained orthogonal frequency

division multiplexing (OFDM) to combat the THz channel frequency selectivity. OFDM technique achieves such purpose, by converting the selective channel into a set of frequency-flat subchannels, which number is equal to the number of subcarriers used in the OFDM scheme. Furthermore, code division multiple access (CDMA), consisting in assigning a different code per targeted transmit device, allows to support multiple access in SM architectures. We agree, to refer, in the MIMO in-VIVO setting, to the interference at the receiver emanating from the multiple transmitting antennas of the intended physiological signal as ICI. Similarly, the one originated from a transmitting device other than the intended signal is conventionnally termed as multiple access interfernce (MAI). The combination of OFDM, SM and CDMA techniques, targetting to increase the data rate, while mitigating the ICI and the MAI in THz frequency selective channel, gives birth to the new concept of SM-OFDM-CDMA.

4.3 Channel characterization and modeling

The in-VIVO THz channel is challenging to characterize and estimate but has attracted lately the research interest because of the development witnessed in nanotechnology and device miniaturization. The in-body electromagnetic waves at the THz band cross different media wihin the human body, each with different electrical and magnetic properties. In this work, we represent the skin tissues, as shown in Fig.4.1, by a three-layer model, namely the stratum corneum (SC), the epidermis, and the dermis. To accurately emulate the electromagnetic propagation inside the human tissues and the

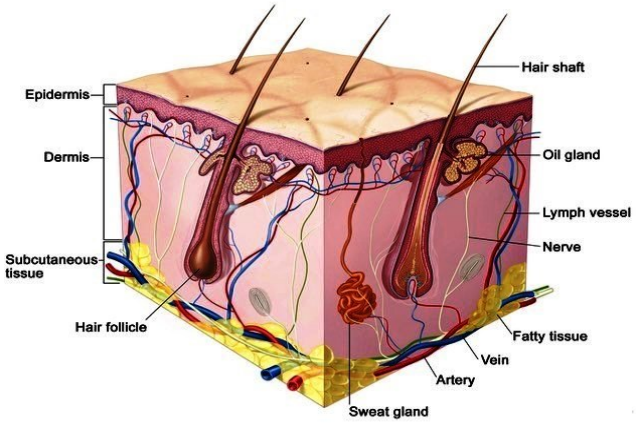

Figure 4.1 — Representation of skin tissues.

resulting losses they generate within a given signal, the epidermis region was supposed containing sweat glands or sweat ducts, which are of spiral shape. We have developed a large scale model in [185] and validated it through time-domain spectroscopy (THz-TDS) experiments carried out at Queen Mary University of London (QMUL) [199] by using two layers, the epidermis extracted from a real being skin, and an artificially cultured collagen emulating the dermis. The collected phase and amplitude of received pulses are processed via transfer equation-based algorithm, which allows the evaluation of the pathloss and other material parameters [200]. For readers interest, more details on the system setup and performed measurements could be found in [185]. The modified Friis equation proposed in [182] which evaluates the path loss in the water vapor channel at the THz band considers two phenomenons, namely the expansion of electromagnetic (EM) waves in the tissue giving rise to the spreading path loss (PL_{spr}), and absorption of the waves in the tissues producing the absorption path loss (PL_{abs}). Accordingly, the path loss in the human tissues could be written as:

$$PL_{total}[dB] = PL_{spr}(f,d)[dB] + PL_{abs}(f,d)[dB] \tag{4.1}$$

where f refers to the frequency in THz, and d to transmitter-receiver distance expressed in millimiters. However, this slow fading model is concerned only with the frequency and distance operation parameters, and overlooks the physiological particularities of the internal part of the human skin. This was taken into account in the model we developed in [185] inferred from the THz-TDS skin measurements, and encompassing the number of sweat ducts in the skin. Unlike our previous works, we are targeting herein a MIMO configuration, and we define our path loss model in each l^{th} multipath signal component between each j^{th} receive antenna and i^{th} transmit antenna of the in-body nano nodes, by complying with the two-step data fitting procedure with the measurements, which yields the following model:

$$\begin{aligned} PL^{l}_{j,i} = -0.2 * N + 3.98 + (0.44 * N + 98.48) d_{j,i}^{0.65} \\ +(0.068 * N + 2.4) f^{4.07} \end{aligned} \tag{4.2}$$

with N being the number of sweat ducts and $l = \{1, 2, ..., L\}$ indicates the number of multipath channel components. In the following, the impingements of the characteristics of the nano-scale in-body environment, the operation frequency and the inter-nodes

distance on the channel path loss are investigated, and the obtained results are illustrated in Fig.4.2 through Fig.4.4. According to Fig.4.2, it appears that the variation of the

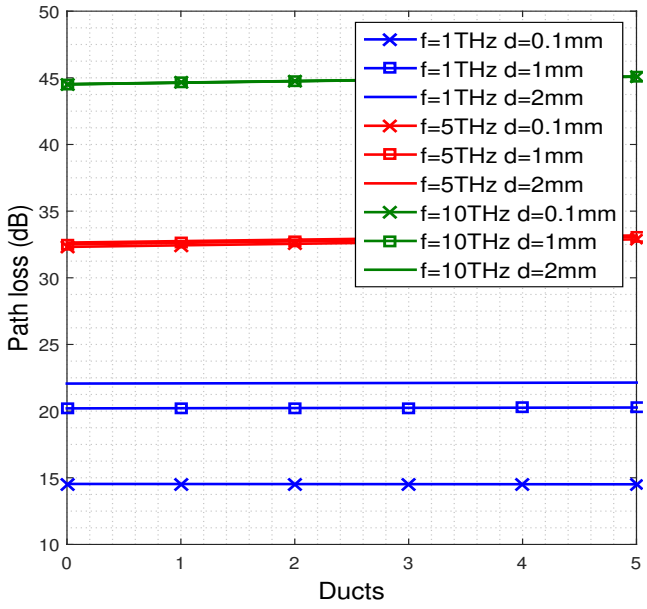

Figure 4.2 — Path loss with respect to the number of ducts

number of ducts in the chosen range has a negligeable effect on the path loss, whatever the operation frequency is. Hence a displacement from an in-body area to a neighbouring region does not induce an appreciable variation in the path loss. At a given number of ducts, increasing the transmitting-receiving elements distance results in a path loss increase at f=1THz, unlike the other frequency of interest, i.e. f=5THz and f=10THz, at which the same path loss is attained, regardless of the distance. On the other hand, Fig.4.3 shows the path loss in terms of the distance for different numbers of ducts and frequencies. From that figure it appears that the path loss observed when varying the distance is the same, regardless of the number of ducts. Furthermore, the increase of the operating frequency results in a higher path loss. When f=1THz, and up to a distance of 1mm, the path loss scales linearly with the variation of the distance, and a small variation of the distance by an order of 0.1mm results in approximately 1dB increase of the path loss. Beyond this value, the path loss at f=1THz is only slightly affected by the distance. For the other higher frequencies of interest, the path loss is not impinged by the distance at the investigated range. Finally, the effect of the operation frequency on the path loss is addressed and the corresponding results are reported in Fig. 4.4. As it can be noted, the path loss remains constant at 22 dB when the frequency is below 2

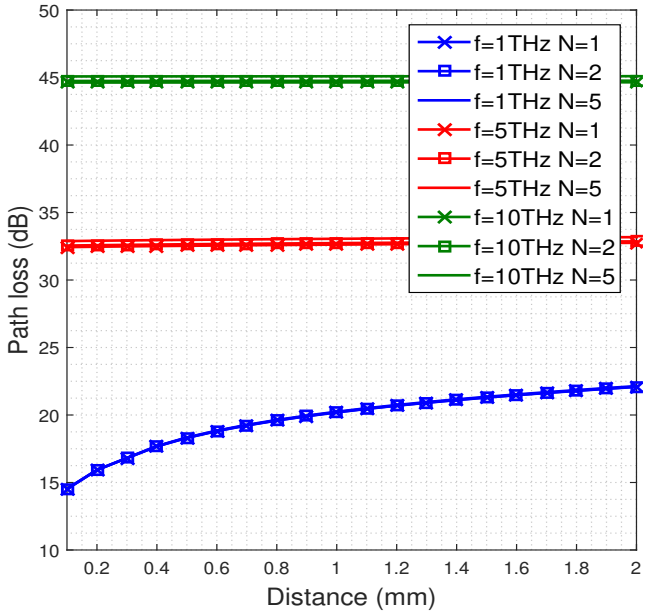

Figure 4.3 — Path loss with respect to the distance

THz. After this threshold, the path loss increases almost linearly by a step of 5 dB at each 1 THz-frequency increase.

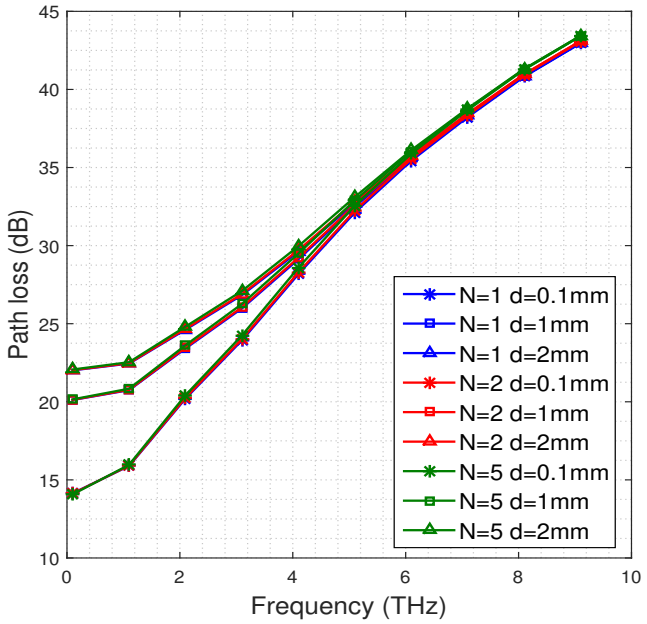

Figure 4.4 — Path loss with respect to the frequency (f)

4.4 Hybrid Spatial Modulation Scheme with CDMA multiple access

Our scenario involves numerous nano-sensors placed within the body, where each, to comply with hardware and energy constraints, is equipped with a sole antenna. Subsets of them are regrouped to form virtual MIMO configurations, where each of those is dedicated to a given application (physiological data), referred to herein as user, thus forming a multiuser system. Index modulation scheme conveys additional information in the data block beside the transmitted symbol, which can be an index of the temporal, spatial, or the frequency resource activated for such a transmission. In this work, the index pertains to the spatial dimension, leading to the particular case of SM. By randomly activating only one antenna, the ICI is mitigated and the only remaining interference is the MAI coming from the co-existence of multiple physiological signals (users) sharing the same frequency and temporal resources and co-communicating with the same reception unit. This MAI will be reduced by resorting to CDMA scheme. Indeed, these spatially distributed nano-networks, are virtually regrouped such that to use N_t nano transmit nodes for a given application, and K users (referring to different applications or different physiological signals) are simultaneously communicating with the receive unit consisting of N_r distributed receive nodes. Figure 4.5 shows an example of SM-OFDM scheme with $N_t = 2$ and 4 OFDM sub-carriers, and which adopts 4QAM modulation resulting in 3 bits/symbol/sub-carrier transmission. The SM-OFDM information block pertaining to each subcarrier is mapped into the index of the activated transmit antenna and the emitted symbol. Let us assume for instance that the input data sequence corresponding to the first sub–carrier is $[0 \quad 1 \quad 1]^T$. Since we are concerned with only two transmit antennas, the first element in the information block (the value zero herein) refers to the antenna index, while the remaining elements are the data block. Hence, this example corresponds in SM mapping to the transmission of the symbol $1 - i$ from the first transmit antenna, while at that time instant the second antenna is kept silent. Hence, the transmit symbol vector for the first sub-carrier is $[1 - i \quad 0]^T$. The block diagram of the used architecture is shown in Fig.4.6. At the transmitter side, the input data sequence $\mathbf{d}(k)$ corresponding to the k^{th} biophysical signal is first encoded, interleaved and then inserted into the SM block to generate the

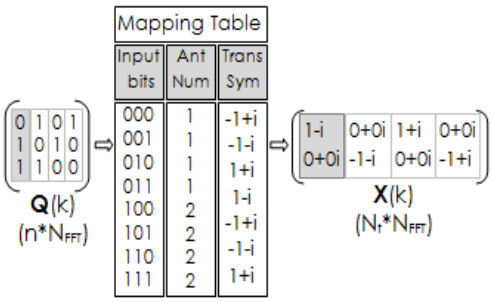

Figure 4.5 — SM-OFDM: 3bits/symbol/subcarrier in 4QAM modulation.

sequence $\mathbf{q}(k)$. Hence, in the SM architecture, the first $log_2 N_t$ of the resulting block are

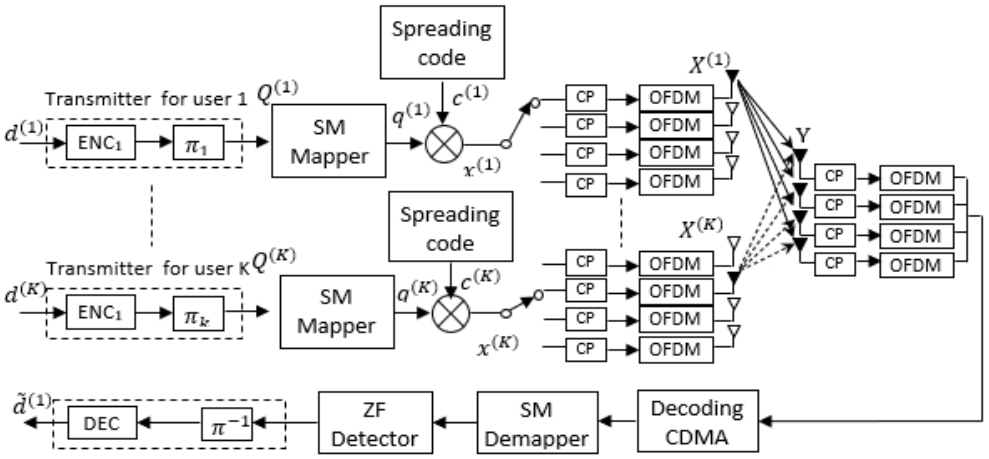

Figure 4.6 — SM-CDMA-OFDM system transceiver block diagram.

dedicated to the coding of the antenna index, while the second $log_2 M$ bits contains the emitted symbol. Therefore, the number of bits/symbol per user that this SM scheme allows to transmit in each block is given, as presented in [128], by:

$$b_{SM} = log_2 N_t + log_2 M \tag{4.3}$$

In each k^{th} application-dedicated system, $k = \{1, ..., K\}$, the signal vector $\mathbf{x}(k)$ is CDMA-spread by performing the Hadamard product between an array of the signal $\mathbf{q}(k)$ repeated N_t times and the spreading code $\mathbf{c}^{(k)} \in \mathbf{C}^{N_t \times P}$ [201]. Hence, the CDMA encoded signal could be written as:

$$\mathbf{x}^{(k)} = \mathbf{q}^{(k)}. \quad \mathbf{c}^{(k)} \in \{-1, +1\}^{1 \times P} \tag{4.4}$$

with P being the length of the spreading code. Afterwards, in each transmitter, the input sequence is transformed to the time domain by applying the inverse fast Fourier transform (IFFT). Subsequently, a cyclic prefix (CP) is inserted to eliminate the inter-symbol interference (ISI) between OFDM symbols, and the resulting signals are transmitted over the channel. The multipath signal received at the ϱ^{th} antenna element from transmit antennas could be written as:

$$\mathbf{y}_{\varrho}(t) = \sum_{i=0}^{K} \mathbf{h}_{\varrho\nu}(t) \otimes \mathbf{x}_{\nu}(t) + \mathbf{w}_{\varrho}(t) \tag{4.5}$$

where $\mathbf{x}_{\nu}(t)$ is the signal emanating from the ν^{th} activated antenna, $\mathbf{w}_{\varrho}(t)$ is the additive white Gaussian noise vector with $CN(0, \sigma^2)$ elements, $\otimes$ denotes the time convolution operator and $\mathbf{h}_{\varrho\nu}(t) = \left[h_{\varrho\nu}(t)^1 \; h_{\varrho\nu}(t)^2 \cdots h_{\varrho\nu}(t)^L)\right]$ stands for the $L \times 1$ channel vector between the pair of ν^{th}transmit-ϱ^{th}receive antennas encompassing the L significant multipath channel components. The receiver at the branch corresponding to the retrieval of the k^{th} user signal, as illustrated in Fig.4.6, comprises simply the blocks performing the reverse ordered operations of the transmitter side. First, OFDM demodulation is carried out, then, the resulting signal is multiplied by the CDMA code associated with the k^{th} application, and summed up such that to re-obtain the despread signal. Then, the SM decoding operation is launched by estimating the index of the activated antenna from the signal block part reserved to the indices, and then demodulating the associated signal using zero forcing (ZF) detector; which is viewed as an element-wise division of the OFDM demodulated signal by the transfer function of the discrete channel response. The so-mentioned channel transfer function is computed by a DFT of the zero-padded discrete time channel impulse response. It follows that the per-carrier ZF is performed as described in [43]:

$$\tilde{\mathbf{z}}^{s}(k) = \frac{\mathbf{y}^{s}(k)}{\mathbf{h}_{j}^{s}(k)} \tag{4.6}$$

where s stands for the index of the subcarrier. Afterwards, spatial location of the transmit antenna index, from which the symbol was transmitted, needs to be estimated. This is done by finding the location of the maximum absolute value of the output vector from the ZF equalizer $\tilde{\mathbf{z}}^{s}(k)$ for each sub-carrier s, which is described in the following

equation:

$$\hat{j}^s = arg \max_j |\tilde{\mathbf{z}}^s(k)| \ for \ j = \{1, 2, .., N_t\} \ s = \{1, 2, .., FFT\} \tag{4.7}$$

where $\hat{j}^s$ denotes the estimated value of the antenna index. Then, the symbol is detected using the following equation:

$$\hat{q}^s = Q(\tilde{\mathbf{z}}^s(k)_{(j=\hat{j}^s)}) \tag{4.8}$$

where Q refers to the quantization operation pertaining to the symbol detection. After the SM-OFDM demapping, decoding and de-interleaving operations are applied, as shown in the Fig. 4.6.

4.5 Simulation results

To study the performance of the proposed multiple access spatial modulation scheme incorporating virtual MIMO-OFDM configuration in the in-VIVO THz channel, simulations are carried out to study the impact of different parameters on such a performance. In the following, we comply with the SM notation adopted in multiple papers when

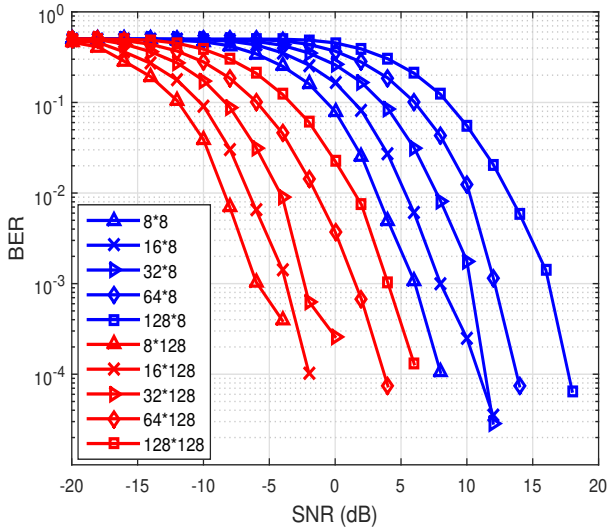

Figure 4.7 — Comparison of BER performances of SM-OFDM-CDMA scheme with the variation of transmit and receive antenna numbers with f=1THz, $2PSK, FFT = 128, N_c = 128, N = 1, d = 0.1mm$

referring to the resulting MIMO system adopting M-PSK modulation, i.e. $N_t \times N_r$ M-PSK. We next analyze the effect of transmit and receive antenna (TX-RX) number

on the BER performance, with: $N_t = \{8, 16, 32, 64, 128\}$ and $N_r = \{8, 128\}$, whereas the length of the spreading CDMA code (N_c) and the number of subcarriers (FFT) are fixed at 128, and 2PSK modulation is retained. As depicted in figure 4.7, the performance significantly improves when increasing the number of receive antennas. However, this same performance degrades when the number of transmit antennas is greater than the number of receive antennas. This consolidates the finding in papers [202–204], where it was shown that the transmit antenna index is better detected and accurately estimated in the presence of a lower number of TX-antennas than the receive ones. It follows that for the investigated cases, the best performance is achieved when $N_t = 8$ and $N_r = 128$.

Fig. 4.8 investigates the BER performance when fixing the spectral efficiency per

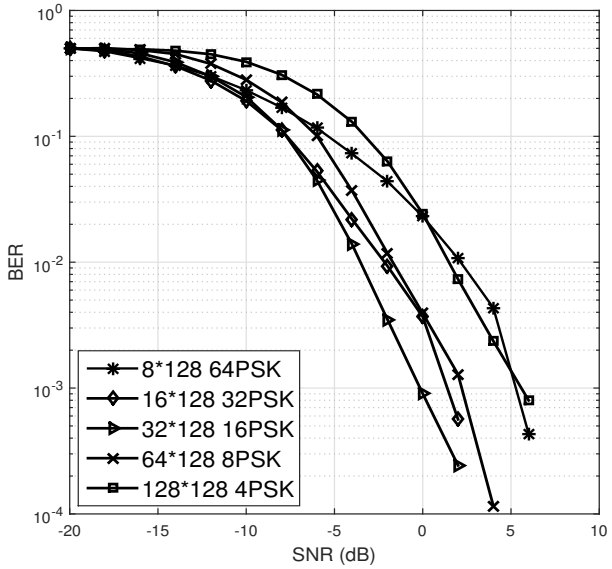

Figure 4.8 — Comparison of BER performances of SM-OFDM-CDMA scheme with the variation of the modulation order M, f = 1THz, $FFT = 128, N_c = 128, N = 1, d = 0.1mm$

subcarrier, as given by the expression in Eq. 4.3, at the value 9 bits/s/Hz, for instance. This is achieved by increasing the order of the modulation from 2 to 128 PSK, with a power of 2, while decreasing the number of transmit antennas, such that to maintain the spectral efficiency constant, as per Eq. 4.3. It can be seen from Fig. 4.8 that the higher modulation orders, such as 64 PSK and 32 PSK, experience a quite acceptable penalty in terms of data reliability thanks to the balance provided by a number of transmit antennas which is below the one of receive antennas. On the other hand, the schemes incorporating the lower modulation orders, i.e 4 PSK and 8 PSK, exhibit

performances which are below the ones expected due to a corresponding numbers of transmit antennas that are close to receive antennas. The scheme which yields the best compromise between the number of transmit antennas and the modulation type is the one supporting 16 PSK, resulting in the best performance.

In next simulation the impingement of the variation of the number of subcarriers on the performance of the proposed system is investigated when the operating frequency is f=1THz, $(N_t, N_r) = (8, 128)$, the 2 PSK modulation is adopted and the distance is maintainted at d=0.1mm. As expected, increasing the number of subcarriers corresponds to affording more parallel frequency branches to transmission, hence enhancing the frequency diversity. It follows that the BER performance is significantly enhanced; for instance migrating from a system supporting 32 subcarriers to a one supporting 128 allows reducing the SNR by more than 5 dB at a required BER of 10^{-3}. The

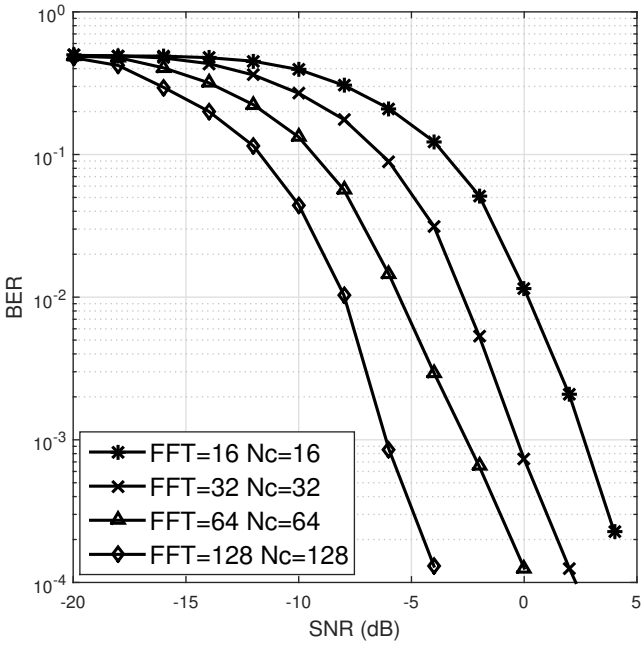

Figure 4.9 — Comparison of BER performances of SM-OFDM-CDMA scheme with the variation of FFT size and N_c at $N_t = 8, N_r = 128, N = 1$, f=1THz, $d = 0.1mm$

performance of the proposed systems is discussed in the same setting when varying the number of subcarriers and the operating frequencies, and the associated results are illustrated in Fig. 4.10. As mentioned earlier, the impact of the operation frequency on the performance is the most critical compared to other parameters. Indeed, increasing the frequency from f = 1THz to 5 THz, induces an approximate penalty of 20 dB in

terms of SNR and of more than 10 dB when migrating from 5THz to 10THz. Moreover, for a given operation frequency, increasing the number of carriers from 64 to 128 results in an average gain of 3 dB in terms of performance. Next, the effect of multiple access

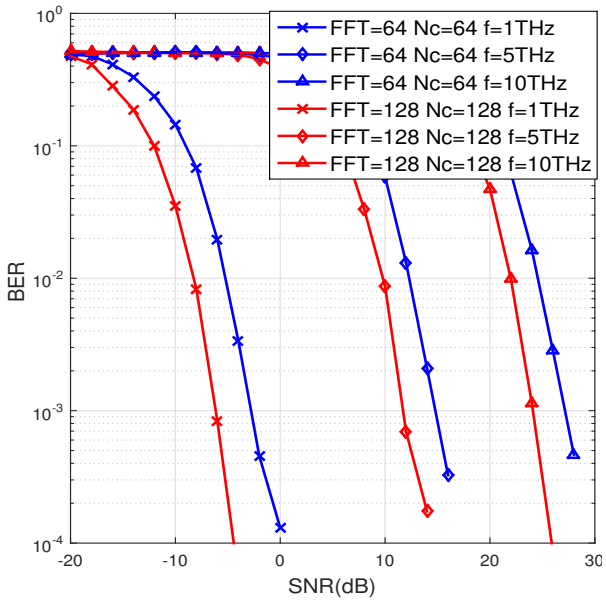

Figure 4.10 — Comparison of BER performances of SM-OFDM-CDMA scheme with the variation of FFT size and N_c at $N_t = 8, N_r = 128, N = 1$, $d = 0.1mm$ and different frequencies.

interference on the performance of the proposed solution is of interest. For this purpose, the parameters are chosen as follows: the number of users (corresponding to different physiological signals) is varied as $K = \{1, 2, 5\}$, the operating frequency is selected from the set $f = \{1, 5, 10\}$THz, the Tx-Rx distance is maintained at 0.1mm, and the remaining parameters are fixed at $(N_t, N_r, M, FFT) = (8, 128, 2, 128)$. Moreover, for simplification purposes, the length of the spreading CDMA code is $N_c = 128$, and we have incorporated in each frame only one OFDM block. As it can be seen from Fig.4.11, the reliability of the data at a given frequency is degraded by the users number increase, which is what was expected. For instance, moving from a scenario supporting only 1 user to the one containing 5 users results in an approximate penalty of 7 dB in terms of SNR. Operating at the lowest frequencies of the terahertz band seems to be more interesting in practice, because of the cost of the higher ones in SNR increase. The balance of this at those high frequency range could be achieved by significantly increasing the number of subcarriers, at the price of a more significant hardware complexity. At f= 1THz,

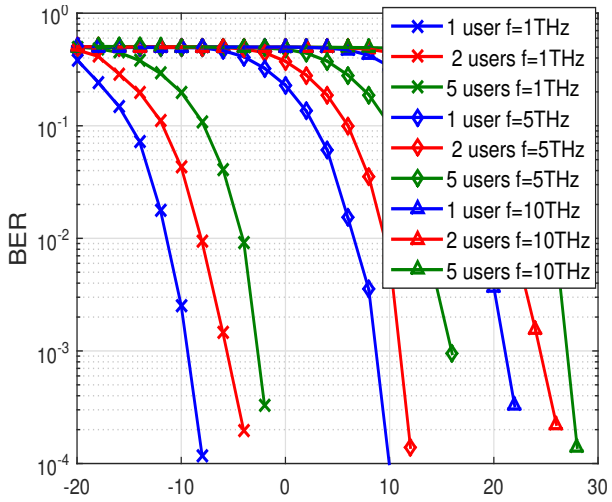

Figure 4.11 — Comparison of BER performances of SM-OFDM-CDMA scheme with the variation of the number of users $N_t = 8, N_r = 128, 2PSK, FFT = 128, N_c = 128, N = 1$, $d = 0.1mm$ and different frequencies

the immunity of our proposed solution to such an interference is confirmed, since less than -2 dB in SNR level is required to support 5 users simultaneously communicating with a BER which is inferior to 10^{-3}. In the following, the effect of the variation of

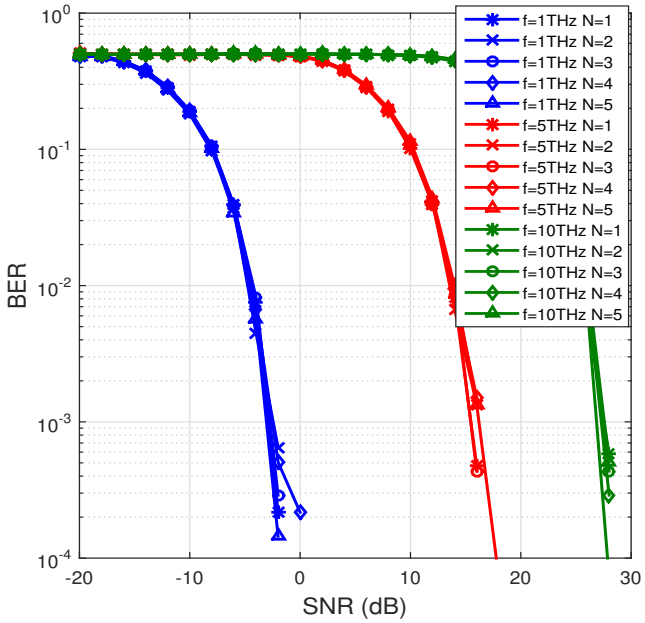

Figure 4.12 — Comparison of BER performances of SM-OFDM-CDMA scheme with the variation of the number of ducts $N_t = 8, N_r = 128, 2PSK, FFT = 128, N_c = 128, d = 0.1mm$, five users and different frequencies

the physiological media is studied at a transmitter-receiver distance of 0.1 mm and a frequency chosen from the set f= {1, 5, 10 }THz in the presence of a MAI level consisting of five users, and the pertaining results are reported in Fig.4.12. As observed, it is again shown that the achievable performance for a given frequency, is independent of the media in which the communication scheme is embedded, for the ones incorporating a number of ducts ranging from 1 to 5. This consolidates the results reported in Fig.4.2 through Fig. 4.4, where the path loss is shown to be the same regardless the number of ducts.

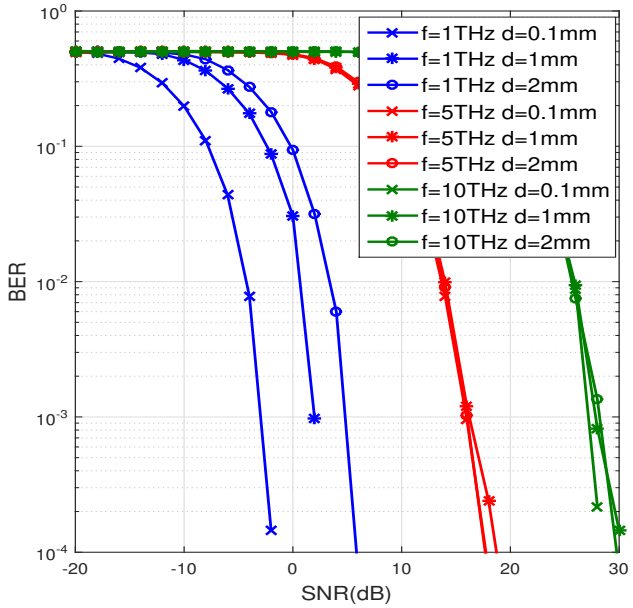

Figure 4.13 — Comparison of BER performances of SM-OFDM-CDMA scheme with the variation of the distance $N_t = 8, N_r = 128, 2PSK, FFT = 128, N_c = 128$, N=1, five users and different frequencies

Figure 4.13 discusses the extent of the impact of the transmitter-receiver distance on the quality of reception, in the presence of MAI and when the operation frequency is varied in the set f= {1, 5, 10 }THz and the number of co-communicating users is 5. Similarly to the trend seen in Fig .4.2 and .4.3, it is demonstrated that the BER performance in the presence of MAI is sensitive to the distance only at the lower range of THz frequencies. At 5 THz and 10 THz frequencies, the performance is very slightly impacted by the distance. At 1 THz, in order to ensure the required BER value of 10^{-3}, an additional SNR of 6.5 dB is necessary when moving the receiver from d=0.1 mm to 1 mm apart from the transmitter. In Fig.4.14, the achievable performance of

the proposed 2PSK-supporting scheme in terms of the frequency of operation and the number of receive antennas is addressed in the presence of MAI. To carry out this study, the number of users is 5, the number of ducts is 1, and the distance is d=0.1mm. As observed, the reliability of the data is altered by the RX number decrease what ever is the used frequency, which is what was expected. However, the most important issue is that, despite the high level of co-supported and acquired physiological signals, i.e. 5 in this case, decreasing the transmit antenna number and increasing that of receive antennas allows to enhance the BER performance, regardless of the operating frequency. This consolidates again the statement of SM better performance when the number of receive antennas exceeds the transmit antennas.

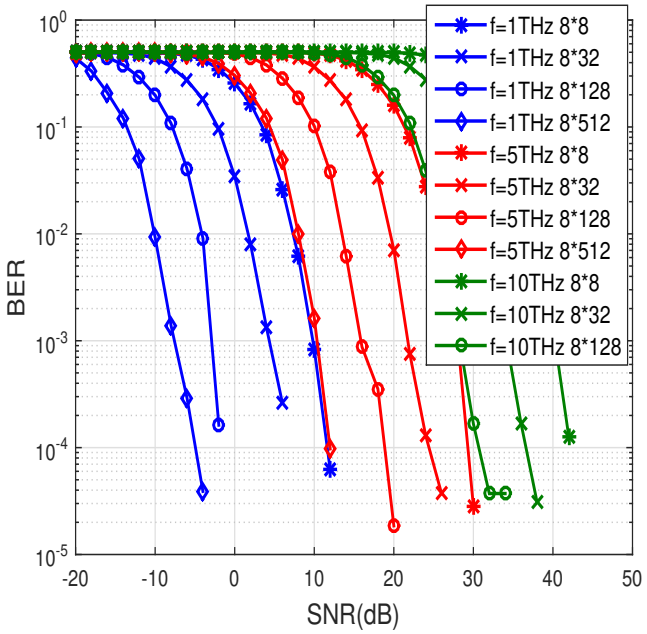

Figure 4.14 — Comparison of BER performances of SM-OFDM-CDMA scheme with the variation of the number of receive antennas $N_t = 8, 2PSK, FFT = 128, N_c = 128, N = 1, d = 0.1mm$ and five users

4.6 Summary

The main objective of this work was to propose an architecture based on spatial modulation which meets the requirements of future generations of health mobile networks, in terms of quality of service and system complexity, while ensuring multiple signal acquisition in in-VIVO Nano networks. It was shown that to ensure a better

performance and signal retrieval at the reception, the number of transmit antenna should be less or equal to the number of receive antennas. Furthermore, because of the in-body channel sensitivity to the high frequencies in the terahertz band, the reliability of the received data is altered. Hence, unless it becomes necessay the lower range of terahertz band should be targeted, and otherwise endow the system with a higher number of subcarrier branches to ensure a more performant OFDM signaling. The impact of the physiological media reflected by the number of ducts was demonstrated to be negligible at these frequencies and the transmitter-receiver element distance was also shown to be of importance only at lower frequencies. The robustness of the resulting architecture to the multiple access and multipath fading interferences has been confirmed. The number of different influential signals (users) has been maximed at 5, which is a reasonnable assumption, however the ambient noise was assumed to be Gaussian. A more accurate distribution of that may bring a new insight towards the incorporation of advanced wireless communication nanonetworks within the body. A new scheme combining SM-OFDM and CDMA is proposed inside the human skin at terahertz frequencies by considering different distances, number of sweat ducts and frequencies, combating strongly the effect of path loss and multiple access interference and keeping the hardware complexity as simple as possible at a required quality of service (QoS). Hence, the reported analysis highlights the novel method to cater the communication challenges in such environment and paved a way for further studies in this harsh environment, for health-care applications.

Conclusion and future work

The wireless community is a few steps away from the implementation of 5G and beyond wireless networks, which are expected to provide ubiquitous communication capabilities. IM considers new dimensions, such as the indices of transmit antennas of a MIMO system, subcarriers of an OFDM system or RF mirrors of an RA, for the transmission of digital information through on/off keying of the building blocks of the considered communication systems.

IM is an up and coming digital modulation concept that has a great potential for next-generation wireless communication systems due to spectrum/energy-efficient as well as low complexity solutions it offers for emerging single/multi-carrier, single/multi-user MIMO, massive MU-MIMO, cooperative communication. Thus, IM technique has attracted the full attention from the academia and industry, and numerous relevant researches have been proposed in the past few years. Spatial modulation is one of the promising MIMO techniques that will be adopted in the 5G-and-beyond communication standards. It offers an improved spectral efficiency, compared to single-input single-output systems, as well as complexity reduction. Indeed, in conventional spatial modulation architectures, only one RF chain is used for transmitting data streams and the spatial position of the switched transmit antenna is utilized as an additional source of information. At the receiver side, designing an appropriate detector which allows to achieve the best average bit error ratio, while keeping a low complexity level, is the most indispensable and essential part. Obviously, this detector should be able to accurately estimate the transmit antenna index at the first stage, then detect the emitted signal in the second stage.

Through this thesis, a study of the different architectures that combine SM/multiuser SM, OFDM, STBC and CDMA exploited in 5G and beyond network systems, has been carried out. We have reviewed the basic principles, advantages, the most recent and promising developments and possible implementation scenarios of SM mapping

paradigm, which is one of the popular applications of the IM concept. For each scheme of SM-based systems, we have provided the corresponding system model, followed by the transceiver design of the typical SM-aided systems, to help the reader to better understand SM principles. Performance evaluation, in terms of bit error rate (BER), have been presented, along with a brief introduction of the different used detectors. Novel architectures combining SM and other schemes such as GFDM and OFTS, as alternatives to OFDM-based solutions, have been introduced, and their performance in frequency selective channels has been demonstrated. Moreover, the exploitation of cooperative diversity in SM has been conducted to offer a higher data immunity against errors. Furthermore, a novel multiple access SM-OFDM-MIMO architecture has been proposed to combat the channel frequency selectivity in In-VIVO environment while offering a high data rate, as compared to conventional SM schemes proposed in literature. In this thesis, special emphasis has been placed on SM-OFDM schemes. We believe this is helpful to the understanding of other SM-aided systems, since their fundamental principles are the same as the SM-OFDM. Based on the survey for the current development of SM, the potential challenges and open issues have been summarized to shed light on the future research. By addressing these challenges, we believe full benefits of the SM technique can be realized, and this attractive novel technique will play an important role in 5G and beyond communications. The following points summarizes some findings from the thesis:

- SM allows to avoid ICI at the receiver input, produces no correlation between the transmit antennas and requires no synchronization between them.
- The performance of SM-OFDM scheme has been investigated with different detectors. It was found that, in ideal correlation and CSI conditions, and using Rayleigh fading, SM-OFDM with OD detector outperforms MMSE and SVD alternatives.
- It is illustrated from simulation results, that the proposed SM-OFDM architectures, which are a combination of SM, STBC, OFDM, and CDMA, are well adapted for 5G and beyond communication network systems, more particularly for massive MIMO. Moreover, they are able to offer a highly reliable low complexity multiple access communication in frequency selective channels. The resulting robustness

and improved performance of the proposed patterns have been confirmed.

- The proposed multi-access SM-OFDM architectures were investigated in Nakagami channels, it was shown, that they were quite sensitive to the increase of spatial correlation and CSI imprecisions, regardless of the used detector. Relaying mechanisms were also tackled in such configurations and the data reliability enhancement yield by the cooperative diversity was highlighted.

- Furtheremore, we contributed with an architecture, based on spatial modulation which meets the requirements of future generations of health mobile networks. it was illustrated, that the robustness of the resulting architecture to the multiple access and multipath fading interferences has been confirmed. In other words, a novel architecture, which combines SM-OFDM and CDMA is proposed inside the human skin at terahertz frequencies by considering different distances, number of sweat ducts and frequencies, and fights hardly against the effect of path loss and multiple access interference and keeping the hardware complexity as simple as possible at a required quality of service (QoS).

With a comprehensive review, we have demonstrated that SM schemes can offer interesting trade-offs in terms of error performance, complexity and spectral efficiency; as a result, they have positioned themselves as possible and strong candidates for next generation (5G and beyond) wireless communication networks.

From very interesting findings achieved within the scope of this thesis, the following research directions are suggested to further investigate this research topic:

- The design of novel generalized/enhanced/differential SM schemes with higher spectral and/or energy efficiency, lower transceiver complexity and better error performance.

- The investigation of a new multiuser schemes that combine SM and other multiple access technique, such as IDMA.

- The optimization and integration of SM techniques to cognitive, massive MU-MIMO, spectrum sharing, M2M and V2X communication systems to be employed in 5G and beyond wireless networks and the design of novel uplink/downlink/point-to-point transmission protocols.

Author's communications

Journal publications

F. Berrahma, K. Ghanem, H. Bousbia-Salah, A. Alomainy, M. Imran, and Q. Abbasi, "Integration of spatial modulation scheme with code division multiple access for vivo based frequency selective nano sensor networks." IEEE Sensors Journal, 2022.

Conference publications

1. Fadila Berrahma, Khalida Ghanem and Mustapha Djeddou, "Performance of Spatial Modulation OFDM Detectors over Adverse Nakagami-m Fading Channel in the Presence of Spatial Correlation", the 3rd International Conference on Electrical Engineering (CEE), EMP, Algiers, Algeria, 2019.

2. F. Berrahma, K. Ghanem, M. Nedil, and H. Bousbia-salah, "A novel multi-user spatial modulation-based code division multiple access scheme," in 2019 IEEE International Symposium on Antennas and Propagation and USNC-URSI Radio Science Meeting. IEEE, 2019, pp. 1587-1588.

3. F. Berrahma, K. Ghanem, H. Bousbia-salah, and M. Nedil, "Incorporation of spatial modulation in in vivo frequency selective nano networks," in 2021 IEEE International Symposium on Antennas and Propagation and USNC-URSI Radio Science Meeting (APS/URSI). IEEE, 2021, pp. 1295-1296.

4. F. Berrahma, K. Ghanem, H. Bousbia-Salah, and M. Nedil, "A novel nonorthogonal frequency division multiplexing scheme for interference avoidance in sm-stbc systems," in 2021 IEEE International Symposium on Antennas and Propagation and USNC-URSI Radio Science Meeting (APS/URSI). IEEE, 2021, pp. 347-348.

5. F. Berrahma, K. Ghanem, and H. Bousbia-Salah, "A new multi-user spatial modulation scheme combining stbc-ofdm and cdma," in 2022 7th International Conference on Image and Signal Processing and their Applications (ISPA). IEEE, 2022, pp. 1-3.

Bibliography

[1] F. Rusek, D. Persson, B. K. Lau, E. G. Larsson, T. L. Marzetta, O. Edfors, and F. Tufvesson, "Scaling up mimo: Opportunities and challenges with very large arrays," *IEEE signal processing magazine*, vol. 30, no. 1, pp. 40–60, 2012.

[2] D. Gesbert, S. Hanly, H. Huang, S. S. Shitz, O. Simeone, and W. Yu, "Multi-cell mimo cooperative networks: A new look at interference," *IEEE journal on selected areas in communications*, vol. 28, no. 9, pp. 1380–1408, 2010.

[3] E. Basar, "Index modulation techniques for 5g wireless networks," *IEEE Communications Magazine*, vol. 54, no. 7, pp. 168–175, 2016.

[4] R. Steele and L. Hanzo, *Mobile radio communications: second and third generation cellular and WATM systems*. IEEE Press-John Wiley, 1999.

[5] M. Rumney *et al.*, *LTE and the evolution to 4G wireless: Design and measurement challenges*. John Wiley & Sons, 2013.

[6] H. Schulze and C. Lüders, *Theory and applications of OFDM and CDMA: Wideband wireless communications*. John Wiley & Sons, 2005.

[7] J. Parikh and A. Basu, "Lte advanced: The 4g mobile broadband technology," *International Journal of Computer Applications*, vol. 13, no. 5, pp. 17–21, 2011.

[8] A. Yastrebova, R. Kirichek, Y. Koucheryavy, A. Borodin, and A. Koucheryavy, "Future networks 2030: Architecture & requirements," in *2018 10th International Congress on Ultra Modern Telecommunications and Control Systems and Workshops (ICUMT)*. IEEE, 2018, pp. 1–8.

[9] S. Zhang, C. Xiang, and S. Xu, "6g: Connecting everything by 1000 times price reduction," *IEEE Open Journal of Vehicular Technology*, vol. 1, pp. 107–115, 2020.

[10] S. Hossain, "5g wireless communication systems," *American Journal of Engineering Research (AJER) e-ISSN*, pp. 2320–0847, 2013.

[11] M. Vaezi, Z. Ding, and H. V. Poor, *Multiple access techniques for 5G wireless networks and beyond*. Springer, 2019, vol. 159.

[12] R. Gayathri, V. Sangeetha, S. Prabha, D. Meenakshi, and N. Raajan, "Papr reduction in ofdm using partial transmit sequence (pts)," *International Journal of Engineering and Technology (IJET)*, vol. 5, no. 2, pp. 1428–1431, 2013.

[13] H. Viswanathan and P. E. Mogensen, "Communications in the 6g era," *IEEE Access*, vol. 8, pp. 57 063–57 074, 2020.

[14] S. Dang, O. Amin, B. Shihada, and M.-S. Alouini, "What should 6g be?" *Nature Electronics*, vol. 3, no. 1, pp. 20–29, 2020.

[15] N. H. Mahmood, H. Alves, O. A. López, M. Shehab, D. P. M. Osorio, and M. Latva-Aho, "Six key features of machine type communication in 6g," in *2020 2nd 6G Wireless Summit (6G SUMMIT)*. IEEE, 2020, pp. 1–5.

[16] B. Sklar, *Digital communications*. Prentice hall Upper Saddle River, NJ, USA:, 2001, vol. 2.

[17] A. Kammoun, M.-S. Alouini *et al.*, "Elevation beamforming with full dimension mimo architectures in 5g systems: A tutorial," *IEEE Communications Surveys & Tutorials*, vol. 21, no. 4, pp. 3238–3273, 2019.

[18] T. S. Rappaport *et al.*, *Wireless communications: principles and practice*. prentice hall PTR New Jersey, 1996, vol. 2.

[19] V. Erceg, L. J. Greenstein, S. Y. Tjandra, S. R. Parkoff, A. Gupta, B. Kulic, A. A. Julius, and R. Bianchi, "An empirically based path loss model for wireless channels in suburban environments," *IEEE Journal on selected areas in communications*, vol. 17, no. 7, pp. 1205–1211, 1999.

[20] M. Pätzold, M. Patzold, and M. Paetzold, *Mobile fading channels*. Wiley Online Library, 2002.

[21] D. Tse and P. Viswanath, *Fundamentals of wireless communication*. Cambridge university press, 2005.

[22] T. Rappaport, "Wireless communications: Principles and practice 2nd edition prentice-hall ptr," 2002.

[23] L. Rayleigh, "Xii. on the resultant of a large number of vibrations of the same pitch and of arbitrary phase," *The London, Edinburgh, and Dublin Philosophical Magazine and Journal of Science*, vol. 10, no. 60, pp. 73–78, 1880.

[24] Z. Hadzi-Velkov, N. Zlatanov, and G. K. Karagiannidis, "On the second order statistics of the multihop rayleigh fading channel," *IEEE Transactions on Communications*, vol. 57, no. 6, pp. 1815–1823, 2009.

[25] R. Y. Mesleh, "Spatial modulation: a spatial multiplexing technique for efficient wireless data transmission," Ph.D. dissertation, Jacobs University Bremen, 2007.

[26] M. Nakagami, "The m-distribution-a general formula of intensity distribution of rapid fading," *Statistical Method of Radio Propagation*, 1960.

[27] N. C. Beaulieu and C. Cheng, "Efficient nakagami-m fading channel simulation," *Vehicular Technology, IEEE Transactions on*, vol. 54, no. 2, pp. 413–424, 2005.

[28] M. D. Yacoub, "Nakagami-m phase-envelope joint distribution: An improved model," in *Microwave and Optoelectronics Conference (IMOC), 2009 SBMO/IEEE MTT-S International*. IEEE, 2009, pp. 335–339.

[29] I. Dioum, "Conception de systèmes multi-antennaires pour techniques de diversité et mimo: application aux petits objets nomades communicants," Ph.D. dissertation, Université Nice Sophia Antipolis; Université Cheikh Anta Diop de Dakar, 2013.

[30] "MS Windows NT kernel description," http://www.teletopix.org/4g-lte/lte-mimo-4g-lte/lte-mimo-types-of-inputs-and-outputs/, accessed: 2010-09-30.

[31] L. C. Godara, "Application of antenna arrays to mobile communications. ii. beamforming and direction-of-arrival considerations," *Proceedings of the IEEE*, vol. 85, no. 8, pp. 1195–1245, 1997.

[32] D. Gesbert, M. Shafi, D.-s. Shiu, P. J. Smith, and A. Naguib, "From theory to practice: an overview of mimo space-time coded wireless systems," *Selected Areas in Communications, IEEE Journal on*, vol. 21, no. 3, pp. 281–302, 2003.

[33] S. M. Alamouti, "A simple transmit diversity technique for wireless communications," *Selected Areas in Communications, IEEE Journal on*, vol. 16, no. 8, pp. 1451–1458, 1998.

[34] D. Brennan, "Linear diversity combining techniques," *Proceedings of the IEEE*, vol. 91, no. 2, pp. 331–356, 2003.

[35] ——, "Linear diversity combining techniques," *Proceedings of the IRE*, vol. 47, no. 6, pp. 1075–1102, 1959.

[36] L. Hanzo, T. H. Liew, and B. L. Yeap, *Turbo coding, turbo equalisation and space-time coding*. John Wiley & Sons, 2002.

[37] L. Hanzo, L.-L. Yang, E. Kuan, and K. Yen, *Single-and multi-carrier DS-CDMA: multi-user detection, space-time spreading, synchronisation, standards and networking*. John Wiley & Sons, 2003.

[38] V. Tarokh, N. Seshadri, and A. R. Calderbank, "Space-time codes for high data rate wireless communication: Performance criterion and code construction," *Information Theory, IEEE Transactions on*, vol. 44, no. 2, pp. 744–765, 1998.

[39] V. Tarokh, A. Naguib, N. Seshadri, and A. R. Calderbank, "Space-time codes for high data rate wireless communication: performance criteria in the presence of channel estimation errors, mobility, and multiple paths," *Communications, IEEE Transactions on*, vol. 47, no. 2, pp. 199–207, 1999.

[40] H. Jafarkhani, "A quasi-orthogonal space-time block code," *Communications, IEEE Transactions on*, vol. 49, no. 1, pp. 1–4, 2001.

[41] P. W. Wolniansky, G. J. Foschini, G. Golden, R. Valenzuela *et al.*, "V-blast: An architecture for realizing very high data rates over the rich-scattering wireless channel," in *Signals, Systems, and Electronics, 1998. ISSSE 98. 1998 URSI International Symposium on*. IEEE, 1998, pp. 295–300.

[42] A. Jamalipour, T. Wada, and T. Yamazato, "A tutorial on multiple access technologies for beyond 3g mobile networks," *Communications Magazine, IEEE*, vol. 43, no. 2, pp. 110–117, 2005.

[43] R. Mesleh, H. Haas, C. W. Ahn, and S. Yun, "Spatial modulation-a new low complexity spectral efficiency enhancing technique," in *2006 First International Conference on Communications and Networking in China*. IEEE, 2006, pp. 1–5.

[44] J. Jeganathan, A. Ghrayeb, L. Szczecinski, and A. Ceron, "Space shift keying modulation for mimo channels," *Wireless Communications, IEEE Transactions on*, vol. 8, no. 7, pp. 3692–3703, 2009.

[45] E. Başar, Ü. Aygölü, E. Panayirci, and H. V. Poor, "Space-time block coded spatial modulation," *Communications, IEEE Transactions on*, vol. 59, no. 3, pp. 823–832, 2011.

[46] E. C. Van Der Meulen, "Three-terminal communication channels," *Advances in applied Probability*, pp. 120–154, 1971.

[47] T. M. Cover and A. E. Gamal, "Capacity theorems for the relay channel," *Information Theory, IEEE Transactions on*, vol. 25, no. 5, pp. 572–584, 1979.

[48] A. Sendonaris, E. Erkip, and B. Aazhang, "User cooperation diversity. part i. system description," *Communications, IEEE Transactions on*, vol. 51, no. 11, pp. 1927–1938, 2003.

[49] T. L. Marzetta, *Fundamentals of massive MIMO*. Cambridge University Press, 2016.

[50] G. Hill, "Peak power reduction in orthogonal frequency division multiplexing transmitters," Ph.D. dissertation, Victoria University, 2011.

[51] F. Hu, *Opportunities in 5G networks: A research and development perspective*. CRC press, 2016.

[52] A. Hammoodi, L. Audah, and M. A. Taher, "Green coexistence for 5g waveform candidates: a review," *IEEE Access*, vol. 7, pp. 10 103–10 126, 2019.

[53] X. Zhang, M. Jia, L. Chen, J. Ma, and J. Qiu, "Filtered-ofdm-enabler for flexible waveform in the 5th generation cellular networks," in *2015 IEEE Global Communications Conference (GLOBECOM)*. IEEE, 2015, pp. 1–6.

[54] R. Hadani, S. Rakib, M. Tsatsanis, A. Monk, A. J. Goldsmith, A. F. Molisch, and R. Calderbank, "Orthogonal time frequency space modulation," in *2017 IEEE Wireless Communications and Networking Conference (WCNC)*. IEEE, 2017, pp. 1–6.

[55] I. Akyildiz, F. Brunetti, and C. Blazquez, "Nanonetworking: A new communication paradigm," *Computer Networks Journal*.

[56] I. F. Akyildiz, J. M. Jornet, and M. Pierobon, "Nanonetworks: A new frontier in communications," *Communications of the ACM*, vol. 54, no. 11, pp. 84–89, 2011.

[57] F. Dressler and O. B. Akan, "A survey on bio-inspired networking," *Computer networks*, vol. 54, no. 6, pp. 881–900, 2010.

[58] F. Dressler, *Self-organization in sensor and actor networks*. John Wiley & Sons, 2008.

[59] F. Dressler and O. B. Akan, "Bio-inspired networking: from theory to practice," *IEEE Communications Magazine*, vol. 48, no. 11, pp. 176–183, 2010.

[60] B. Alberts, A. Johnson, J. Lewis, M. Raff, K. Roberts, and P. Walter, "Molecular biology or the cell," in *Molecular biology or the cell*, 2002.

[61] B. Krüger and F. Dressler, "Molecular processes as a basis for autonomous networking," *IPSI Transactions on Advances Research: Issues in Computer Science and Engineering*, vol. 1, no. 1, pp. 43–50, 2005.

[62] M. Pierobon and I. F. Akyildiz, "Noise analysis in ligand-binding reception for molecular communication in nanonetworks," *IEEE Transactions on Signal Processing*, vol. 59, no. 9, pp. 4168–4182, 2011.

[63] T. Nakano, T. Suda, M. Moore, R. Egashira, A. Enomoto, and K. Arima, "Molecular communication for nanomachines using intercellular calcium signaling," in *5th IEEE Conference on Nanotechnology, 2005.* IEEE, 2005, pp. 478–481.

[64] M. Moore, A. Enomoto, T. Nakano, R. Egashira, T. Suda, A. Kayasuga, H. Kojima, H. Sakakibara, and K. Oiwa, "A design of a molecular communication system for nanomachines using molecular motors," in *Fourth Annual IEEE International Conference on Pervasive Computing and Communications Workshops (PERCOMW'06)*. IEEE, 2006, pp. 6–pp.

[65] Y. Moritani, S. Hiyama, T. Suda, R. Egashira, A. Enomoto, M. Moore, and T. Nakano, "Molecular communications between nanomachines," in *24th IEEE Conference on Computer Communications (IEEE INFOCOM 2005), Miami, FL*, 2005.

[66] K. Jensen, J. Weldon, H. Garcia, and A. Zettl, "Nanotube radio," *Nano letters*, vol. 7, no. 11, pp. 3508–3511, 2007.

[67] M. Pierobon and I. F. Akyildiz, "A physical end-to-end model for molecular communication in nanonetworks," *IEEE Journal on Selected Areas in Communications*, vol. 28, no. 4, pp. 602–611, 2010.

[68] M. Gregori and I. F. Akyildiz, "A new nanonetwork architecture using flagellated bacteria and catalytic nanomotors," *IEEE Journal on selected areas in communications*, vol. 28, no. 4, pp. 612–619, 2010.

[69] I. F. Akyildiz and J. M. Jornet, "Electromagnetic wireless nanosensor networks," *Nano Communication Networks*, vol. 1, no. 1, pp. 3–19, 2010.

[70] M. S. Mannoor, H. Tao, J. D. Clayton, A. Sengupta, D. L. Kaplan, R. R. Naik, N. Verma, F. G. Omenetto, and M. C. McAlpine, "Graphene-based wireless bacteria detection on tooth enamel," *Nature communications*, vol. 3, no. 1, pp. 1–9, 2012.

[71] A. Guney, B. Atakan, and O. B. Akan, "Mobile ad hoc nanonetworks with collision-based molecular communication," *IEEE Transactions on Mobile Computing*, vol. 11, no. 3, pp. 353–366, 2011.

[72] H. Lee, T. K. Choi, Y. B. Lee, H. R. Cho, R. Ghaffari, L. Wang, H. J. Choi, T. D. Chung, N. Lu, T. Hyeon *et al.*, "A graphene-based electrochemical device with thermoresponsive microneedles for diabetes monitoring and therapy," *Nature nanotechnology*, vol. 11, no. 6, pp. 566–572, 2016.

[73] N. A. Ali and M. Abu-Elkheir, "Internet of nano-things healthcare applications: Requirements, opportunities, and challenges," in *2015 IEEE 11th International Conference on Wireless and Mobile Computing, Networking and Communications (WiMob)*. IEEE, 2015, pp. 9–14.

[74] P. Honeine, F. Mourad, M. Kallas, H. Snoussi, H. Amoud, and C. Francis, "Wireless sensor networks in biomedical: Body area networks," in *International Workshop on Systems, Signal Processing and their Applications, WOSSPA*. IEEE, 2011, pp. 388–391.

[75] D. Cypher, N. Chevrollier, N. Montavont, and N. Golmie, "Prevailing over wires in healthcare environments: benefits and challenges," *IEEE Communications Magazine*, vol. 44, no. 4, pp. 56–63, 2006.

[76] S. D. Digambar, T. P. Shahu, S. A. Gorakshanath, P. S. Appasaheb, and M. D. Sitaram, "In vivo networking (ivn): Need of present era." 2020.

[77] H. Haas, S. Sinanovic, C. Ahn, and S. Yun, "Spatial modulation," *IEEE Trans. Veh. Technol*, vol. 57, no. 4, pp. 2228–41, 2008.

[78] E. Basar, M. Wen, R. Mesleh, M. Di Renzo, Y. Xiao, and H. Haas, "Index modulation techniques for next-generation wireless networks," *IEEE access*, vol. 5, pp. 16 693–16 746, 2017.

[79] Q. Ma, P. Yang, Y. Xiao, H. Bai, and S. Li, "Error probability analysis of ofdm-im with carrier frequency offset," *IEEE Communications Letters*, vol. 20, no. 12, pp. 2434–2437, 2016.

[80] E. Memisoglu, E. Basar, and H. Arslan, "Fading-aligned ofdm with index modulation for mmtc services," *Physical Communication*, vol. 35, p. 100680, 2019.

[81] J. Jeganathan, A. Ghrayeb, and L. Szczecinski, "Spatial modulation: Optimal detection and performance analysis," *IEEE Communications Letters*, vol. 12, no. 8, pp. 545–547, 2008.

[82] R. Zhang, L.-L. Yang, and L. Hanzo, "Error probability and capacity analysis of generalised pre-coding aided spatial modulation," *IEEE Transactions on Wireless Communications*, vol. 14, no. 1, pp. 364–375, 2014.

[83] A. Kammoun, A. Chaaban, M. Debbah, M.-S. Alouini *et al.*, "Asymptotic max-min sinr analysis of reconfigurable intelligent surface assisted miso systems," *IEEE Transactions on Wireless Communications*, vol. 19, no. 12, pp. 7748–7764, 2020.

[84] J. Zhao, "A survey of intelligent reflecting surfaces (irss): Towards 6g wireless communication networks," *arXiv preprint arXiv:1907.04789*, 2019.

[85] S. Gong, X. Lu, D. T. Hoang, D. Niyato, L. Shu, D. I. Kim, and Y.-C. Liang, "Toward smart wireless communications via intelligent reflecting surfaces: A contemporary survey," *IEEE Communications Surveys & Tutorials*, vol. 22, no. 4, pp. 2283–2314, 2020.

[86] E. Basar, "Reconfigurable intelligent surface-based index modulation: A new beyond mimo paradigm for 6g," *IEEE Transactions on Communications*, vol. 68, no. 5, pp. 3187–3196, 2020.

[87] R. Abu-Alhiga and H. Haas, "Subcarrier-index modulation ofdm," in *2009 IEEE 20th International Symposium on Personal, Indoor and Mobile Radio Communications*. IEEE, 2009, pp. 177–181.

[88] M. Nakao, T. Ishihara, and S. Sugiura, "Single-carrier frequency-domain equalization with index modulation," *IEEE Communications Letters*, vol. 21, no. 2, pp. 298–301, 2016.

[89] G. Kaddoum, M. F. Ahmed, and Y. Nijsure, "Code index modulation: A high data rate and energy efficient communication system," *IEEE Communications Letters*, vol. 19, no. 2, pp. 175–178, 2014.

[90] A. K. Khandani, "Media-based modulation: A new approach to wireless transmission," in *2013 IEEE international symposium on information theory*. IEEE, 2013, pp. 3050–3054.

[91] P. Yang, Y. Xiao, Y. L. Guan, K. Hari, A. Chockalingam, S. Sugiura, H. Haas, M. Di Renzo, C. Masouros, Z. Liu *et al.*, "Single-carrier sm-mimo: A promising design for broadband large-scale antenna systems," *IEEE Communications Surveys & Tutorials*, vol. 18, no. 3, pp. 1687–1716, 2016.

[92] E. Seifi, M. Atamanesh, and A. K. Khandani, "Media-based mimo: Outperforming known limits in wireless," in *2016 IEEE International Conference on Communications (ICC)*. IEEE, 2016, pp. 1–7.

[93] Y. Naresh and A. Chockalingam, "On media-based modulation using rf mirrors," *IEEE Transactions on Vehicular Technology*, vol. 66, no. 6, pp. 4967–4983, 2016.

[94] E. Basar, "Media-based modulation for future wireless systems: A tutorial," *IEEE Wireless Communications*, vol. 26, no. 5, pp. 160–166, 2019.

[95] J. Zhang, Y. Wang, J. Zhang, and L. Ding, "Polarization shift keying (polarsk): System scheme and performance analysis," *IEEE Transactions on Vehicular Technology*, vol. 66, no. 11, pp. 10 139–10 155, 2017.

[96] I. A. Hemadeh, P. Xiao, Y. Kabiri, L. Xiao, V. Fusco, and R. Tafazolli, "Polarization modulation design for reduced rf chain wireless," *IEEE Transactions on Communications*, vol. 68, no. 6, pp. 3890–3907, 2020.

[97] A. Younis, N. Serafimovski, R. Mesleh, and H. Haas, "Generalised spatial modulation," in *2010 conference record of the forty fourth Asilomar conference on signals, systems and computers*. IEEE, 2010, pp. 1498–1502.

[98] A. Younis, R. Mesleh, and H. Haas, "Quadrature spatial modulation performance over nakagami-m fading channels," *IEEE Transactions on Vehicular Technology*, vol. 65, no. 12, pp. 10 227–10 231, 2015.

[99] C.-C. Cheng, H. Sari, S. Sezginer, and Y. T. Su, "Enhanced spatial modulation with multiple signal constellations," *IEEE Transactions on Communications*, vol. 63, no. 6, pp. 2237–2248, 2015.

[100] E. Başar, U. Aygölü, E. Panayirci, and H. V. Poor, "Space-time block coded spatial modulation," *IEEE transactions on communications*, vol. 59, no. 3, pp. 823–832, 2010.

[101] E. Başar, Ü. Aygölü, E. Panayırcı, and H. V. Poor, "Orthogonal frequency division multiplexing with index modulation," *IEEE Transactions on signal processing*, vol. 61, no. 22, pp. 5536–5549, 2013.

[102] E. Ozturk, E. Basar, and H. A. Cirpan, "Generalized frequency division multiplexing with index modulation," in *2016 IEEE Globecom Workshops (GC Wkshps)*. IEEE, 2016, pp. 1–6.

[103] T. Ishihara and S. Sugiura, "Faster-than-nyquist signaling with index modulation," *IEEE Wireless Communications Letters*, vol. 6, no. 5, pp. 630–633, 2017.

[104] M. Nakao and S. Sugiura, "Dual-mode time-domain single-carrier index modulation with frequency-domain equalization," in *2017 IEEE 86th Vehicular Technology Conference (VTC-Fall)*. IEEE, 2017, pp. 1–5.

[105] Q. Li, M. Wen, E. Basar, and F. Chen, "Ofdm spread spectrum with index modulation," in *2017 IEEE Globecom Workshops (GC Wkshps)*. IEEE, 2017, pp. 1–6.

[106] E. Basar and I. Altunbas, "Space-time channel modulation," *IEEE Transactions on Vehicular Technology*, vol. 66, no. 8, pp. 7609–7614, 2017.

[107] Z. Yigit and E. Basar, "Space-time media-based modulation," *IEEE Transactions on Signal Processing*, vol. 67, no. 9, pp. 2389–2398, 2019.

[108] Y. Bian, X. Cheng, M. Wen, L. Yang, H. V. Poor, and B. Jiao, "Differential spatial modulation," *IEEE Transactions on Vehicular Technology*, vol. 64, no. 7, pp. 3262–3268, 2014.

[109] S. Sugiura, S. Chen, and L. Hanzo, "Coherent and differential space-time shift keying: A dispersion matrix approach," *IEEE Transactions on Communications*, vol. 58, no. 11, pp. 3219–3230, 2010.

[110] M. Driusso, F. Babich, M. I. Kadir, and L. Hanzo, "Ofdm aided space-time shift keying for dispersive downlink channels," in *2012 IEEE Vehicular Technology Conference (VTC Fall)*. IEEE, 2012, pp. 1–5.

[111] S. Jacob, T. L. Narasimhan, and A. Chockalingam, "Space-time index modulation," in *2017 IEEE Wireless Communications and Networking Conference (WCNC)*. IEEE, 2017, pp. 1–6.

[112] B. Shamasundar, S. Bhat, S. Jacob, and A. Chockalingam, "Multidimensional index modulation in wireless communications," *IEEE Access*, vol. 6, pp. 589–604, 2017.

[113] F. Çögen, E. Aydin, N. Kabaoğlu, E. Bagar, and H. Ilhan, "A novel mimo scheme based on code-index modulation and spatial modulation," in *2018 26th Signal Processing and Communications Applications Conference (SIU)*. IEEE, 2018, pp. 1–4.

[114] I. Yildirim, E. Basar, and I. Altunbas, "Quadrature channel modulation," *IEEE Wireless Communications Letters*, vol. 6, no. 6, pp. 790–793, 2017.

[115] S. Dhanasekaran, "Space-polarization shift keying modulation for mimo channels," *Wireless Personal Communications*, vol. 86, no. 3, pp. 1509–1539, 2016.

[116] G. Zafari, M. Koca, and H. Sari, "Dual-polarized spatial modulation over correlated fading channels," *IEEE Transactions on Communications*, vol. 65, no. 3, pp. 1336–1352, 2016.

[117] ——, "Spatial modulation with dual-polarized antennas," in *2015 IEEE International Conference on Communications (ICC)*. IEEE, 2015, pp. 2375–2380.

[118] M. Au, G. Kaddoum, M. S. Alam, E. Basar, and F. Gagnon, "Joint code-frequency index modulation for iot and multi-user communications," *IEEE Journal of Selected Topics in Signal Processing*, vol. 13, no. 6, pp. 1223–1236, 2019.

[119] I. A. Hemadeh, M. El-Hajjar, S. Won, and L. Hanzo, "Multi-set space-time shift-keying with reduced detection complexity," *IEEE Access*, vol. 4, pp. 4234–4246, 2016.

[120] P. Botsinis, I. Hemadeh, D. Alanis, Z. Babar, H. V. Nguyen, D. Chandra, S. X. Ng, M. El-Hajjar, and L. Hanzo, "Joint-alphabet space time shift keying in mm-wave non-orthogonal multiple access," *IEEE Access*, vol. 6, pp. 22 602–22 621, 2017.

[121] S. Lu, I. A. Hemadeh, M. El-Hajjar, and L. Hanzo, "Compressed-sensing-aided space-time frequency index modulation," *IEEE Transactions on Vehicular Technology*, vol. 67, no. 7, pp. 6259–6271, 2018.

[122] Y. Chau, S.-H. Yu *et al.*, "Space modulation on wireless fading channels," in *Vehicular Technology Conference, 2001. VTC 2001 Fall. IEEE VTS 54th*, vol. 3. IEEE, 2001, pp. 1668–1671.

[123] H. Haas, E. Costa, and E. Schulz, "Increasing spectral efficiency by data multiplexing using antenna arrays," in *Personal, Indoor and Mobile Radio Communications, 2002. The 13th IEEE International Symposium on*, vol. 2. IEEE, 2002, pp. 610–613.

[124] S. Song, Y. Yang, Q. Xionq, K. Xie, B.-J. Jeong, and B. Jiao, "A channel hopping technique i: Theoretical studies on band efficiency and capacity," in *Communications, Circuits and Systems, 2004. ICCCAS 2004. 2004 International Conference on*, vol. 1. IEEE, 2004, pp. 229–233.

[125] R. Mesleh, H. Haas, Y. Lee, and S. Yun, "Interchannel interference avoidance in mimo transmission by exploiting spatial information," in *Personal, Indoor and Mobile Radio Communications, 2005. PIMRC 2005. IEEE 16th International Symposium on*, vol. 1. IEEE, 2005, pp. 141–145.

[126] R. Mesleh, H. Haas, C. W. Ahn, S. Yun *et al.*, "On the performance of spatial modulation ofdm," in *Signals, Systems and Computers, 2006. ACSSC'06. Fortieth Asilomar Conference on*. IEEE, 2006, pp. 1825–1829.

[127] R. Mesleh, S. Ganesan, and H. Haas, "Impact of channel imperfections on spatial modulation ofdm," in *Personal, Indoor and Mobile Radio Communications, 2007. PIMRC 2007. IEEE 18th International Symposium on*. IEEE, 2007, pp. 1–5.

[128] R. Y. Mesleh, H. Haas, S. Sinanović, C. W. Ahn, and S. Yun, "Spatial modulation," *Vehicular Technology, IEEE Transactions on*, vol. 57, no. 4, pp. 2228–2241, 2008.

[129] S. U. Hwang, S. Jeon, S. Lee, and J. Seo, "Soft-output ml detector for spatial modulation ofdm systems," *IEICE Electronics Express*, vol. 6, no. 19, pp. 1426–1431, 2009.

[130] M. Di Renzo and H. Haas, "Spatial modulation with partial-csi at the receiver: optimal detector and performance evaluation," in *Sarnoff Symposium, 2010 IEEE*. IEEE, 2010, pp. 1–6.

[131] E. Başar, Ü. Aygölü, E. Panayırcı, and H. V. Poor, "Performance of spatial modulation in the presence of channel estimation errors," *Communications Letters, IEEE*, vol. 16, no. 2, pp. 176–179, 2012.

[132] R. Mesleh and S. S. Ikki, "On the effect of gaussian imperfect channel estimations on the performance of space modulation techniques," in *Vehicular Technology Conference (VTC Spring), 2012 IEEE 75th.* IEEE, 2012, pp. 1–5.

[133] R. Mesleh, R. Mehmood, H. Elgala, and H. Haas, "Indoor mimo optical wireless communication using spatial modulation," in *Communications (ICC), 2010 IEEE International Conference on.* IEEE, 2010, pp. 1–5.

[134] T. Fath, H. Haas, M. D. Renzo, and R. Mesleh, "Spatial modulation applied to optical wireless communications in indoor los environments," in *Global Telecommunications Conference (GLOBECOM 2011), 2011 IEEE.* IEEE, 2011, pp. 1–5.

[135] Y. Yang and B. Jiao, "Information-guided channel-hopping for high data rate wireless communication," *Communications Letters, IEEE*, vol. 12, no. 4, pp. 225–227, 2008.

[136] M. Di Renzo, H. Haas, A. Ghrayeb *et al.*, "Spatial modulation for mimo wireless systems," in *IEEE Wireless Communications and Networking Conference-WCNC 2013*, 2013.

[137] M. D. Renzo and H. Haas, "Bit error probability of sm-mimo over generalized fading channels," *Vehicular Technology, IEEE Transactions on*, vol. 61, no. 3, pp. 1124–1144, 2012.

[138] A. Stavridis, S. Sinanovic, M. Di Renzo, and H. Haas, "Energy evaluation of spatial modulation at a multi-antenna base station," in *Vehicular Technology Conference (VTC Fall), 2013 IEEE 78th.* IEEE, 2013, pp. 1–5.

[139] Y. Li, J. H. Winters, and N. R. Sollenberger, "Mimo-ofdm for wireless communications: signal detection with enhanced channel estimation," *Communications, IEEE Transactions on*, vol. 50, no. 9, pp. 1471–1477, 2002.

[140] P. Yang, M. Di Renzo, Y. Xiao, S. Li, and L. Hanzo, "Design guidelines for spatial modulation," *Communications Surveys & Tutorials, IEEE*, vol. 17, no. 1, pp. 6–26, 2015.

[141] A. Younis, R. Mesleh, H. Haas, and P. M. Grant, "Reduced complexity sphere decoder for spatial modulation detection receivers," in *Global Telecommunications Conference (GLOBECOM 2010), 2010 IEEE*. IEEE, 2010, pp. 1–5.

[142] A. Younis, S. Sinanovic, M. Di Renzo, R. Mesleh, and H. Haas, "Generalised sphere decoding for spatial modulation," *Communications, IEEE Transactions on*, vol. 61, no. 7, pp. 2805–2815, 2013.

[143] N. R. Naidoo, H.-J. Xu, and T. Al-Mumit Quazi, "Spatial modulation: optimal detector asymptotic performance and multiple-stage detection," *Communications, IET*, vol. 5, no. 10, pp. 1368–1376, 2011.

[144] Q. Tang, Y. Xiao, P. Yang, Q. Yu, and S. Li, "A new low-complexity near-ml detection algorithm for spatial modulation," *Wireless Communications Letters, IEEE*, vol. 2, no. 1, pp. 90–93, 2013.

[145] J. Zheng, "Signal vector based list detection for spatial modulation," *Wireless Communications Letters, IEEE*, vol. 1, no. 4, pp. 265–267, 2012.

[146] M. O. Damen, H. El Gamal, and G. Caire, "On maximum-likelihood detection and the search for the closest lattice point," *Information Theory, IEEE Transactions on*, vol. 49, no. 10, pp. 2389–2402, 2003.

[147] R. M. Legnain, R. H. Hafez, I. D. Marsland, and A. M. Legnain, "A novel spatial modulation using mimo spatial multiplexing," in *Communications, Signal Processing, and their Applications (ICCSPA), 2013 1st International Conference on*. IEEE, 2013, pp. 1–4.

[148] E. Viterbo and J. Boutros, "A universal lattice code decoder for fading channels," *Information Theory, IEEE Transactions on*, vol. 45, no. 5, pp. 1639–1642, 1999.

[149] X. Xia, H. Hu, and H. Wang, "Reduced initial searching radius for sphere decoder," in *Personal, Indoor and Mobile Radio Communications, 2007. PIMRC 2007. IEEE 18th International Symposium on*. IEEE, 2007, pp. 1–4.

[150] A. Younis, "Spatial modulation: theory to practice," 2014.

[151] E. Soujeri and G. Kaddoum, "Performance comparison of spatial modulation detectors under channel impairments," in *Ubiquitous Wireless Broadband (ICUWB), 2015 IEEE International Conference on*. IEEE, 2015, pp. 1–5.

[152] N. Michailow, S. Krone, M. Lentmaier, and G. Fettweis, "Bit error rate performance of generalized frequency division multiplexing," in *2012 IEEE Vehicular Technology Conference (VTC Fall)*. IEEE, 2012, pp. 1–5.

[153] N. Serafimovski, S. Sinanović, M. D. Renzo, and H. Haas, "Multiple access spatial modulation," *EURASIP Journal on Wireless Communications and Networking*, vol. 2012, no. 1, pp. 1–20, 2012.

[154] M. Di Renzo and H. Haas, "Bit error probability of space-shift keying mimo over multiple-access independent fading channels," *IEEE transactions on vehicular technology*, vol. 60, no. 8, pp. 3694–3711, 2011.

[155] Y. Chen, L. Wang, Z. Zhao, M. Ma, and B. Jiao, "Secure multiuser mimo downlink transmission via precoding-aided spatial modulation," *IEEE Communications Letters*, vol. 20, no. 6, pp. 1116–1119, 2016.

[156] L. He, J. Wang, J. Song, and L. Hanzo, "On the multi-user multi-cell massive spatial modulation uplink: How many antennas for each user?" *IEEE Transactions on Wireless Communications*, vol. 16, no. 3, pp. 1437–1451, 2016.

[157] R. Kohno, R. Meidan, and L. B. Milstein, "Spread spectrum access methods for wireless communications," *IEEE Communications magazine*, vol. 33, no. 1, pp. 58–67, 1995.

[158] A. J. Viterbi, *CDMA: principles of spread spectrum communication*. Addison Wesley Longman Publishing Co., Inc., 1995.

[159] R. Pickholtz, D. Schilling, and L. Milstein, "Theory of spread-spectrum communications-a tutorial," *IEEE transactions on Communications*, vol. 30, no. 5, pp. 855–884, 1982.

[160] F. Ghanem, G. Delisle, T. Denidni, and K. Ghanem, "A directive dual-band antenna based on metallic electromagnetic crystals," *IEEE Antennas and Wireless Propagation Letters*, vol. 5, no. 1, pp. 384–387, 2006.

[161] A. Sumathi, S. K. Mohideen, and A. Anitha, "Performance analysis of space time block coded spatial modulation," 2012.

[162] A. Hedayat, T. Hunter, and A. Nosratinia, "Cooperative communication in wireless networks," *IEEE Communications Magazine*, vol. 42, no. 10, pp. 74–80, 2004.

[163] J. N. Laneman, D. N. Tse, and G. W. Wornell, "Cooperative diversity in wireless networks: Efficient protocols and outage behavior," *IEEE Transactions on Information theory*, vol. 50, no. 12, pp. 3062–3080, 2004.

[164] N. Serafimovski, S. Sinanovic, M. Di Renzo, and H. Haas, "Dual-hop spatial modulation (dh-sm)," in *2011 IEEE 73rd Vehicular Technology Conference (VTC Spring)*. IEEE, 2011, pp. 1–5.

[165] P. Som and A. Chockalingam, "Performance analysis of space-shift keying in decode-and-forward multihop mimo networks," *IEEE Transactions on Vehicular Technology*, vol. 64, no. 1, pp. 132–146, 2014.

[166] R. Mesleh, S. S. Ikki, E.-H. M. Aggoune, and A. Mansour, "Performance analysis of space shift keying (ssk) modulation with multiple cooperative relays," *EURASIP Journal on Advances in Signal Processing*, vol. 2012, no. 1, p. 201, 2012.

[167] R. Mesleh and S. S. Ikki, "Space shift keying with amplify-and-forward mimo relaying," *Transactions on Emerging Telecommunications Technologies*, vol. 26, no. 4, pp. 520–531, 2015.

[168] R. Mesleh, S. Ikki, and M. Alwakeel, "Performance analysis of space shift keying with amplify and forward relaying," *IEEE Communications Letters*, vol. 15, no. 12, pp. 1350–1352, 2011.

[169] R. Mesleh and S. S. Ikki, "Performance analysis of spatial modulation with multiple decode and forward relays," *IEEE Wireless Communications Letters*, vol. 2, no. 4, pp. 423–426, 2013.

[170] P. Som and A. Chockalingam, "End-to-end ber analysis of space shift keying in decode-and-forward cooperative relaying," in *2013 IEEE wireless communications and networking conference (WCNC)*. IEEE, 2013, pp. 3465–3470.

[171] X. Yang, D. Fan, A. Ren, N. Zhao, and M. Alam, "5g-based user-centric sensing at c-band," *IEEE Transactions on Industrial Informatics*, vol. 15, no. 5, pp. 3040–3047, 2019.

[172] B. Amouri, K. Ghanem, and M. Kaddeche, "Hybrid relay selection-based scheme for uwb bans combining mb-ofdm and decode-and-forward cooperative architectures," *Electronics Letters*, vol. 52, no. 24, pp. 2017–2019, 2016.

[173] K. Ghanem, P. Hall, and R. Langley, "Interference cancellation in body-area networks using linear multiuser receivers," *International Journal of Wireless Information Networks*, vol. 17, no. 3, pp. 126–136, 2010.

[174] O. Kerdjidj, A. Amira, K. Ghanem, N. Ramzan, S. Katsigiannis, and F. Chouireb, "An fpga implementation of the matching pursuit algorithm for a compressed sensing enabled e-health monitoring platform," *Microprocessors and Microsystems*, vol. 67, pp. 131–139, 2019.

[175] K. Ghanem, I. Khan, P. Hall, and L. Hanzo, "Mimo channel modeling and capacity of body area networks," *IEEE Trans. Antennas Propag.*, vol. 60, no. 6, pp. 2980–2986, 2012.

[176] K. Ghanem and P. S. Hall, "Power and bit allocation in on-body channels using mimo antenna arrays," *IEEE transactions on vehicular technology*, vol. 62, no. 1, pp. 404–408, 2012.

[177] ——, "Interference cancellation using cdma multi-user detectors for on-body channels," in *2009 IEEE 20th international symposium on personal, indoor and mobile radio communications*. IEEE, 2009, pp. 2152–2156.

[178] K. Ghanem, "Effect of channel correlation and path loss on average channel capacity of body-to-body systems," *IEEE transactions on Antennas and propagation*, vol. 61, no. 12, pp. 6260–6265, 2013.

[179] M. El Azhari, M. Nedil, Y. S. Alj, I. B. Mabrouk, K. Ghanem, and L. Talbi, "Off-body los and nlos channel characterization in a mine environment," in *2015 International Conference on Electrical and Information Technologies (ICEIT)*. IEEE, 2015, pp. 114–118.

[180] M. E. H. El Azhari, M. Nedil, I. B. Mabrouk, K. Ghanem, and L. Talbi, "Characterization of an off-body channel at 2.45 ghz in an underground mine environment," *Progress In Electromagnetics Research M*, vol. 43, pp. 91–100, 2015.

[181] W. Dib, K. Ghanem, M. Radi, F. Z. Bouchibane, and A. Maali, "An experiemental system-based analyis of humain body motions using embedded sensors," in *2014 IEEE Antennas and Propagation Society International Symposium (APSURSI)*. IEEE, 2014, pp. 981–982.

[182] J. M. Jornet and I. F. Akyildiz, "Channel modeling and capacity analysis for electromagnetic wireless nanonetworks in the terahertz band," *IEEE Transactions on Wireless Communications*, vol. 10, no. 10, pp. 3211–3221, 2011.

[183] K. Yang, A. Pellegrini, A. Brizzi, A. Alomainy, and Y. Hao, "Numerical analysis of the communication channel path loss at the thz band inside the fat tissue," in *2013 IEEE MTT-S International Microwave Workshop Series on RF and Wireless Technologies for Biomedical and Healthcare Applications (IMWS-BIO)*. IEEE, 2013, pp. 1–3.

[184] P. Boronin, D. Moltchanov, and Y. Koucheryavy, "A molecular noise model for thz channels," in *2015 IEEE International Conference on Communications (ICC)*. IEEE, 2015, pp. 1286–1291.

[185] Q. H. Abbasi, H. El Sallabi, N. Chopra, K. Yang, K. A. Qaraqe, and A. Alomainy, "Terahertz channel characterization inside the human skin for nano-scale body-centric networks," *IEEE Transactions on Terahertz Science and Technology*, vol. 6, no. 3, pp. 427–434, 2016.

[186] J. M. Jornet and I. F. Akyildiz, "Low-weight channel coding for interference mitigation in electromagnetic nanonetworks in the terahertz band," in *2011 IEEE international conference on communications (ICC)*. IEEE, 2011, pp. 1–6.

[187] J. M. Jornet, "Low-weight error-prevention codes for electromagnetic nanonetworks in the terahertz band," *Nano Communication Networks*, vol. 5, no. 1-2, pp. 35–44, 2014.

[188] V. Petrov, D. Moltchanov, and Y. Koucheryavy, "On the efficiency of spatial channel reuse in ultra-dense thz networks," in *2015 IEEE Global Communications Conference (GLOBECOM)*. IEEE, 2015, pp. 1–7.

[189] ——, "Interference and sinr in dense terahertz networks," in *2015 IEEE 82nd Vehicular Technology Conference (VTC2015-Fall)*. IEEE, 2015, pp. 1–5.

[190] V. Petrov, M. Komarov, D. Moltchanov, J. M. Jornet, and Y. Koucheryavy, "Interference and sinr in millimeter wave and terahertz communication systems with blocking and directional antennas," *IEEE Transactions on Wireless Communications*, vol. 16, no. 3, pp. 1791–1808, 2017.

[191] R. Zhang, K. Yang, Q. H. Abbasi, K. A. Qaraqe, and A. Alomainy, "Analytical characterisation of the terahertz in-vivo nano-network in the presence of interference based on ts-ook communication scheme," *IEEE Access*, vol. 5, pp. 10 172–10 181, 2017.

[192] S. Cui, A. J. Goldsmith, and A. Bahai, "Energy-efficiency of mimo and cooperative mimo techniques in sensor networks," *IEEE Journal on selected areas in communications*, vol. 22, no. 6, pp. 1089–1098, 2004.

[193] A. Del Coso, U. Spagnolini, and C. Ibars, "Cooperative distributed mimo channels in wireless sensor networks," *IEEE Journal on Selected Areas in Communications*, vol. 25, no. 2, pp. 402–414, 2007.

[194] F. Berrahma, K. Ghanem, M. Nedil, and H. Bousbia-salah, "A novel multi-user spatial modulation-based code division multiple access scheme," in *2019 IEEE International Symposium on Antennas and Propagation and USNC-URSI Radio Science Meeting*. IEEE, 2019, pp. 1587–1588.

[195] N. Serafimovski, A. Younis, R. Mesleh, P. Chambers, M. Di Renzo, C.-X. Wang, P. M. Grant, M. A. Beach, and H. Haas, "Practical implementation of spatial modulation," *IEEE Transactions on Vehicular Technology*, vol. 62, no. 9, pp. 4511–4523, 2013.

[196] W. Belaoura, K. Ghanem, M. A. Imran, A. Alomainy, and Q. H. Abbasi, "A cooperative massive mimo system for future in vivo nanonetworks," *IEEE Systems Journal*, 2020.

[197] N. Serafimovski, S. Sinanović, A. Younis, M. Di Renzo, and H. Haas, "2-user multiple access spatial modulation," in *2011 IEEE GLOBECOM Workshops (GC Wkshps)*. IEEE, 2011, pp. 343–347.

[198] Y. Liu, L.-L. Yang, and L. Hanzo, "Spatial modulation aided sparse code-division multiple access," *IEEE Transactions on Wireless Communications*, vol. 17, no. 3, pp. 1474–1487, 2017.

[199] O. Sushko, "Terahertz dielectric study of bio-molecules using time-domain spectrometry and molecular dynamics simulations," Ph.D. dissertation, Queen Mary University of London, 2014.

[200] T. D. Dorney, R. G. Baraniuk, and D. M. Mittleman, "Material parameter estimation with terahertz time-domain spectroscopy," *JOSA A*, vol. 18, no. 7, pp. 1562–1571, 2001.

[201] M. Fukuma and K. Ishii, "Space-time code division multiple access based on spatial modulation," in *2015 IEEE 82nd Vehicular Technology Conference (VTC2015-Fall)*. IEEE, 2015, pp. 1–5.

[202] M. Di Renzo, H. Haas, and P. M. Grant, "Spatial modulation for multiple-antenna wireless systems: A survey," *IEEE Communications Magazine*, vol. 49, no. 12, pp. 182–191, 2011.

[203] J. Mietzner, R. Schober, L. Lampe, W. H. Gerstacker, and P. A. Hoeher, "Multiple-antenna techniques for wireless communications-a comprehensive literature survey," *IEEE communications surveys & tutorials*, vol. 11, no. 2, pp. 87–105, 2009.

[204] M. Renzo, H. Haas, A. Ghrayeb, L. Hanzo, and S. Sugiura, "Spatial modulation for multiple-antenna communication," 2016.